Title
Sources, Fate, and Transport of Fecal Indicator and Antibiotic Resistance Bacteria in Coastal Environments

Author
Cira, Marisol

Publication Date
2023

Peer reviewed|Thesis/dissertation

UNIVERSITY OF CALIFORNIA

Los Angeles

Sources, Fate, and Transport of Fecal Indicator and Antibiotic Resistance Bacteria in Coastal Environments

A dissertation submitted in partial satisfaction of the

requirements for the degree Doctor of Philosophy

in Civil Engineering

by

Marisol Alejandria Cira

2023

ABSTRACT OF THE DISSERTATION

Sources, Fate, and Transport of Fecal Indicator and Antibiotic Resistance Bacteria in Coastal Environments

by

Marisol Alejandria Cira

Doctor of Philosophy in Civil Engineering

University of California, Los Angeles, 2023

Professor Jennifer A. Jay, Chair

Microbial contamination of coastal waters is a global environmental and public health concern. However, monitoring and tracking of microbial contaminants may require technical expertise and may be costly and labor-intensive. Thus, to address this environmental issue in both developed and developing countries, current methods need to be cross-validated, and more accessible methods need to be proposed.

Therefore, this dissertation investigates the sources, fate, and transport of fecal indicator and antibiotic resistant bacteria in coastal watersheds. This dissertation utilizes culture-, molecular-, and satellite-based techniques to provide cross comparison. Additionally, this dissertation implements these techniques into course-based research experiences (CREs) for graduate students to assess whether CREs influence graduate students' confidence and interest in research.

In chapter 1, a team of collaborators from University of California, Los Angeles (UCLA), the University of Pennsylvania, the Jet Propulsion Laboratory, and Health the Bay investigate oceanic responses to the 2018 Woolsey Fire using in-situ data of fecal indicator bacteria and satellite-derived data of turbidity. Chapter 2 examines commercially available garden products as sources of antibiotic resistance genes. In Chapter 3, researchers from UCLA and the Autonomous University of Baja California evaluate the effects of reclaimed water irrigation on antibiotic resistance gene levels in a coastal agricultural region in Mexico. Further, chapter 4 and 5 implement traditional and novel culture- and molecular-based methods to quantify antibiotic resistant bacteria and antibiotic resistance genes to examine the microbial burden hospital sewage discharges to the sewershed and to assess impacts of urbanization by comparing an urbanized watershed to an adjacent natural watershed. Lastly, chapter 6 incorporates these methods into a CRE for graduate students. Ultimately, this dissertation showcases the utility of equitable research methodologies in the field and the classroom.

The dissertation of Marisol Alejandria Cira is approved.

Shaily Mahendra

Sanjay K. Mohanty

Adriane C. Jones

Christine M. Lee

Jennifer A. Jay, Committee Chair

University of California, Los Angeles

2023

Dedication Page

Se la dedico a mi familia en Estados Unidos, mis abuelos en México, y mi tía en el cielo. Gracias por todo su apoyo, amor, y sacrificios. Un agradecimiento especial para mi madre que siempre me alentó y nunca me apuro, a pesar de las dificultades. Los amo.

Table of Contents

List of Figures

List of Tables

Acknowledgements

I would like to thank my committee: Dr. Jennifer Jay, Dr. Shaily Mahendra, Dr. Sanjay Mohanty, Dr. Adriane Jones, and Dr. Christine Lee. Thank you for all your guidance and feedback.

Thank you to all the collaborators at UCLA, the Jet Propulsion Laboratory, the University of Pennsylvania, Heal the Bay, the Autonomous University of Baja California, Mount St. Mary's University, the Ronald Reagan UCLA Medical Center, and LA Sanitation.

Thanks to all the members of the Jay Lab, specially my mentors and incredible team of undergraduate and high school researchers.

Chapter 1 was published in Nature Scientific Reports with the following co-authors: Anisha Bafna, Christine M. Lee, Yuwei Kong, Benjamin Holt, Luke Ginger, Kerry Cawse-Nicholson, Lucy Rieves, and Jennifer A. Jay. Chapter 2 was published in Environmental Science and Pollution Research with the following co-authors: Cristina M. Echeverria-Palencia, Ileana Callejas, Karina Jimenez, Rafael Herrera Jr, Wei-Cheng Hung, Nicolas Colima, Amanda Schmidt, and Jennifer A. Jay. Chapter 3 is in preparation for publication with the following co-authors: Victoria Whitener, Wayne Hung, Max Menczer, Ileana Callejas, Leopoldo Mendoza-Espinosa, and Jennifer A. Jay. Chapter 4 is in preparation for publication with the following co-authors: Pratika Nagpal, Laura Kubiatko, Adriane Jones, and Jennifer A. Jay. Chapter 5 is in preparation for publication with the following co-authors: Pratika Nagpal, Laura Kubiatko, Onja Davidson, Adriane Jones, and Jennifer A. Jay. Chapter 6 is in preparation for publication with the following co-authors: Laila Shaaban, Yuwei Kong, Karina Jimenez, and Jennifer A. Jay.

Vita

EDUCATION

M.S. Civil Engineering, University of California, Los Angeles	2019
B.S. Civil Engineering, University of California, Los Angeles	2018

AWARDS

Achievement Award for Student Welfare, UCLA Samueli	2023
Switzer Fellowship, Robert and Patricia Switzer Foundation	2022 – 2023
Early-Career Fellowship, UCLA Center for Diverse Leadership in Science	2020 – 2023
Eugene V. Cota-Robles Fellowship, UCLA	2019 – 2023
Ford Predoctoral Fellowship, Ford Foundation	2019 – 2022
Competitive Edge Fellowship, UCLA	2019
Outstanding Master of Science Award, UCLA Civil and Environmental Engineering	2019
Graduate Opportunity Fellowship, UCLA	2018 – 2019
Achievement Award for Student Welfare, UCLA Samueli	2018

TEACHING EXPERIENCE

Mount Saint Mary's University	2022 – 2023
Instructor – BIO 003L: Introduction to Microbiology	
UCLA Civil and Environmental Engineering	2022
Teaching Assistant – CEE 154: Chemical Fate and Transport in Aquatic Environments	
Level Playing Field Institute	2016
Engineering Teaching Assistant – Summer Math and Science Honors (SMASH) Academy	

PEER-REVIEWED PUBLICATIONS

Ghavanloughajar, M., Borthakur, A., **Cira, M.**, Jay, J., Stenstrom, M.K., and Mohanty, S.K. (in press) Adding a submerged layer to the stormwater biofilter design could increase antibiotic resistance genes concentration in the effluent. *Journal of Environmental Engineering*.

Cira, M., Bafna, A., Lee, C. M., Kong, Y., Holt, B., Ginger, L., ... & Jay, J. A. (2022). Turbidity and fecal indicator bacteria in recreational marine waters increase following the 2018 Woolsey Fire. *Nature Scientific reports*, *12*(1), 2428.

Cira, M.*, Echeverria-Palencia, C. M.*, Callejas, I., Jimenez, K., Herrera, R., Hung, W. C., ... & Jay, J. A. (2021). Commercially available garden products as important sources of antibiotic resistance genes—a survey. *Environmental Science and Pollution Research*, *28*, 43507-43514.

Hung, W. C., **Hernandez-Cira, M.**, Jimenez, K., Elston, I., & Jay, J. A. (2018). Preliminary assessment of lead concentrations in topsoil of 100 parks in Los Angeles, California. *Applied Geochemistry*, *99*, 13-21.

Echeverria-Palencia, C. M., Thulsiraj, V., Tran, N., Ericksen, C. A., Melendez, I., Sanchez, M. G., ... & Jay, J. A. (2017). Disparate antibiotic resistance gene quantities revealed across 4 major cities in California: a survey in drinking water, air, and soil at 24 public parks. *ACS omega*, *2*(5), 2255-2263.

CONFERENCE PRESENTATIONS

Cira, M.*, Bafna, A., Lee, C. M., Kong, Y., Holt, B., Ginger, L., ... & Jay, J. A. (2022). "Turbidity and fecal indicator bacteria in recreational marine waters increase following the 2018 Woolsey Fire". (oral) Ocean Sciences Meeting, 27 February – 4 March 2022, Remote.

Whitener, V., **Cira, M.***, Hung, W., Callejas, I., Menczer, M., Mendoza Espinoza, L., Jay, J. A. "Reclaimed Water as a Source of Antibiotic Resistance in Agricultural Soil, Northern Mexico." (poster) Ford Conference, 9 – 10 October 2020, Remote.

Cira, M.*, Callejas, I., Echeverria-Palencia, C., Jay, J. A. "Antibiotic Resistance Gene Quantities in Commercially Available Garden Products." (poster) Ford Conference, 3 – 5 October 2019, San Juan, PR.

Cira, M.*, Callejas, I., Echeverria-Palencia, C., Jay, J. A. "Antibiotic Resistance Gene Quantities in Commercially Available Garden Products." (poster) American Chemical Society National Meeting, 25 – 29 August 2019, San Diego, CA.

Chapter 1: Turbidity and fecal indicator bacteria in recreational marine waters increase following the 2018 Woolsey Fire

1. Introduction

In the western United States, wildfire activity has increased since the late 20th century[1,2] in frequency, duration, and season length[3,4]. Wildfire activity is projected to surge in the second half of the 21st century in response to future climate changes[2]. In Southern California, where wildfire activity is driven by precipitation and aridity[5-7], and wildfire growth is driven by Santa Ana winds[8-10], a projected reduction in precipitation[11], accretion in aridity[12], and seasonal shift in Santa Ana wind events[13] are expected to exacerbate wildfire conditions.

As wildfire activity increases, soil hydrology and, by extension, water quality will increasingly become affected. More specifically, wildfire accelerates soil erosion rates by removing vegetation and litter cover, intensifying and translocating soil hydrophobicity, and inducing soil sealing[14-20]. During and immediately after a wildfire, soil erosion begins as dry ravel. At the onset of rainfall, runoff is unable to infiltrate burned soils, resulting in soil erosion via rill networks and debris flows[21]. Ultimately, these processes produce heightened runoff and sediment yields[16,17,22] that mobilize and transport contaminants to downstream ecosystems.

Wildfires have been shown to alter the physical and chemical water quality of receiving streams. For example, elevated turbidity levels in stream waters post-wildfire are well documented[23-31]. However, wildfire impacts on microbial water quality remain elusive[32]. Most notably, water quality responses to wildfire in receiving oceans have been overlooked[33]. Additionally, studies have been largely limited by sparse sampling, hindering broad spatial and temporal observations[34].

Satellite remote sensing can be used to help resolve gaps in spatial and temporal sampling of water quality to help evaluate coastal conditions following wildfire events. Water quality

variables, such as turbidity, can be derived using optical data acquired through remote sensing platforms including Landsat and Sentinel-2. A semi-empirical algorithm for turbidity[35] has been applied and evaluated in water bodies across the world of varying optical complexities[36,37]. Good agreement between satellite-derived and *in situ* turbidity measurements indicate that satellite imagery can be used as a complement to on-going monitoring programs that include collection and analysis of water samples, with the potential to expand spatial and temporal coverage across regions and decades. This study focuses on the remote sensing data processing and interpretation, and relies on previous validation studies[35-37]. Nonetheless, this study did show consistency between satellite-derived turbidity and coincident *in situ* light transmissivity measurements (Supplementary Text S1 and Supplementary Fig. A1-1).

The goal of this study was to investigate spatial and temporal shifts in coastal water quality associated with the 2018 Woolsey Fire. We analyze long-term and high-frequency turbidity and fecal indicator bacteria (FIB) datasets to examine water quality before, during, and after the Woolsey Fire. We hypothesize that increases in monthly mean sediment and FIB levels will be associated with beaches draining the fire burn area, compared with beaches adjacent to or outside the fire burn area.

2. Data and Methods

2.1 Study Area

The Santa Monica Mountains are located in the Southwestern United States. The Santa Monica Mountains are part of the east-west trending Transverse Ranges of Southern California. The dominant vegetation communities, chaparral and coastal sage scrub, are adapted to the Mediterranean climate conditions of wet winters, dry summers, and frequent fires[38].

Despite temperatures in the mid-70°Fs, the Santa Monica Mountains faced extreme fire weather conditions on November 8, 2018. At 10 am local time, relative humidity dropped to 5%

and wind gusts soared to 35 mph. At 2 pm, a powerline failure near the Santa Susana Field Lab ignited the Woolsey Fire[39], and the Santa Ana winds, Southern California foehn winds, pushed the fire south into the Santa Monica Mountains. The Woolsey Fire burned nearly 100,000 acres and destroyed nearly 2,000 structures in the Ventura and Los Angeles counties before being fully contained on November 21, 2018[40]. Post-fire, the California Watershed Emergency Response Team used hydrological models to assess flood and debris flow risks, and their watershed modeling approximated a 2 to 5 fold increase in post-fire flows[40].

To study the impact of increased flow and sediment delivery to the coast, we divided our study area into three regions using the Woolsey Fire and watershed boundaries (Fig. 1-1). The "inside" region received discharges from burned watersheds. The "adjacent" region, immediately to the west and east of the Woolsey Fire, received runoff primarily from unburned watersheds that were adjacent to burned watersheds. The "outside" region, to the east of the Woolsey Fire, received flows from unburned watersheds. Unlike the adjacent region, we did not define an outside region to the west of the Woolsey Fire due to a difference in land use and land cover. Namely, this region received runoff primarily from agriculture and salt marsh, while the rest of our study area received runoff primarily from chaparral and coastal sage scrub[38]. The coordinates of these regions can be found in Supplementary Table A1-1.

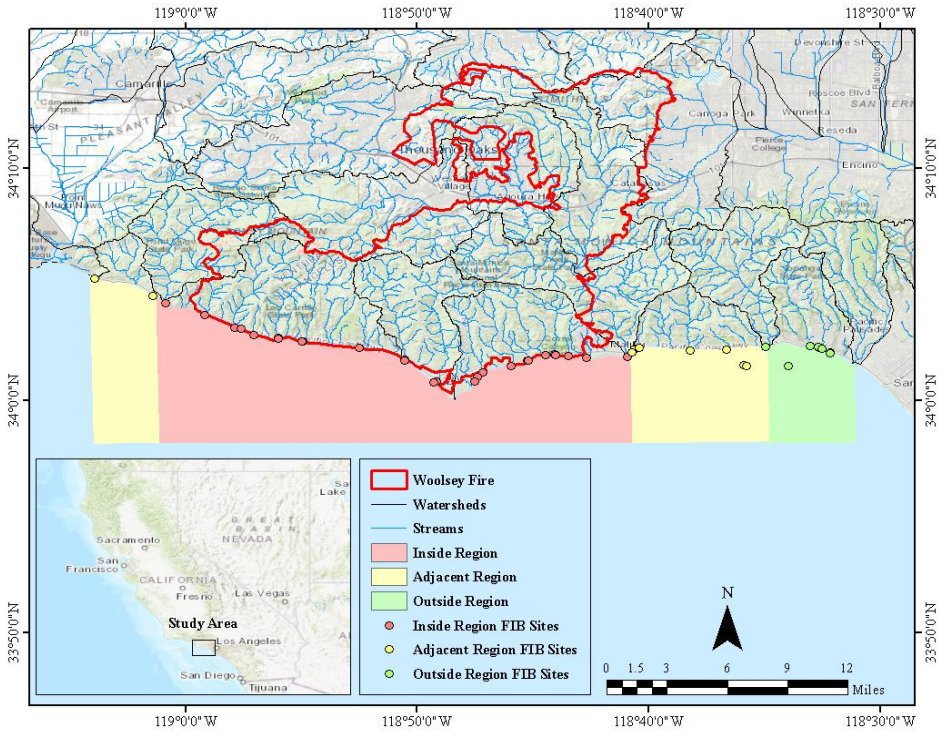

Figure 1-1. The study area map shows the Woolsey Fire (red lines), watersheds (black lines), and streams (blue lines) in the Santa Monica Mountains coastal range. The map also indicates the location of the 26 FIB sites (red circles) in the inside region (red), 10 FIB sites (yellow circles) in the adjacent region (yellow), and 8 FIB sites (green circles) in the outside region (green).

2.2 Sentinel-2 Image Acquisition and Processing

We used the Sentinel-2 imagery Level-1C product T11SLT tile available to users via EarthExplorer (https://earthexplorer.usgs.gov/). We obtained 48 cloud-free Sentinel-2 images spanning from August 2016 to April 2020. The European Space Agency's Copernicus Sentinel-2 mission utilizes a constellation of two identical satellites, in the same orbit 180° apart, to provide a high revisit time. Sentinel-2A was launched on June 23, 2015, and Sentinel-2B was launched on March 7, 2017. Sentinel-2 images land and coastal areas with a wide swath high-resolution multispectral imager. Sentinel-2 revisit time, spatial resolution, swath width, and spectral bands are listed in Supplementary Table A1-2.

Sentinel-2 imagery, for the study area and each region of the study area, were atmospherically corrected and processed in ACOLITE, an open-source software downloadable

from GitHub (https://github.com/acolite/acolite)[36,37]. The image outputs were visualized in ArcGIS.

ACOLITE uses a dark spectrum fitting algorithm and an exponential extrapolation algorithm to atmospherically correct images[41,42]. ACOLITE derives turbidity, in Formazine Nephelometric Units (FNU), from water surface reflectance as shown in equation (1):

$$T = \frac{A\,\rho_w}{1-\frac{\rho_w}{C}} \quad (1)$$

where ρ_w is the water-leaving radiance reflectance, and A and C are band-specific calibration coefficients. This study uses the Dogliotti et al. (2015) algorithm in ACOLITE, which uses the calibration coefficients corresponding to the red band (645 nm) when ρ_w(645 nm) < 0.05 and the near-infrared band (859 nm) when ρ_w (645 nm) > 0.07. When 0.05 < ρ_w (645 nm) < 0.07, the Dogliotti et al. (2015) algorithm uses a linear weighting function to calculate turbidity.

Assessing the detection limit of the Dogliotti et al. (2015) algorithm was not within the scope of this study given that it has been validated in optically diverse waters[36,37]. However, false positives were of concern due to clouds, fog, and wind. Therefore, we screened manually for clouds, utilized a cloud mask, and flagged for outliers to minimize any false positives.

2.3 Turbidity Threshold and Plume Surface Area Calculations

We developed an automated plume detection algorithm in Python to characterize an increase in turbidity resulting from the wildfire. To determine the turbidity threshold of our plume detection algorithm, we utilized the November 30, 2018, image of the inside region, which captured discharges from burned watersheds after a rain event. Four 2 km squares were utilized as the regions of interest around discharge points. For each square, 1,000 unique points were randomly selected. For each point, we extracted the mean turbidity from a 5x5 pixel window. The minimum, lower quartile, mean, median, upper quartile, and maximum values were calculated for

all points in each square. The lower quartile, which was 4.6 FNU, was selected as the turbidity threshold. While not shown, we evaluated the probability density functions within plume and non-plume regions and verified that the threshold of 4.6 FNU was consistently higher than background levels (2.3 FNU, considered for 5 scenes), providing confidence that 4.6 FNU was sufficient to minimize any false positives in plume detection.

To compute the plume surface area from an image, we assigned a binary value to each pixel. If a pixel had a turbidity value above the turbidity threshold, then the pixel was assigned a 1, otherwise, the pixel was assigned a 0. The pixels assigned a 1 were counted and converted to surface area. We performed the turbidity threshold and plume surface area calculations in Python. We calculated plume surface area monthly means by region and date range in RStudio.

2.4 Fecal Indicator Bacteria Data

FIB originate from the gastrointestinal tracts of humans and other warm-blooded animals and are therefore used as proxies for fecal contamination. Although they are not typically harmful themselves, FIB are used as pathogen indicators since fecal matter may contain a myriad of disease-causing organisms[43]. Studies have demonstrated that rainstorms increase FIB levels in seawater[44-46] and that seawater exposure after a rainstorm increases incidence rates of swimming-associated illnesses[47]. Therefore, the California Department of Public Health advises beachgoers to stay out of the water for a minimum of 3 days after a storm event greater than 0.1 inches. Additionally, the State Water Resources Control Board (SWRCB) has set the standards for recreational marine waters at 10,000 colony-forming units (CFU)/100 mL for total coliform (TC) and 104 CFU/100 mL for *Enterococcus* (ENT)[48].

To assess the effects of wildfire on bacterial water quality, we accessed FIB data from July 2008 to June 2020 for the Los Angeles County and Ventura County coast from SWRCB

(https://www.waterboards.ca.gov/water_issues/programs/beaches/search_beach_mon.html). The FIB data included TC and ENT measurements in most probable number (MPN)/100 mL. For this study area, measurements were taken at 26 sites in the inside region (n = 8,978), 10 sites in the adjacent region (n = 2,758), and 8 sites in the outside region (n = 3,279) (Fig. 1-1). For the sites in Los Angeles County, measurements were taken at a minimum of once a week throughout the year. However, for the sites in Ventura County, measurements were only taken at a minimum of once a week from April to October. In RStudio, monthly means and standard errors were calculated for TC and ENT by region, date range, and weather condition.

2.5 Precipitation Data

We acquired daily precipitation data from the NOAA National Climatic Data Center (https://www.ncdc.noaa.gov), for the Los Angeles International Airport, from June 2008 to June 2020. We used RStudio to calculate 3-day and monthly precipitation totals. The 3-day precipitation totals were used to categorize our FIB data by weather condition. FIB data with a 3-day precipitation total greater than 0.1 inches was categorized as wet weather data, otherwise, it was categorized as dry weather data[49]. We also computed the means and standard errors of monthly precipitation totals by date range, where possible. Date ranges were ordered by rainfall season, which runs from July 1 through June 30. The 2016-2020 and 2008-2020 monthly precipitation totals are shown in Supplementary Fig. A1-2.

2.6 Statistics

We used histograms and quantile-quantile (Q-Q) plots to test whether the FIB data were normal. The data were found to be non-normal. Therefore, two-sided Wilcoxon rank-sum tests with continuity correction were used to compare 2008-2018 to 2018-2019 by month, region, and weather condition.

We also performed Pearson correlations and linear regressions for all variables. A multiple linear regression using 3-day precipitation totals, region, and fire year (2018-2019) and non-fire years (2016-2017, 2017-2018, and 2019-2020) to predict plume surface area was further examined. Residual diagnostics were evaluated to check the validity of the assumptions made when fitting the multiple linear regression model. Linear regressions of plume surface area and 3-day precipitation totals were visualized by region and fire year and non-fire years. A sensitivity analysis was also performed by removing data points with 3-day precipitation totals equal to 0 to test the influence of these data points. All statistical computations were performed in RStudio.

2.7 Systematic Literature Review

We conducted a systematic review on March 12, 2021, using Web of Science. The following three searches were performed: (1) "wildfire" and "turbidity" (41 results, 11 retained), (2) "wildfire" and "total coliforms OR fecal coliforms OR Escherichia coli OR Enterococcus" (13 results, 1 retained), (3) "wildfire," "water quality," and "remote sensing" (9 results, 1 retained). Studies that did not directly investigate the impacts of wildfire in the Western United States were removed. Retained studies are summarized in Supplementary Table A1-3. The current study is novel in that it is the first to investigate the impacts of wildfire on ocean turbidity and FIB. In addition, it is the second to apply remote sensing and *in situ* techniques to study the effects of wildfire on coastal water quality.

3. Results

3.1 Remote Sensing Analysis: Turbidity and Plume Surface Area

The remote sensing analysis revealed notable changes in physical water quality in response to the 2018 Woolsey Fire. Imagery of the study area from 2018 to 2019 (Fig. 1-2) indicated an increase in plume intensity and extent in post-fire images (Fig. 1-2i-q), in comparison to pre-fire images (Fig. 1-2a-g). Generally, more turbidity values in the 4.6 to greater than 6.5 FNU range

were observed post-fire. More specifically, the surface area of plumes exceeding the 4.6 FNU threshold shifted from 9 to 27 km^2 pre-fire to 8 to 200 km^2 post-fire. These changes in turbidity were mostly attributed to post-fire rain events (Fig. 1-2i, m).

Imagery of similar rain events from 2016 to 2019 further illustrated that the turbidity from post-fire rain events was anomalous (Fig. 1-3d, e), compared to pre-fire rain events (Fig. 1-3a-c). For example, a previous rain event of 2.94 inches (Fig. 1-3c) produced a smaller plume than a post-fire rain event of 1.49 inches (Fig. 1-3d). Moreover, while images of previous rain events indicated that regions closest to urban areas were normally more impacted, images of post-fire rain events indicated that the region below the Woolsey Fire was more impacted.

Plume surface area monthly means from 2016 to 2020 by region further confirmed that the 2018-2019 plume extent was atypical, particularly for the inside region, which received surface runoff from burned watersheds (Fig. 1-4). Prior to the Woolsey Fire, the 2018-2019 plume surface area monthly means were similar to those observed in other years for all regions. However, in November, the 2018-2019 plume surface area monthly average increased to 64, 18, and 22 km^2 in the inside region, adjacent region, and outside region, respectively. In January, the 2018-2019 plume surface area monthly mean also increased in all regions, however, only the inside region's 45 km^2 plume differed from those observed in other years.

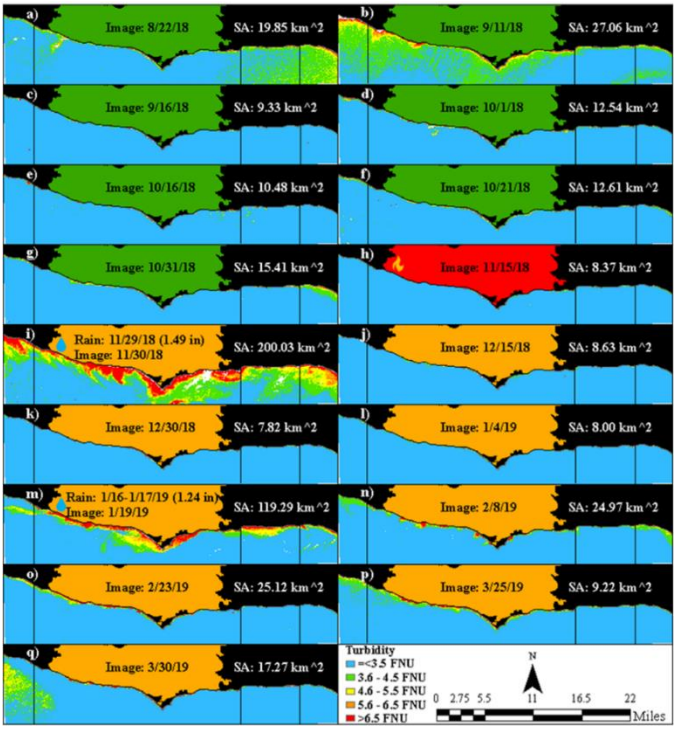

Figure 1-2. Imagery of the study area from 2018-2019, where available, with turbidity and plume surface area (SA). (**a**)-(**g**) Pre-fire images, (**h**) active Woolsey Fire (November 8-21, 2018) image, (**i**)-(**q**) post-fire images, and (**i**),(**m**) images within three days of a rain event. Vertical black lines correspond to region boundaries in Figure 1-1. Post-fire rain events produced up to 200 km^2 plumes (exceeding the 4.6 FNU threshold).

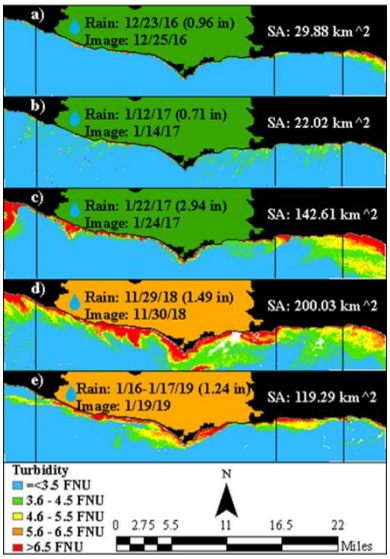

Figure 1-3. Imagery within three days of a rain event greater than 0.7 inches, where possible, with turbidity and plume surface area (SA). (**a**)-(**c**) Pre-fire rain events and (**d**),(**e**) post-fire rain events. There were no cloud-free images within three days of a rain event greater than 0.7 inches in 2020. Vertical black lines correspond to region boundaries in Figure 1-1. Rain events from 2016-2019 show post-fire rain events produced plumes (exceeding the 4.6 FNU threshold) of greater extent and intensity.

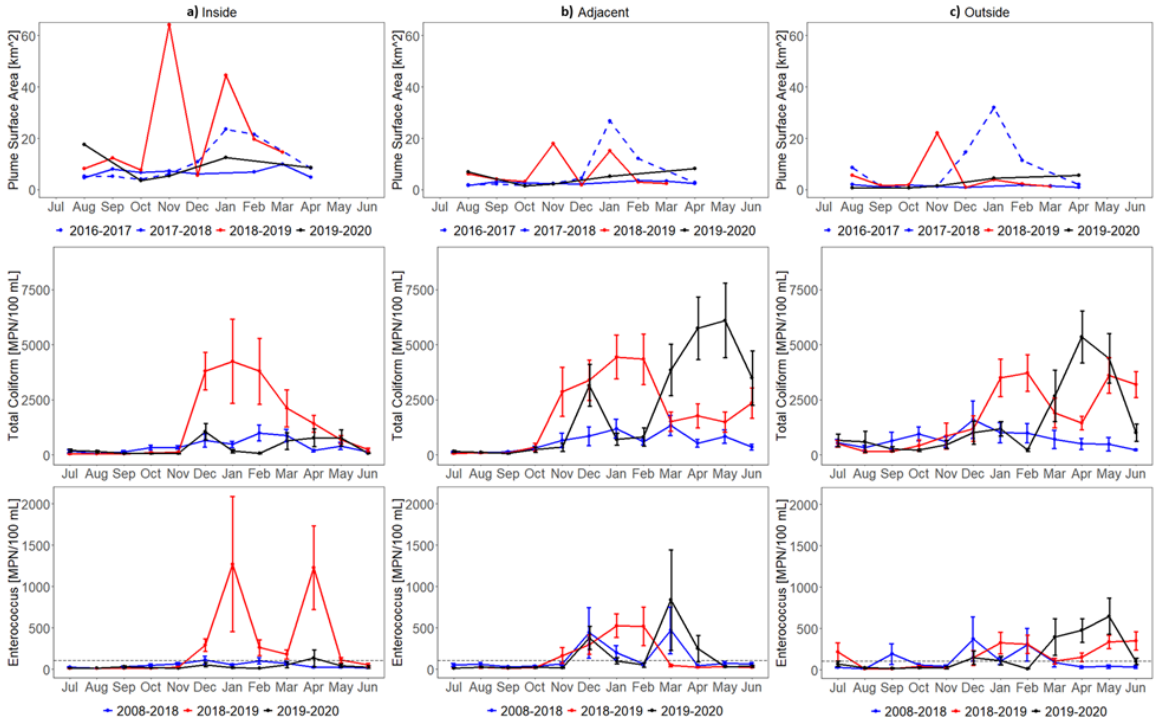

Figure 1-4. Plume surface area (exceeding the 4.6 FNU threshold, 2016-20020) and FIB (TC and ENT, 2008-2020) monthly means and standard errors for the (**a**) inside, (**b**) adjacent, and (**c**) outside region. The SWRCB standards are indicated with a black dotted line. Please see Figure 1-1 for region locations. Plume surface area, TC, and ENT increase in 2018-2019 following the Woolsey Fire (November 8-21, 2018), particularly in the inside region.

3.2 *In Situ* Analysis: Fecal Indicator Bacteria

The *in situ* analysis also showed microbial water quality responses to the wildfire. FIB monthly means from 2008 to 2020 by region showed marked increases post-fire, primarily in the inside region, which drained the burned area (Fig. 1-4). Before the Woolsey Fire, the 2018-2019 TC monthly means were comparable to those observed in other years for all regions. However, in December, the 2018-2019 TC monthly average in the inside region increased and remained elevated through March. Compared to 2008-2018 TC monthly means in the inside region, these elevations were statistically significant in December ($W = 43$, $Z = -3.16$, $p = 0.002$, $r = 0.47$) and statistically highly significant in January ($W = 79$, $Z = -3.90$, $p < 0.001$, $r = 0.47$), February ($W = 62$, $Z = -4.06$, $p < 0.001$, $r = 0.51$), and March ($W = 148$, $Z = -3.92$, $p < 0.001$, $r = 0.46$) (Supplementary Table A1-4). The 2018-2019 TC monthly average was also discernable between

other years in the adjacent region in November (W = 221, Z = -2.92, p = 0.003, r = 0.38), January (W = 274, Z = -4.19, p < 0.001, r = 0.48), and February (W = 203, Z = -4.04, p < 0.001, r = 0.49) and in the outside region in January (W = 251, Z = -4.22, p < 0.001, r = 0.49), February (W = 157, Z = -4.73, p < 0.001, r = 0.57), and June (W = 113, Z = -6.04, p <0.001, r = 0.67). ENT displayed similar behavior as TC. Prior to the Woolsey Fire, the 2018-2019 ENT monthly means were similar to those observed in other years in all three regions. In December, the 2018-2019 ENT monthly mean average in the inside region also increased and remained elevated through May. In comparison to 2008-2018 ENT monthly means in the inside region, these elevations were statistically significant in December (W = 57, Z = -2.75, p = 0.006, r = 0.40), January (W = 143, Z = -2.84, p = 0.004,r = 0.34), and February (W = 117, Z = -3.06, p = 0.002,r = 0.39) and statistically highly significant in March (W = 174, Z = -3.56, p < 0.001, r = 0.42), April (W = 164, Z = -5.94, p < 0.001, r = 0.58), and May (W = 161, Z = -4.94, p < 0.001, r = 0.51). The 2018-2019 ENT monthly means were also distinguishably different from other years in the adjacent region in January (W = 358, Z = -3.31, p <0.001, r = 0.38) and February (W = 294, Z = -2.88, p = 0.004, r = 0.35) and in the outside region in January (W = 402, Z = -2.55, p = 0.011, r = 0.30) and June (W = 259, Z = -4.57, p < 0.001, r = 0.51). While the January and February observations may be partly in response to unusual monthly precipitation totals (Supplementary Fig. A1-2), results do indicate that they are also in response to the wildfire. Namely, the 2018-2019 ENT monthly average in January in the inside region (1,270 MPN/100 mL) was substantially higher than that of the adjacent region (526 MPN/100 mL) and outside region (326 MPN/100 mL). It is also worth noting that the 2019-2020 TC and ENT monthly means in the inside region did not respond to abnormal precipitation totals in December, March, and April as seen in the adjacent and outside regions.

Examining FIB by weather conditions demonstrated that the shifts in 2018-2019 TC and ENT in the inside region occurred during both wet and dry weather (Supplementary Fig. A1-3). More precisely, the wet weather 2018-2019 TC monthly means were distinguishably higher than those observed in other years in the inside region in January (W = 3, Z = -2.22, p = 0.026, r = 0.55) and in the adjacent region in November (W = 9, Z = -2.10, p = 0.035, r = 0.53) and February (W = 15, Z = -2.22, p = 0.026, r = 0.52) (Fig. 1-5, Supplementary Table A1-5). Figure 1-5 and Supplementary Table A1-5 also illustrated that the wet weather 2018-2019 ENT monthly averages were distinctly different in the adjacent region in January (W = 35, Z = -2.14, p = 0.032, r = 0.44) and February (W = 17, Z = -2.05, p = 0.041, r = 0.48). While there were other highly visible increases in wet weather 2018-2019 TC and ENT monthly means, they were not statistically significant increases (Supplementary Table A1-5).

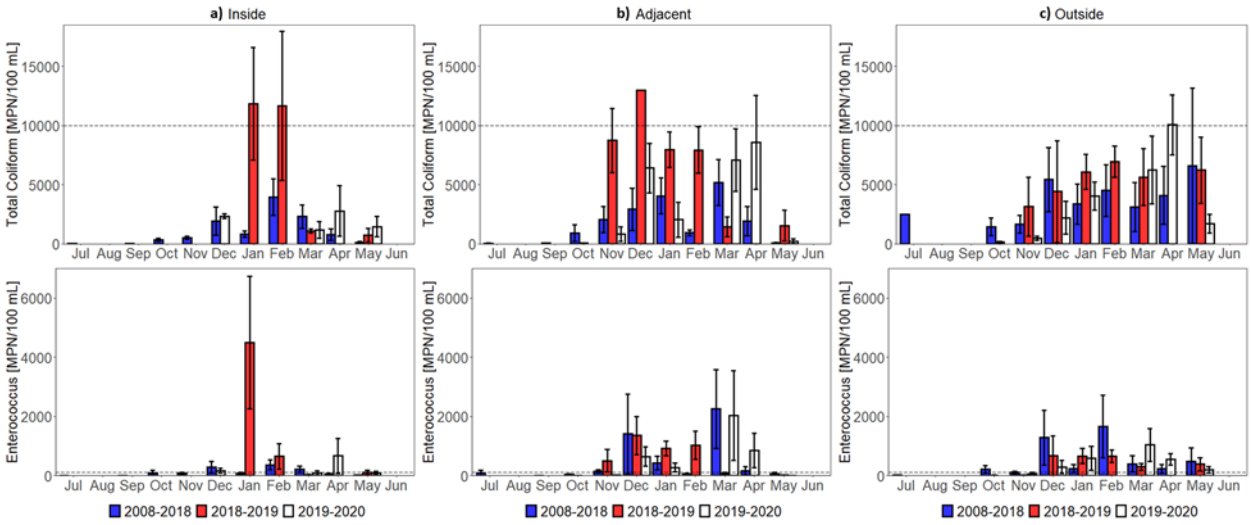

Figure 1-5. Wet weather FIB (2008-2020) monthly means and standard errors for the (**a**) inside, (**b**) adjacent, and (**c**) outside region. The SWRCB standards are indicated with a black dotted line. Note that the y-axis was changed. Statistics are shown in Supplementary Table A1-5. Wet weather (3-day precipitation totals greater than 0.1 inches) TC and ENT increase in 2018-2019 following the Woolsey Fire (November 8-21, 2018), more substantially in the inside region.

Dry weather 2018-2019 FIB monthly means were more aligned with 2018-2019 FIB monthly means. For instance, the dry weather 2018-2019 TC monthly averages were notably greater than those observed in other years in the inside region in December ($W = 25$, $Z = -3.36$, $p < 0.001$, $r = 0.55$), January ($W = 41$, $Z = -3.42$, $p < 0.001$, $r = 0.48$), February ($W = 20$, $Z = -4.18$, $p < 0.001$, $r = 0.58$), March ($W = 69$, $Z = -4.28$, $p < 0.001$, $r = 0.55$), and April ($W = 126$, $Z = -5.96$, $p < 0.001$, $r = 0.60$), in the adjacent region in November ($W = 105$, $Z = -2.91$, $p = 0.004$, $r = 0.44$) and January ($W = 109$, $Z = -3.31$, $p < 0.001$, $r = 0.45$), and in the outside region in December ($W = 100$, $Z = -3.18$, $p = 0.001$, $r = 0.48$), February ($W = 65$, $Z = -3.93$, $p < 0.001$, $r = 0.55$), and June ($W = 113$, $Z = -6.04$, $p < 0.001$, $r = 0.67$) (Fig. 1-6, Supplementary Table A1-6). Furthermore, the dry weather 2018-2019 ENT monthly means were statistically different in the inside region in December ($W = 37$, $Z = -2.90$, $p = 0.004$, $r = 0.48$), February ($W = 67$, $Z = -3.01$, $p = 0.003$, $r = 0.42$), March ($W = 76$, $Z = -4.16$, $p < 0.001$, $r = 0.53$), April ($W = 138$, $Z = -5.92$, $p < 0.001$, $r = 0.60$), and May ($W = 134$, $Z = -4.44$, $p < 0.001$, $r = 0.48$) and in the outside region in February ($W = 109$, $Z = -3.25$, $p = 0.001$, effective size $r = 0.46$), March ($W = 200$, $Z = -3.07$, $p = 0.002$, $r = 0.40$), and June ($W = 259$, $Z = -4.57$, $p < 0.001$, $r = 0.51$). Dry weather 2018-2019 FIB monthly averages also affirmed that the January and February observations from 2018-2019 FIB monthly averages were also in response to the wildfire since they were also derived during dry weather conditions.

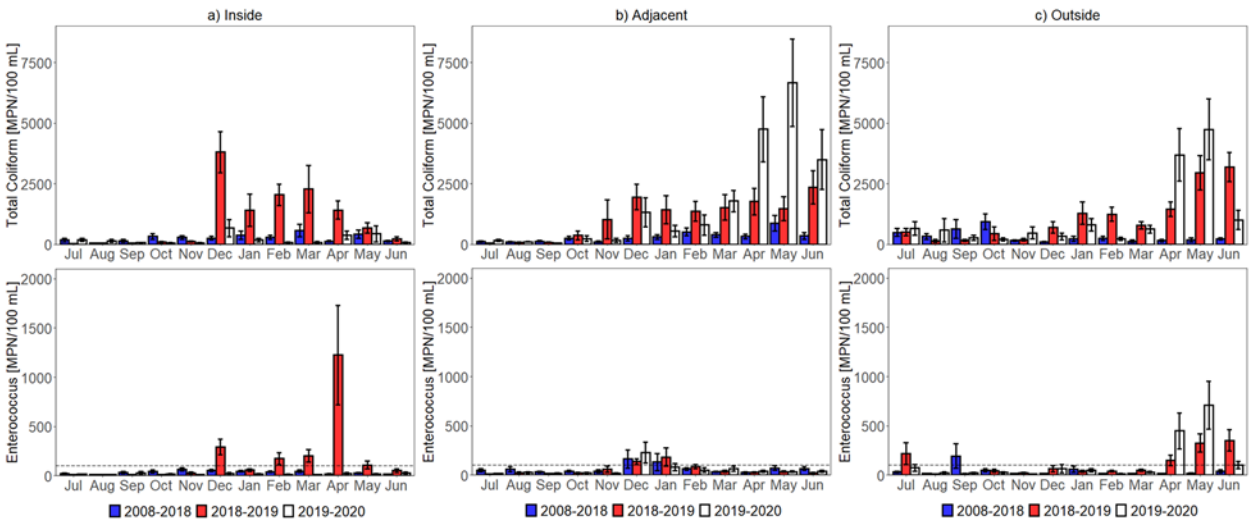

Figure 1-6. Dry weather FIB (2008-2020) monthly means and standard errors for the (**a**) inside, (**b**) adjacent, and (**c**) outside region. The SWRCB standards are indicated with a black dotted line. Statistics shown in Supplementary Table A1-6. Dry weather (3-day precipitation totals not greater than 0.1 inches) TC and ENT increase in 2018-2019 following the Woolsey Fire (November 8-21, 2018), more notably in the inside region.

3.3 Statistical Analysis

Moderate Pearson correlations were found between TC and ENT ($r = 0.545$, $p < 0.001$), plume surface area and TC ($r = 0.547$, $p < 0.001$), and plume surface area and 3-day precipitation totals ($r = 0.634$, $p < 0.001$) (Supplementary Table A1-7). The multiple linear regression used to predict plume surface area based on 3-day precipitation totals, region, and fire year (2018-2019) and non-fire years (2016-2017, 2017-2018, and 2019-2020) was found to be significant ($F(4, 285) = 73.82$, $p < 0.001$, $R^2 = 0.509$). Examination of individual predictors indicated that 3-day precipitation totals ($t = 15.78$, $p < 0.001$), the inside region ($t = 4.93$, $p < 0.001$), and the fire year ($t = 4.27$, $p < 0.001$) were significant predictors in the model. Residual diagnostics showed that the linearity and normality assumptions made when fitting the multiple linear regression model were valid. In the residuals versus fitted values plot (Supplementary Fig. A1-4a), residuals were close to and spread along the 0 line with mild departures. In the residuals Q-Q plot (Supplementary Fig. A1-4b), observations lied along the 45° line with few exceptions. Additionally, all residual normality tests were statistically highly significant (p-value < 0.001) (Supplementary Table A1-

8). Linear regressions of plume surface area and 3-day precipitation totals for the fire year and non-fire years by region confirmed that 2018-2019 post-fire rainstorms produced plumes with greater surface area that were more substantial in the inside region (Fig. 1-7), as suggested by the satellite imagery. Further, differences between fire year and non-fire years were most notable in the inside region. While the sensitivity analysis (Supplementary Fig. A1-5) greatly reduced the amount of data, regressions still followed similar trends shown in Fig. 1-7, indicating that 3-day precipitation totals equal to 0 had little influence on the resulting fit.

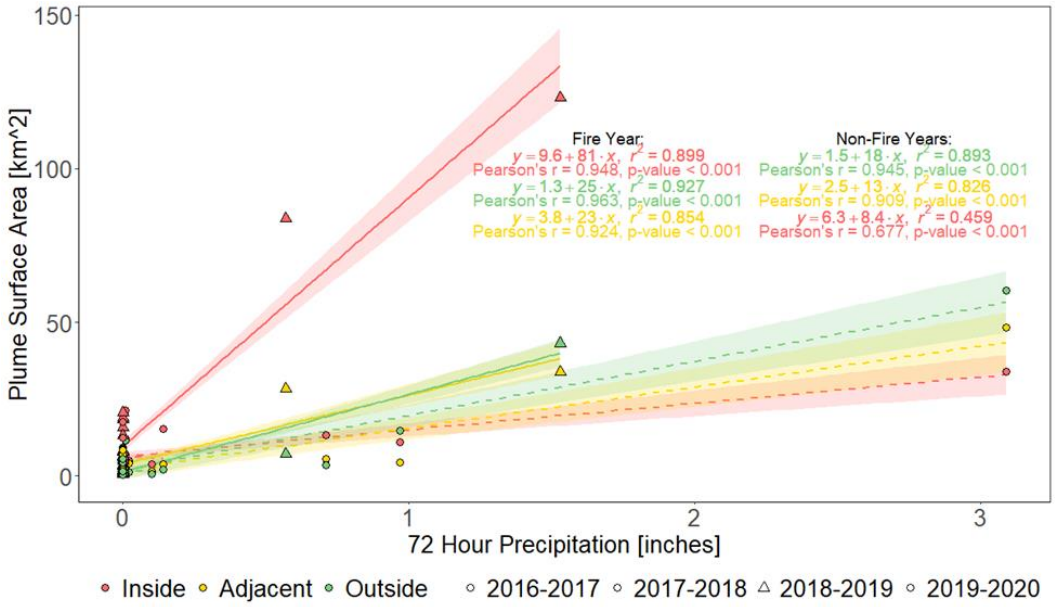

Figure 1-7. Linear regressions of plume surface area and 3-day precipitation totals for non-fire years (circles, dashed lines) and fire year (triangles, solid lines) in the inside region (red), adjacent region (yellow), and outside region (green) with their respective 95% confidence interval (shaded). Three-day precipitation totals produced plumes (exceeding the 4.6 FNU threshold) with greater surface area during 2018-2019 (fire year), more notably in the inside region

4. Discussion

Results indicate that the 2018 Woolsey Fire impacted the physical water quality. Imagery of the study area from 2018 to 2019 and of similar rain events from 2016 to 2019 illustrated shifts in plume intensity and extent following post-fire rain events. Plume surface area monthly means from 2016 to 2020 showed that following the wildfire beaches receiving discharges from burned

watersheds experienced increases in 2018-2019 plumes in November and January that were up 10 and 9 times greater than 2016-2017 and 2017-2018 plumes, respectively. A multiple linear regression predicting plume surface area revealed that 3-day precipitation totals, the inside region, and the fire year were significant predictors. Further, linear regressions of plume surface area and 3-day precipitation totals by region and fire year and non-fire years demonstrated that post-fire 2018-2019 3-day precipitation totals produced larger plumes, particularly in beaches draining the burn area.

While the effects of wildfire on turbidity in ocean ecosystems have not been previously documented, investigations on the effects of wildfire on turbidity in stream ecosystems have associated heightened turbidity levels to burn severity[29] and precipitation events[23,25-28,30,31]. In addition, when compared to plumes from urban stormwater runoff in the Santa Monica Bay[50,51], plumes from burned area surface runoff were greater. This suggests that post-fire runoff is a considerable source of sediment and other debris into ocean ecosystems. These results also suggest that as wildfire activity increases, the Santa Monica Bay (a wildland-urban interface) will experience the cumulative impacts of both wildfire and urbanization. Given that the Transverse Range rivers, which include the Santa Monica Mountain creeks, are responsible for over 75% of the total sediment flux in Southern California[52], increased wildfire disturbance in this area has the potential to substantially increase sediment delivery to ocean ecosystems.

Results also suggest that the Woolsey Fire degraded the microbial water quality of recreational beaches, and that proximity to wildfire burn areas also plays a role. FIB monthly means from 2016 to 2020 showed that following the Woolsey Fire beaches draining the burned area experienced elevations in 2018-2019 TC from December to March and ENT from December to May that were 9 and 53 times greater than 2008-2018 monthly means, respectively. Results here

indicate that post-wildfire runoff and sediments may carry harmful pollutants that may affect beachgoer health.

It is worth noting that FIB may also be delivered to beaches via debris flows. Disastrous debris flows can damage sanitary sewers and septic tanks, contaminating downstream ecosystems with fecal matter. Local agencies may also clear contaminated sediments in public rights-of-way and creek channels and deposit them onto beaches[53]. Fires, floods, and debris flows also have the potential of damaging wastewater treatment plants or deeming them inoperable, which may result in untreated raw sewage being discharged into coastal waters.

Increased sediments may also promote the persistence of FIB. It has been shown that sediments provide nutrients and protection from ultraviolet radiation, temperature fluctuations, and predation[54-59]. However, it is unclear whether burned sediments can affect the survival of FIB in marine waters[32].

Greater abundance of TC post-wildfire may be due to their widespread occurrence in nature; they are present in plants, soils, and feces from humans and other warm-blooded animals[60]. Greater persistence of ENT post-wildfire may be due to their distinguished ability to survive in salt water[61]. Since ENT are more human-specific[60] and are more highly associated with gastrointestinal illnesses in marine waters[43,62-65], dramatic increases in ENT, above the SWRCB standards, are of particular concern. While we did not analyze fecal coliform and *Escherichia coli* (*E.coli*), due to a lack of data, Barron (2020) found that post-fire (2018-2020) mean *E.coli* levels were 10 times greater than pre-fire (2015-2018) mean *E.coli* levels in the surface waters of the North Santa Monica Bay Coastal Watersheds. However, Valenca et al. (2020) reported that the growth and persistence of *E.coli* in surface water in the presence of Woolsey Fire residues was less than that in the presence of unburned soil particles. Therefore, future studies should study

differences in FIB behavior in different environmental compartments. Future studies could also utilize watershed modeling to help elucidate processes that contribute to observed increases in plumes and FIB.

While FIB are known to increase following rainstorms[44-46], increases following post-fire rainstorms were greater than what has been observed in the past for TC and ENT during comparable rain events. The beaches draining the burned area exhibited wet weather 2018-2019 TC and ENT monthly means that were up to 14 and 54 times greater than 2008-2018 monthly means, respectively. Further, while Arnold et al. (2017) reported wet weather ENT means of approximately up to 300 CFU/100 mL in beaches receiving urban discharges, the current study found wet weather ENT monthly means of up to 4,496 MPN/100 mL in beaches receiving runoff and sediment discharges from burned areas.

Due to slow watershed recovery, post-fire sediment yields can remain elevated for three months to ten years[19]. Accordingly, studies have reported short-term[23,24,26,28,30] and long-term[25,27,29,31] turbidity increases in streams post-fire. The current study did observe short-term increases in turbidity, within three months of the Woolsey Fire. Further, while the TC and ENT responses were more persistent, they also returned to background levels within six months of the Woolsey Fire. Since the present study only analyzed a year and a half of post-fire data, future investigations could continue to monitor for any long-term impacts as watersheds recover.

To our knowledge, only one other study has employed remote sensing and *in situ* techniques to study the effects of wildfire on coastal water quality[67]. This study illustrates how using both satellite and *in situ* measurements results in a more complete assessment of coastal water quality. For example, with satellite and *in situ* measurements we were able to evaluate both the physical and microbial water quality. Further, one of the limitations of this study was that we

could not obtain *in situ* FIB measurements for the Ventura County coast from November to March. However, by utilizing satellite turbidity measurements of the Ventura County coast, we were able to gain some indication of the water quality. Similarly, previous studies examining the impacts of wildfire in aquatic ecosystems listed sparse sampling as a limitation that hindered meaningful spatial observations; however, this study's use of satellite imagery did allow for a supraregional investigation.

This novel approach can be implemented to assess coastal water quality after a major fire event. Results could guide monitoring and public health agencies in sampling and treatment efforts, as well as beach closures. Additionally, researchers could apply this methodology to further investigate the effects of wildfire on coastal water quality. For example, future studies can evaluate oceanic responses to smaller fires or fires that occur more upslope. Future research can also study the effects of post-fire increases in stream nutrients[68-70] on chlorophyll-a, colored dissolved organic matter, and harmful algal blooms.

There are various remote sensing techniques for detecting plumes. Coastal plumes exhibit differences in turbidity, color, temperature, and salinity from ambient background water that can be observed via multispectral and hyperspectral imagers, thermal infrared (TIR) radiometers, microwave radiometers, and Synthetic Aperture Radar (SAR)[71]. In the Southern California Bight, ocean color imagery from SeaWiFS[72], MODIS[73-75], and Landsat[76] have been utilized and combined with radiometers[77,78] and SAR[50] to delineate and track plumes.

There does exist some caveats to using satellite imagery. For instance, Sentinel-2 is affected by cloud cover, fog, and wind, and is limited by repeat frequency and time of day of acquisition, making it challenging to study water quality responses to precipitation events. Further,

while rapid data processing is possible, real-time image acquisition remains a challenge. Although, efforts are underway to decrease the time for satellite data release to within a day.

In addition, there are challenges to defining turbidity thresholds. Various methods have been used to define a turbidity threshold to delineate plumes. Studies have used an arbitrary value relevant to coral reef health as the turbidity threshold[79]. Studies have also utilized accumulated nLw555 values for 25th and 75th percentile composites[80], river discharge and plume extension correlation coefficients as a function of threshold values[81,82], a histogram of the distribution of radiance nLw645[81], and a finite mixing model[83] to determine turbidity thresholds.

Based on the results of this study we recommend prioritizing low impact development to reduce post-wildfire stormwater and sediment delivery to the coast. However, we also recommend preventative measures for wildfire. In California, most wildfires are caused by human activities, with powerline ignitions representing a substantial proportion of recent wildfire ignition sources[84]. One popular management decision is to de-energize urban areas during times of elevated wildfire risk. However, other options like burying powerlines and replacing aging powerline infrastructure should also be considered. Local governments should also guide development based on wildfire risk[85]. Further, climate change is increasingly creating conditions conducive to wildfire, therefore, a reduction in carbon emissions should also be considered as a strategy for addressing wildfire[86]. Additionally, in Southern California, chaparral is increasingly getting converted to grassland, which poses a higher fire risk[87]. Thus, we should also consider restoring and preserving chaparral landscapes in the wildland-urban interface.

5. Appendix

Text A2-1. Light Transmission Data

We compared satellite turbidity measurements with *in situ* light transmission measurements provided by LA Sanitation for various stations in the Santa Monica Bay. Light transmission measurements taken within 1.5 hours of a Sentinel-2 overpass, which generally occurred at 11:45 am local time, were selected. The mean turbidity from a 5x5 pixel window of each station was extracted. Results are presented in Fig. A1-1.

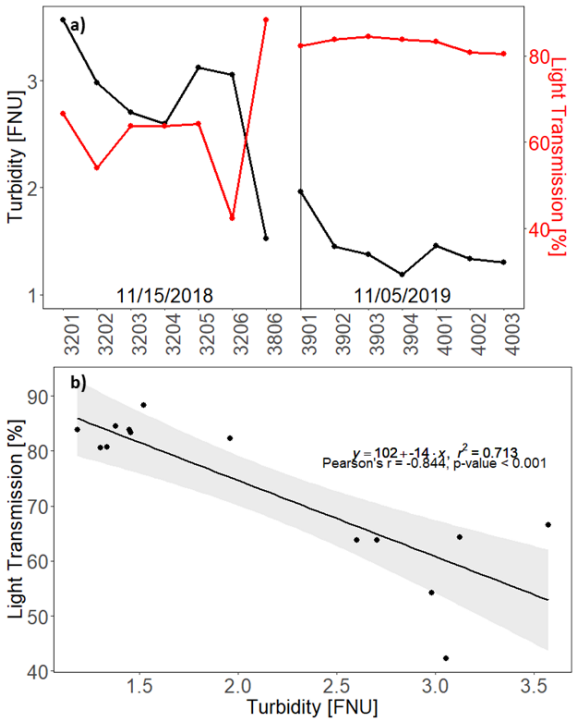

Figure A1-1. Turbidity and light transmission (**a**) matchups and (**b**) linear regression with 95% confidence interval (shaded).

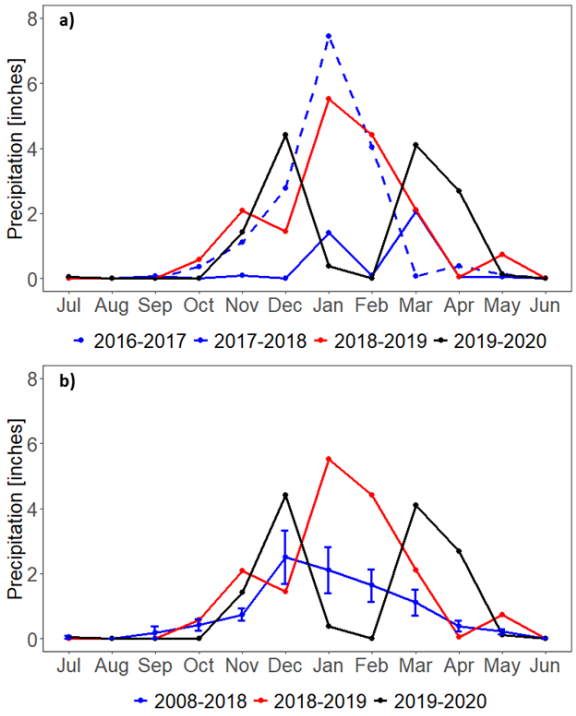

Figure A1-2. Monthly precipitation totals for (**a**) 2016-2020 and (**b**) 2008-2020.

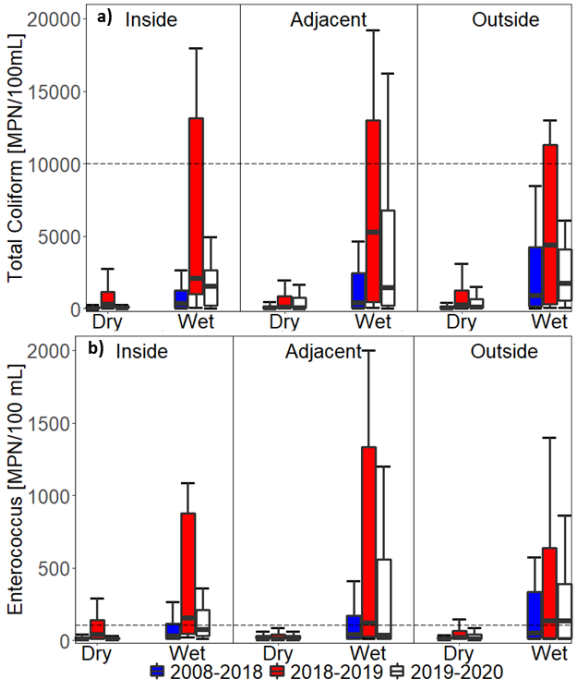

Figure A1-3. Boxplots of (**a**) TC and (**b**) ENT by region and weather condition. The SWRCB standards are indicated with a black dotted line. The 2018-2019 shifts in TC and ENT in the inside region occurred both during wet and dry weather.

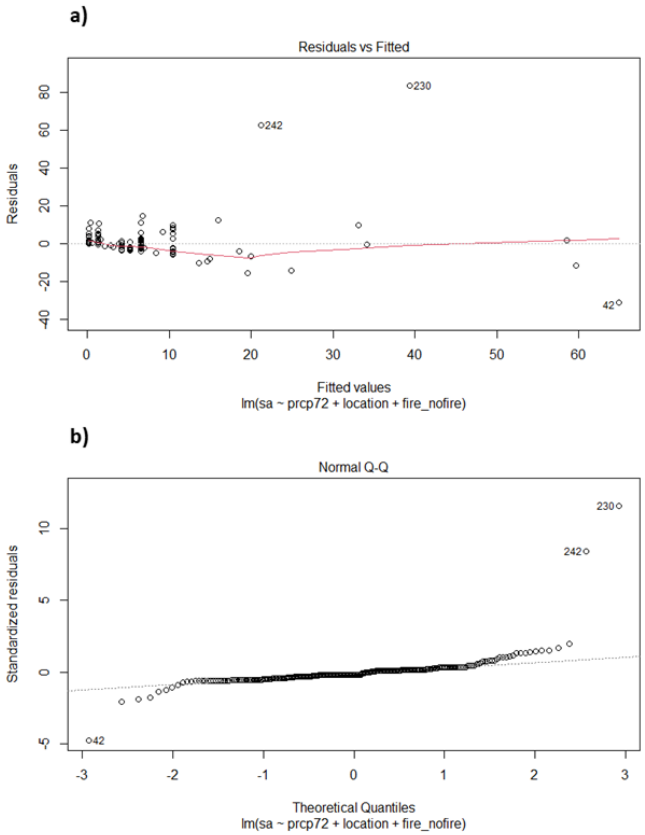

Figure A1-4. Multiple linear regression (a) residuals versus fitted values plot and (b) residuals Q-Q plot.

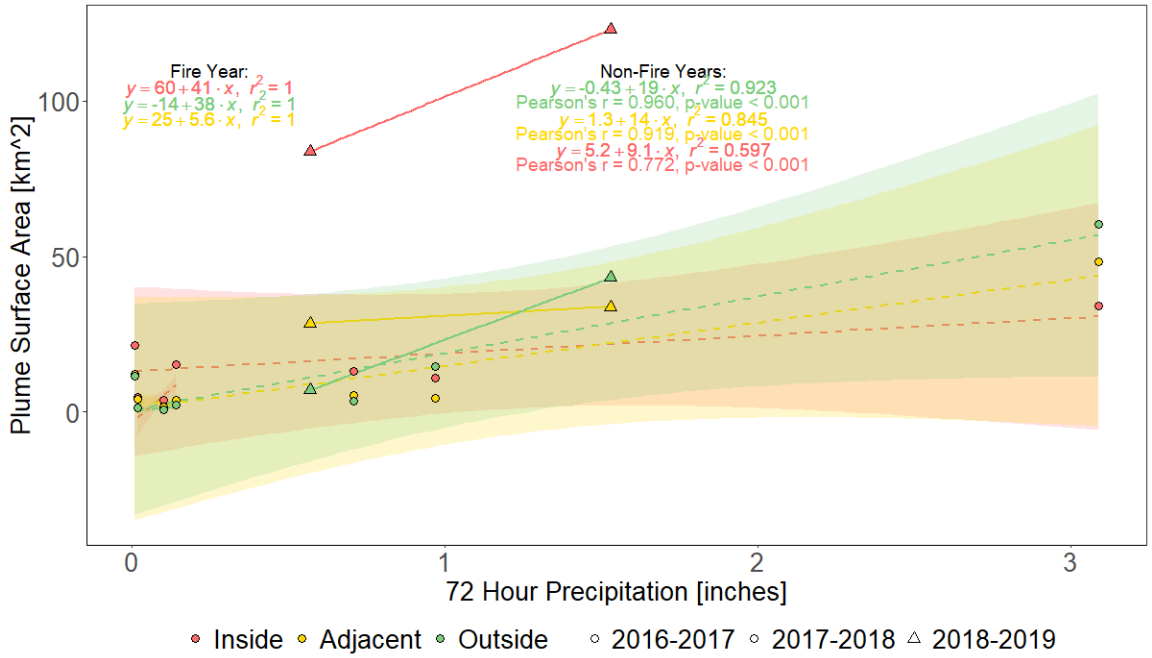

Figure A1-5. Linear regressions of plume surface area and 3-day precipitation totals when excluding data points with 3-day precipitation totals equal to 0.

Table A1-1. Boundary coordinates for the study area and each region.

	South	North	West	East
Study Area	33.9688	34.1266	-119.066	-118.520
Adjacent Left	33.9688	34.1266	-119.066	-119.018
Inside	33.9688	34.1266	-119.018	-118.681
Adjacent Right	33.9688	34.1266	-118.681	-118.582
Outside	33.9688	34.1266	-118.582	-118.520

Table A1-2. Sentinel-2 temporal, spatial, and spectral resolution, and swath.

	Sentinel-2
Revisit Time (days)	5
Spatial Resolution (m/pixel)	10
Swath Width (km)	290
Spectral Bands (in this study)	Band 4: Red (650 - 680 nm)
	Central Wavelength: 665 nm
	Band 8: Near-infrared (780 - 886 nm)
	Central Wavelength: 833 nm

Table A1-3. Systematic literature review summaries.

Search	Author	Location	Findings
"wildfire" and "turbidity"	Earl and Blinn, 2003	New Mexico	Changes in turbidity were dramatic, but short lived (<24 h). Changes in water quality occurred kilometers downstream of the actual fires.
	Rhoades et al., 2011	Colorado	Turbidity in severely burned basins (>45%) was four times greater than in lesser burned basins. Analytes remained elevated through 5 years post-fire.
	Oliver et al., 2012	California	Turbidity increased following the fire, particularly in the wetter second year. Sites (2 and 3) closest to the burned area showed greater increases.
	Murphy et al., 2012	Colorado	High intensity storms resulted in dramatic increases in turbidity at sites downstream from the burned area. Low intensity storms also led to increases in turbidity, but differences between sites upstream and downstream from the burned area remained minimal.
	Dahm et al., 2015	New Mexico	Runoff from burned areas caused turbidity peaks (to 2500 NTU) at least 50 km downstream.
	Reale et al., 2015	New Mexico	Storm events led to elevated turbidity in 1st and 2nd order streams post-fire. Less severe and nominal effects were observed in the 3rd and 4th order streams, respectively.
	Sherson et al., 2015	New Mexico	Post-fire non-monsoonal precipitation led to small increases in turbidity. Post-fire monsoonal precipitation resulted in multi-day increases in turbidity (>100 x background levels).
	Mast et al., 2016	Colorado	Post-fire high intensity rain storms caused short-term turbidity spikes (> 600 NTU).
	Lewis et al., 2018	California	Turbidity impacts of logging, harvesting, and a wildfire. Turbidity increased pre-fire at 4 sites and post-fire at 6 sites. Extreme turbidity measurements became more frequent the year following the fire.
	Thompson et al., 2018	Colorado	High turbidity spates (>1200 NTU) in late July through September 2011 were associated with loss of submerged macrophyte biomass.
	Uzun et al., 2020	California	Burned watersheds showed elevated levels in turbidity during the following two seasons. The more extensively burned watershed showed remarkable decreases in the second year.
"wildfire" and "total coliforms OR fecal coliforms OR Escherichia coli OR Enterococcus"	Valenca et al., 2020	California	Growth or persistence of E. coli in the presence of wildfire residues was less than that in the presence of unburned soil particles. Increased transport of wildfire residues did not result in increased transport of E. coli.
"wildfire," "water quality," and "remote sensing"	Rust et al., 2018	Western United States	Nutrient, major-ion, and metal concentrations and loading rates significantly increased within the first 5 years after fire. Particulate analytes (bounded to sediments) increased, whereas their dissolved counterparts did not. Precipitation events after fire increased particulate concentrations and loading rates.

Table A1-4. Wilcoxon rank sum test p-values for 2008-2018 versus 2018-2019 all weather samples. P-values <0.05, <0.01, and <0.001 are highlighted in yellow, orange, and red, respectively.

Region	Parameter	Jul	Aug	Sep	Oct	Nov	Dec	Jan	Feb	Mar	Apr	May	Jun
Inside	TC	0.931	0.062	0.350	0.552	0.984	0.002	<0.001	<0.001	<0.001	<0.001	<0.001	<0.001
	ENT	0.738	0.837	0.710	0.456	0.668	0.006	0.004	0.002	<0.001	<0.001	<0.001	<0.001
Adjacent	TC	0.026	0.007	0.001	0.566	0.003	<0.001	<0.001	<0.001	0.017	<0.001	<0.001	<0.001
	ENT	0.144	0.178	0.970	0.223	0.472	0.003	<0.001	0.004	0.876	<0.001	0.238	0.543
Outside	TC	0.785	0.266	0.800	0.247	0.973	0.051	<0.001	<0.001	<0.001	<0.001	<0.001	<0.001
	ENT	0.920	0.028	0.026	0.098	0.006	0.620	0.011	<0.001	0.004	0.002	<0.001	<0.001

Table A1-5. Wilcoxon rank sum test p-values for 2008-2018 versus 2018-2019 wet weather samples. P-values <0.05, <0.01, and <0.001 are highlighted in yellow, orange, and red, respectively.

Region	Parameter	Jul	Aug	Sep	Oct	Nov	Dec	Jan	Feb	Mar	Apr	May	Jun
Inside	TC	-	-	-	-	-	-	0.026	0.133	0.830	-	0.154	-
	ENT	-	-	-	-	-	-	0.051	0.197	0.133	-	0.074	-
Adjacent	TC	-	-	-	0.500	0.035	0.064	0.722	0.026	0.329	-	0.085	-
	ENT	-	-	-	0.383	0.335	0.151	0.032	0.041	0.160	-	0.591	-
Outside	TC	-	-	-	0.121	0.624	0.781	0.119	0.182	0.160	-	1.000	-
	ENT	-	-	-	0.121	0.095	0.510	0.296	0.789	0.554	-	0.698	-

Table A1-6. Wilcoxon rank sum test p-values for 2008-2018 versus 2018-2019 dry weather samples. P-values <0.05, <0.01, and <0.001 are highlighted in yellow, orange, and red, respectively.

Region	Parameter	Jul	Aug	Sep	Oct	Nov	Dec	Jan	Feb	Mar	Apr	May	Jun
Inside	TC	0.961	0.062	0.363	0.738	0.600	<0.001	<0.001	<0.001	<0.001	<0.001	<0.001	<0.001
	ENT	0.730	0.837	0.736	0.481	0.833	0.004	0.022	0.003	<0.001	<0.001	<0.001	<0.001
Adjacent	TC	0.023	0.007	0.001	0.362	0.004	<0.001	<0.001	0.004	0.001	<0.001	<0.001	<0.001
	ENT	0.165	0.178	0.995	0.301	0.709	0.006	0.092	0.017	0.766	<0.001	0.266	0.543
Outside	TC	0.666	0.266	0.800	0.346	0.337	0.001	<0.001	<0.001	<0.001	<0.001	<0.001	<0.001
	ENT	0.967	0.028	0.026	0.180	0.036	0.070	0.026	0.001	0.002	<0.001	<0.001	<0.001

Table A1-7. Pearson correlation coefficients. Moderate correlations are highlighted in yellow. P-values <0.05, <0.01, and <0.001 are marked with *, **, and ***, respectively.

Parameter	TC	ENT	SA	PRCP	PRCP72
TC	1.000				
ENT	0.545***	1.000			
SA	0.547***	0.372***	1.000		
PRCP	0.341***	0.328***	0.009	1.000	
PRCP72	0.486***	0.454***	0.634***	0.683***	1.000

Table A1-8. Residual normality tests. P-values <0.05, <0.01, and <0.001 are highlighted in yellow, orange, and red, respectively.

Test	Statistic	p-value
Shapiro-Wilk	0.4879	<0.001
Kolmogorov-Smirnov	0.2499	<0.001
Cramer-von Mises	22.1935	<0.001
Anderson-Darling	30.2435	<0.001

6. References

1. Marlon, J. R. *et al.* Long-term perspective on wildfires in the western USA. *Proc. Natl. Acad. Sci. U. S. A.* **109**, 535–543 (2012).

2. Pechony, O. & Shindell, D. T. Driving forces of global wildfires over the past millennium and the forthcoming century. *Proc. Natl. Acad. Sci. U. S. A.* **107**, 19167–19170 (2010).

3. Westerling, A. L. R. Increasing western US forest wildfire activity: Sensitivity to changes in the timing of spring. *Philos. Trans. R. Soc. B Biol. Sci.* **371**, (2016).

4. Westerling, A. L., Hidalgo, H. G., Cayan, D. R. & Swetnam, T. W. Warming and earlier spring increase Western U.S. forest wildfire activity. *Science (80-.).* **313**, 940–943 (2006).

5. Abatzoglou, J. T. & Williams, A. P. Impact of anthropogenic climate change on wildfire across western US forests. *Proc. Natl. Acad. Sci. U. S. A.* **113**, 11770–11775 (2016).

6. Dennison, P. E., Brewer, S. C., Arnold, J. D. & Moritz, M. A. Large wildfire trends in the western United States, 1984–2011. *Geophys. Res. Lett.* **41**, 2928–2933 (2014).

7. Williams, A. P. *et al.* Observed Impacts of Anthropogenic Climate Change on Wildfire in California. *Earth's Futur.* **7**, 892–910 (2019).

8. Keeley, J. E. & Syphard, A. D. Twenty-first century California, USA, wildfires: fuel-dominated vs. wind-dominated fires. *Fire Ecol.* **15**, (2019).

9. Moritz, M. A., Moody, T. J., Krawchuk, M. A., Hughes, M. & Hall, A. Spatial variation in extreme winds predicts large wildfire locations in chaparral ecosystems. *Geophys. Res. Lett.* **37**, 1–5 (2010).

10. Westerling, A. L., Cayan, D. R., Brown, T. J., Hall, B. L. & Riddle, L. G. Climate, santa ana winds and autumn wildfires in southern california. *Eos (Washington. DC).* **85**, (2004).

11. Barnett, T. P. *et al.* Human-Induced Changes United States. *Science (80-.).* **319**, 1080–1083 (2008).

12. Seager, R. *et al.* Model projections of an imminent transition to a more arid climate in southwestern North America. *Science (80-.).* **316**, 1181–1184 (2007).

13. Miller, N. L. & Schlegel, N. J. Climate change projected fire weather sensitivity: California Santa Ana wind occurrence. *Geophys. Res. Lett.* **33**, 1–5 (2006).

14. De Bano, L. F. Water repellent soils: a state-of-the-art. *US Dep. Agric. For. Serv. Gen.*

Tech. Rep. (1981).

15. Doerr, S. H., Shakesby, R. A. & Walsh, R. P. D. Soil water repellency: Its causes, characteristics and hydro-geomorphological significance. *Earth Sci. Rev.* **51**, 33–65 (2000).

16. Larsen, I. J. *et al.* Causes of Post-Fire Runoff and Erosion: Water Repellency, Cover, or Soil Sealing? *Soil Sci. Soc. Am. J.* **73**, 1393–1407 (2009).

17. Rowe, P. B., Countyman, C. M., & Storey, H. C. Probable peak discharges and erosion rates from southern California watersheds as influences by fire. U. S. Dept. of Agriculture 1–107 (1949).

18. Savage, S. M. Mechanism of Fire-Induced Water Repellency in Soil. *Soil Science Society of America Journal* **38**, 652–657 (1974).

19. Shakesby, R. A. Post-wildfire soil erosion in the Mediterranean: Review and future research directions. *Earth-Science Rev.* **105**, 71–100 (2011).

20. Wells, W. G. Proceedings of the Christchurch Symposium, January 25–31, 1981, Christchurch, New Zealand. Some Effects of Brushfires on Erosion Processes in Coastal Southern California. *International Association of Hydrological Sciences*. (1981).

21. Wells, W. G. Proceedings of the Chaparral Ecosystems Research Conference, May 16-17, 1985, Santa Barbara, California / sponsored by University of California, Water Resources Center ... [et al.] ; editor, Johannes J. DeVries. (1986).

22. Wells, W. G. Proceedings of the 4th International Symposium on Mediterranean Ecosystems, August, 1984, Perth, Western Australia / sponsored by University of Western Australia, Botany Department. Fire Dominates Sediment Production in California Chaparral. (1984).

23. Dahm, C. N., Candelaria-Ley, R. I., Reale, C. S., Reale, J. K. & Van Horn, D. J. Extreme water quality degradation following a catastrophic forest fire. *Freshw. Biol.* **60**, 2584–2599 (2015).

24. Earl, S. R. & Blinn, D. W. Effects of wildfire ash on water chemistry and biota in south-western U.S.A. streams. *Freshw. Biol.* **48**, 1015–1030 (2003).

25. Mast, M. A., Murphy, S. F., Clow, D. W., Penn, C. A. & Sexstone, G. A. Water-quality response to a high-elevation wildfire in the Colorado Front Range. *Hydrol. Process.* **30**, 1811–1823 (2016).

26. Murphy, S. F., Blaine McCleskey, R. & Writer, J. H. Effects of flow regime on stream turbidity and suspended solids after wildfire, Colorado Front Range. *IAHS-AISH Publ.*

354, 51–58 (2012).

27. Oliver, A. A., Reuter, J. E., Heyvaert, A. C. & Dahlgren, R. A. Water quality response to the Angora Fire, Lake Tahoe, California. *Biogeochemistry* **111**, 361–376 (2012).

28. Reale, J. K., Van Horn, D. J., Condon, K. E. & Dahm, C. N. The effects of catastrophic wildfire on water quality along a river continuum. *Freshw. Sci.* **34**, 1426–1442 (2015).

29. Rhoades, C. C., Entwistle, D. & Butler, D. The influence of wildfire extent and severity on streamwater chemistry, sediment and temperature following the Hayman Fire, Colorado. *Int. J. Wildl. Fire* **20**, 430–442 (2011).

30. Sherson, L. R., Van Horn, D. J., Gomez-Velez, J. D., Crossey, L. J. & Dahm, C. N. Nutrient dynamics in an alpine headwater stream: Use of continuous water quality sensors to examine responses to wildfire and precipitation events. *Hydrol. Process.* **29**, 3193–3207 (2015).

31. Uzun, H. *et al.* Two years of post-wildfire impacts on dissolved organic matter, nitrogen, and precursors of disinfection by-products in California stream waters. *Water Res.* **181**, (2020).

32. Valenca, R., Ramnath, K., Dittrich, T. M., Taylor, R. E. & Mohanty, S. K. Microbial quality of surface water and subsurface soil after wildfire. *Water Res.* **175**, 115672 (2020).

33. Kramer, S. J., Bisson, K. M. & Fischer, A. D. Observations of Phytoplankton Community Composition in the Santa Barbara Channel During the Thomas Fire. *J. Geophys. Res. Ocean.* **125**, 1–16 (2020).

34. Rust, A. J., Hogue, T. S., Saxe, S. & McCray, J. Post-fire water-quality response in the western United States. *Int. J. Wildl. Fire* **27**, 203–216 (2018).

35. Dogliotti, A. I., Ruddick, K. G., Nechad, B., Doxaran, D. & Knaeps, E. A single algorithm to retrieve turbidity from remotely-sensed data in all coastal and estuarine waters. *Remote Sens. Environ.* **156**, 157–168 (2015).

36. Braga, F., Scarpa, G. M., Brando, V. E., Manfè, G. & Zaggia, L. COVID-19 lockdown measures reveal human impact on water transparency in the Venice Lagoon. *Sci. Total Environ.* **736**, (2020).

37. Huovinen, P., Ramírez, J., Caputo, L. & Gómez, I. Mapping of spatial and temporal variation of water characteristics through satellite remote sensing in Lake Panguipulli, Chile. *Sci. Total Environ.* **679**, 196–208 (2019).

38. Swenson, J. J. & Franklin, J. The effects of future urban development on habitat

fragmentation in the Santa Monica Mountains. *Landsc. Ecol.* **15**, 713–730 (2000).

39. County of Los Angeles. After Action Review of the Woolsey Fire Incident. *County of Los Angeles* 1–203 (2019).

40. Watershed Emergency Response Team. Woolsey and Hill Fires. *State of California* 1–192 (2018).

41. Vanhellemont, Q. & Ruddick, K. Atmospheric correction of metre-scale optical satellite data for inland and coastal water applications. *Remote Sens. Environ.* **216**, 586–597 (2018).

42. Vanhellemont, Q. & Ruddick, K. ACOLITE processing for Sentinel-2 and Landsat-8: atmospheric correction and aquatic applications. *Ocean Opt. Conf.* (2016).

43. EPA. Recreational Water Quality Criteria. *U. S. Environ. Prot. Agency* 1–69 (2012).

44. Ackerman, D. & Weisberg, S. B. Relationship between rainfall and beach bacterial concentrations on Santa Monica Bay beaches. *J. Water Health* **1**, 85–87 (2003).

45. Noble, R. T., Moore, D. F., Leecaster, M. K., McGee, C. D. & Weisberg, S. B. Comparison of total coliform, fecal coliform, and enterococcus bacterial indicator response for ocean recreational water quality testing. *Water Res.* **37**, 1637–1643 (2003).

46. Schiff, K. C., Morton, J. & Weisberg, S. B. Retrospective evaluation of shoreline water quality along santa monica bay beaches. *Mar. Environ. Res.* **56**, 245–253 (2003).

47. Arnold, B. F. *et al.* Acute Illness among Surfers after Exposure to Seawater in Dry- and Wet-Weather Conditions. *Am. J. Epidemiol.* **186**, 866–875 (2017).

48. State Water Resources Control Board. Water Quality Control Plan Ocean Waters of California. *State Water Resources Control Board California Environmental Protection Agency* (2019).

49. Gold, M. *et al.* Los Angeles County and Orange County Beach Water Quality: Re-Evaluation of the 3-Day Rule. *UCLA Institute of the Environment and Sustainability* 1–30 (2013).

50. Holt, B., Trinh, R. & Gierach, M. M. Stormwater runoff plumes in the Southern California Bight: A comparison study with SAR and MODIS imagery. *Mar. Pollut. Bull.* **118**, 141–154 (2017).

51. Washburn, L., McClure, K. A., Jones, B. H. & Bay, S. M. Spatial scales and evolution of stormwater plumes in Santa Monica Bay. *Mar. Environ. Res.* **56**, 103–125 (2003).

52. Warrick, J. A. & Farnsworth, K. L. Sources of sediment to the coastal waters of the Southern California Bight. *Spec. Pap. Geol. Soc. Am.* **454**, 39–52 (2009).

53. Li, D. *et al.* Surf zone microbiological water quality following emergency beach nourishment using sediments from a catastrophic debris flow. *Water Res.* **176**, 115733 (2020).

54. Craig, D. L., Fallowfield, H. J. & Cromar, N. J. Use of microcosms to determine persistence of Escherichia coli in recreational coastal water and sediment and validation with in situ measurements. *J. Appl. Microbiol.* **96**, 922–930 (2004).

55. Davies, C. M., Long, J. A. H., Donald, M. & Ashbolt, N. J. Survival of fecal microorganisms in marine and freshwater sediments. *Appl. Environ. Microbiol.* **61**, 1888–1896 (1995).

56. Garzio-Hadzick, A. *et al.* Survival of manure-borne E. coli in streambed sediment: Effects of temperature and sediment properties. *Water Res.* **44**, 2753–2762 (2010).

57. Gerba, C. Indicator microorganisms. In Maier, R., Pepper, I. & Gerba, C. (Eds.) Environmental Microbiology. *California: Academic*. 491–503 (2000).

58. Alm, E. W., Burke, J. & Spain, A. Fecal indicator bacteria are abundant in wet sand at freshwater beaches. *Water Res.* **37**, 3978–3982 (2003).

59. Wanjugi, P., Fox, G. A. & Harwood, V. J. The Interplay Between Predation, Competition, and Nutrient Levels Influences the Survival of Escherichia coli in Aquatic Environments. *Microb. Ecol.* **72**, 526–537 (2016).

60. EPA. Volunteer Stream Monitoring: A Methods Manual. *U. S. Environ. Prot. Agency* 180–181 (1997).

61. Byappanahalli, M. N., Nevers, M. B., Korajkic, A., Staley, Z. R. & Harwood, V. J. Enterococci in the Environment. *Microbiol. Mol. Biol. Rev.* **76**, 685–706 (2012).

62. Halliday, E. & Gast, R. J. Coastal Water Quality and Bather Health. *Env. Sci* **45**, 370–379 (2012).

63. Fattal, B., Vasl, R. J., Katzenelson, E., & Shuval, H. I. Survival of Bacterial Indicator Organisms and Enteric Viruses in the Mediterranean Coastal Waters Off Tel-Eviv. *Water Res.* **17**, 397–402 (1983).

64. Wade, T. J. *et al.* Rapidly measured indicators of recreational water quality and swimming-associated illness at marine beaches: a prospective cohort study. *Environ Health* **9,** 66 (2010).

65. Wade, T. J. *et al*. Dufour Rapidly Measured Indicators of Recreational Water Quality Are Predictive of Swimming-Associated Gastrointestinal Illness. *Environmental Health Perspectives* **114**, 24–28 (2006).

66. Barron, S. Water Quality of Coastal Watersheds Following the Woolsey Wildfire: Surface Water Quality of Pollutants of Concern Before and After Fire, and Mitigating the Impact of Wildfires Through Stormwater Management Techniques. *California Stormwater Quality Association* https://www.casqa.org/asca/water-quality-coastal-watersheds-following-woolsey-wildfire-surface-water-quality-pollutants (2021).

67. Tang, W. *et al.* Widespread phytoplankton blooms triggered by 2019–2020 Australian wildfires. *Nature* **597**, 370–375 (2021).

68. Coombs, J. S. & Melack, J. M. Initial impacts of a wildfire on hydrology and suspended sediment and nutrient export in California chaparral watersheds. *Hydrol. Process.* **27**, 3842–3851 (2013).

69. Riggan, P. J. *et al.* Effects of Fire Severity on Nitrate Mobilization in Watersheds Subject to Chronic Atmospheric Deposition. *Environ. Sci. Technol.* **28**, 369–375 (1994).

70. Stein, E. D., Brown, J. S., Hogue, T. S., Burke, M. P. & Kinoshita, A. Stormwater contaminant loading following southern California wildfires. *Environ. Toxicol. Chem.* **31**, 2625–2638 (2012).

71. Martin, S. An Introduction to Ocean Remote Sensing. *United Kingdom: Cambridge University Press* (2014).

72. Nezlin, N. P., Weisberg, S. B. & Diehl, D. W. Relative availability of satellite imagery and ship-based sampling for assessment of stormwater runoff plumes in coastal southern California. *Estuar. Coast. Shelf Sci.* **71**, 250–258 (2007).

73. Lahet, F. & Stramski, D. MODIS imagery of turbid plumes in San Diego coastal waters during rainstorm events. *Remote Sens. Environ.* **114**, 332–344 (2010).

74. Nezlin, N. P. *et al.* Stormwater plume detection by MODIS imagery in the southern California coastal ocean. *Estuar. Coast. Shelf Sci.* **80**, 141–152 (2008).

75. Warrick, J. A. *et al.* River plume patterns and dynamics within the Southern California Bight. *Cont. Shelf Res.* **27**, 2427–2448 (2007).

76. Warrick, J. A., Mertes, L. A. K., Washburn, L. & Siegel, D. A. Dispersal forcing of southern California river plumes, based on field and remote sensing observations. *Geo-Marine Lett.* **24**, 46–52 (2004).

77. Gierach, M. M., Holt, B., Trinh, R., Jack Pan, B. & Rains, C. Satellite detection of

wastewater diversion plumes in Southern California. *Estuar. Coast. Shelf Sci.* **186**, 171–182 (2017).

78. Mertes, L. A. K., Hickman, M., Waltenberger, B., Bortman, A. L., Inlander, E., McKenzie, C., & Dvorsky, J. Synoptic views of sediment plumes and coastal geography of the Santa Barbara Channel, California. *Hydrological Processes* **12**, 967–979 (1998).

79. Restrepo, J. D., Park, E., Aquino, S. & Latrubesse, E. M. Coral reefs chronically exposed to river sediment plumes in the southwestern Caribbean: Rosario Islands, Colombia. *Sci. Total Environ.* **553**, 316–329 (2016).

80. Mendes, R. *et al.* Observation of a turbid plume using MODIS imagery: The case of Douro estuary (Portugal). *Remote Sens. Environ.* **154**, 127–138 (2014).

81. Fernández-Nóvoa, D. et al. Influence of main forcing affecting the Tagus turbid plume under high river discharges using MODIS imagery. PLoS One 12, 1–27 (2017).

82. Guo, K., Zou, T., Jiang, D., Tang, C. & Zhang, H. Variability of Yellow River turbid plume detected with satellite remote sensing during water-sediment regulation. Cont. Shelf Res. 135, 74–85 (2017).

83. Torregroza-Espinosa, A. C. et al. Fluvial and oceanographic influences on suspended sediment dispersal in the Magdalena River Estuary. J. Mar. Syst. 204, 103282 (2020).

84. Keeley, J. E. & Syphard, A. D. Historical patterns of wildfire ignition sources in California ecosystems. *Int. J. Wildl. Fire* **27**, 781–799 (2018).

85. Kramer, H. A. *et al.* Post-wildfire rebuilding and new development in California indicates minimal adaptation to fire risk. *Land use policy* **107**, 105502 (2021).

86. Goss, M. *et al.* Climate change is increasing the likelihood of extreme autumn wildfire conditions across California. *Environ. Res. Lett.* **15**, (2020).

87. Syphard, A. D., Brennan, T. J. & Keeley, J. E. Chaparral Landscape Conversion in Southern California. 323–346 (2018) doi:10.1007/978-3-319-68303-4_12.

Chapter 2: Commercially available garden products as important sources of antibiotic resistance genes—A survey

1. Introduction

Antibiotic resistance threatens the global response to infectious disease, with over 700,000 deaths in 2014 projected to increase to 10 million by 2050 (O'Neill 2016). Concurrently, over 11 million kg of antibiotics are administered to livestock annually for growth promotion and disease prevention (USFDA 2018). An estimated 30-90% of antibiotics administered for agricultural use are not metabolized prior to excretion and are instead introduced into the environment where they exert a selective pressure for antimicrobial resistance (Sarmah et al. 2006). Additionally, consistent animal exposure to antibiotics drives selection within livestock gut microbiomes, resulting in the excretion of antibiotic resistant bacteria (ARB) into the environment (Looft et al. 2012). Confined animal feeding operations (CAFOs) have widely been confirmed as sources of anthropogenic antimicrobial resistance into the environment (Heuer et al. 2011; McEachran et al. 2012; Sancheza et al. 2016) due to use of antibiotics in animal feed. While antibiotic resistance genes (ARGs) also exist in native soils due to selective pressures that occur naturally in the environment (Allen et al. 2010; Hall and Barlow 2004), archived agricultural soils show a significant increase in ARG abundance since 1940, corresponding with the increased use of antibiotics in animal husbandry (Knapp et al. 2010).

Manure from CAFOs is also frequently mixed with soil in rural and urban settings to restore and replenish nutrients. This process constitutes a significant pathway of ARG dissemination from agriculture, with a substantial body of literature confirming that such repeated manure application results in propagation of both antibiotics and ARGs in fields (Dungan et al. 2019; Fahrenfeld et al. 2014; Heuer et al. 2011; Jechalke et al. 2013; Marti et al. 2013; Sandberg and LaPara 2016).

However, there is an important knowledge gap with regard to commercially available garden products containing animal manure, which are readily obtainable by the general public. Animal manure contains antibiotic resistant bacteria (Fahrenfeld et al. 2014; Liu et al. 2016; Marti et al. 2013; Wang et al. 2015), representing a potential route of consumer exposure to ARGs via fertilized gardens, lawns, and parks. In addition to a lack of data on ARG content, there is a lack of regulation over garden product branding. For example, for food, fiber, and feed products, the term "organic" is regulated by the Code of Federal Regulations (Code of Federal Regulations 2020), but for fertilizers, the term "organic" is not federally regulated. Instead the Organic Materials Review Institute (OMRI) and the Demeter Association certifications verify that fertilizers meet the USDA National Organic Program (NOP) regulations. However, the NOP regulations refer to any organic matter containing plant and animal material, including raw manure, as "organic". In addition, there is little transparency on fertilizer treatment prior to purchase, with garden product packaging and online descriptions lacking this information and with the NOP regulations only explicitly outlining treatment methods for vermicomposting. Further, unlike the Code of Federal Regulations, the NOP regulations do not consider propagation of antibiotic resistance, either through regulating antibiotic, ARB, or ARG content (National Organic Program Handbook 2018).

It is critical to comprehensively consider environments existing at the nexus of human-ARG interaction. Understanding sources and scope of dissemination will prove critical in determining potential points of mitigation as well as approach. Therefore, in this study, we sought to measure ARG content in 34 commercially available garden products intended for home use, 3 recently landscaped soils from a community garden, residential lawn, and a park, and 5 native soils from hiking trails. Two sulfonamide resistance genes, *sul*1 and *sul*2, two tetracycline resistance

genes, *tet*(L)and *tet*(W), one macrolide resistance gene, *erm*(F), one class 1 integron-integrase gene, *intI*1, and a total bacterial surrogate, 16S rRNA, were quantified via qPCR. All genes quantified here are good candidates for monitoring the dissemination of ARGs from livestock waste. *tet*, *sul*, and *erm* have conferred resistance to three major classes of antibiotics used in animal husbandry (USFDA 2018) via different resistance mechanisms and are thus the most frequently detected ARG classes in livestock waste (He et al. 2020). Additionally, *int*I1 is a mobile genetic element that can be transferred via horizontal gene transfer (HGT) and is a known proxy for anthropogenic pollution (Gillings et al. 2015; Gilling et al. 2018). All samples were analyzed with respect to per gram of dry soil and per 16S rRNA gene copies, and correlation coefficients between individual ARGs and *intI*1 copies were calculated. Results were cross-referenced with package labeling to determine if existing indicators and/or animal manure sources may be correlated to ARG loading.

2. Materials and Methods

2.1 Sample Collection

All commercially available garden products chosen for this survey were purchased in-person from a manufacturer or retailer at major garden and hardware stores. These garden products were sold internationally (n=6), nationally (n=23), at select states (n=1), or locally (n=4). Garden products specialized to specific plants (i.e. orchid, rose, etc.) were avoided when possible with preference given to garden products branded for general use. Garden products were classified into five major categories: Potting Soil (n=10), Garden Soil (n=7), Fruit Amendment (n=4), Lawn Amendment (n=4), Manure (n=6), and Compost (n=3). Garden products spanned 16 brands and included animal manure sources ranging from poultry litter and dairy cow manure to bat guano (manure was included as a listed ingredient in items not labelled as “Manure”). Product

information made available on packaging or online descriptions such as certifications (Demeter or OMRI), labelling, and manure source are summarized in Table 2-1.

The five native soils were collected throughout January 2019 from relatively remote hiking trails selected based on accessibility, foot traffic, and distance to potential anthropogenic contamination sources such as freeways, industrial sites, farms, and residential areas (Fig. 2-1). For each hiking trail, 1 m^2 plots were randomly selected approximately 3 ft away from the trail where the soil was undisturbed and uncompacted at the beginning, middle, and end of the trail (n=15). Within each 1 m^2 plot, we collected 10 subsamples from different areas from the top 0-2 in. of soil using sterile 50 mL falcon tubes and spatulas. Soil samples were transported in coolers with ice before being stored at 4°C.

The three recently landscaped soils were collected throughout January 2019 from a community garden in Westwood (RL1), a residential lawn in Crenshaw (RL2), and a park in Santa Monica (RL3) (Fig. 2-1). For each site, three 1 m^2 plots were randomly selected (n=9). Within each 1 m^2 plot, we collected 10 subsamples from different areas from the top 0-2 in. of soil using sterile 50 mL falcon tubes and spatulas. The samples were transported in coolers with ice and stored at 4°C.

For processing, soil samples were mixed and triplicate subsamples of 0.25 ± 0.01 g (wet wt.) were measured into sterile 2 mL screwcap tubes loaded with 1.00 ± 0.05 g of 0.7 mm garnet beads (Qiagen, Germantown, MD) for gene quantification analysis. Screwcap tubes were stored at -80°C until DNA extraction. Additionally, triplicate subsamples of 90.00 ± 2.00 g (wet wt.) were measured into sterile glass sample jars and stored at -20 °C for soil characterization.

2.2 DNA Extraction and qPCR

All DNA extractions were completed within two weeks of sample collection using the DNeasy PowerSoil Kit (Qiagen, Germantown, MD) per the manufacturer's guidelines except for the cell lysis step where a BioSpec Mini-BeadBeater-8 (BioSpec Products, Bartlesville, OK) was used for 2 mins, in place of vortexing for 10 mins. All samples were analyzed for *sul*1, *sul*2, *tet*(L), *tet*(W), *erm*(F), *intI*1, and 16S rRNA via qPCR with a StepOne Plus (Applied Biosystems, Foster City, CA). Primers and primer concentrations (Table A2-1) and reaction specifics (Table A2-2) were validated previously in the literature (Ji et al. 2012; Knapp et al. 2010; Luo et al. 2010; Pei et al. 2006; Zhou et al. 2014). Standard curves were designed using sequences obtained through the National Center for Biotechnology (NCBI) database and ordered through IDT Technologies (Echeverria-Palencia et al. 2017).

2.3 Soil Characterization

Sand, silt, and clay distributions were obtained using the particle size analysis hydrometer method. Triplicate subsamples of 80.00 ± 1.00 g (wet wt.) were oven dried at 70℃ for 24 hrs. For each triplicate subsample, 50.00 ± 1.00 g (dry wt.) were measured into a beaker. 100 mL of a 5% (w/w) sodium metaphosphate solution and 200 mL of deionized (DI) water were added to the beaker to mix at 125 rpm for 24 hrs. The contents in the beaker were transferred to 1 L cylinders and DI water was added up to the 1 L mark. The contents in the cylinders were mixed and temperature and hydrometer readings were taken at 40 s to obtain % sand. Without disturbing the cylinders, temperature and hydrometer readings were taken again at 2 hrs. to obtain % clay. The % silt was obtained by subtracting % sand and % clay from 100% (Ashworth et al. 2001).

To obtain moisture content and total solids, triplicate subsamples of 2.00 ± 0.05 g were oven dried at 105℃ for 24 hrs. To determine the fractions of total solids-fixed and total solids-

volatile, the dried subsamples were ignited in a furnace at 550℃ for 2 hrs. (EPA 2001). NA in Table 2-1 indicates insufficient amount of sample for triplicate subsamples to be analyzed.

Fig. 2-1 Map of locations where native soils (black) and recently landscaped soils (brown) were collected.

2.4 Statistics

Microsoft Excel was used to calculate triplicate subsample absolute and relative gene abundances from raw thermocycler data. Average absolute and relative gene abundances were calculated from triplicate subsamples for each sample, category, and gene. The SAS CORR procedure was used to calculate the Pearson correlation coefficients between gene abundances and between gene abundances and soil characteristics. R Studio was used to determine normality for each category and each gene through visual observation of histograms and quantile-quantile (Q-Q) plots. The dataset was found to contain non-normal distributions. The Wilcoxon signed-rank test was used to compare garden products and native soils, OMRI and non-OMRI certified garden products, and manure sourcing and non-manure sourcing.

Table 2-1. Certifications, labelling, and manure source for commercially available garden products and soil properties for all samples.

		Certifications[a]				Particle Size Analysis[a]						
Category	Sample	OMRI	Demeter	Labelling[b]	Manure Source[c]	% Sand	% Silt	% Clay	% Moisture Content[a]	% Total Solids[a]	% Total Solid-Fixed[a]	% Total Solids-Volatile[a]
Potting Soil	POS1	No	No	NA	NA	88.2	10.1	1.7	5.01	94.99	24.19	75.81
	POS2	No	No	O	G	89.3	9.7	1.0	3.84	96.16	23.59	76.41
	POS3	Yes	No	O,P	P	93.0	5.4	1.6	4.16	95.84	45.99	54.01
	POS4	No	No	NA	NA	86.5	13.5	0.0	5.48	94.52	26.80	73.20
	POS5	No	No	O,N	NA	93.2	6.8	0.0	4.66	95.34	27.28	72.72
	POS6	No	No	NA	D	85.9	12.9	1.3	2.86	97.14	45.61	54.39
	POS7	No	No	O,N	P	86.1	13.2	0.7	5.28	94.72	21.35	78.65
	POS8	No	No	NA	NA	95.3	1.9	2.8	3.68	96.32	32.13	67.87
	POS9	No	Yes	O	D	97.3	2.7	0.0	4.75	95.25	54.70	45.30
	POS10	No	No	O,N	NA	91.2	6.1	2.6	4.25	95.75	50.58	49.42
Garden Soil	GS1	Yes	No	O,N	P,G	89.1	5.6	5.3	4.03	95.97	43.52	56.48
	GS2	Yes	No	O,N	P	82.6	10.6	6.8	5.80	94.20	26.61	73.39
	GS3	Yes	No	O,N,P	NA	86.2	7.4	6.4	3.60	96.40	21.12	78.88
	GS4	Yes	No	O	NA	96.1	1.1	2.8	5.27	94.73	61.17	38.83
	GS5	No	No	NA	NA	89.0	7.9	3.2	5.06	94.94	26.46	73.54
	GS6	No	No	NA	NA	91.5	4.2	4.3	4.38	95.62	40.14	59.86
	GS7	No	No	NA	NA	85.1	6.4	8.5	4.62	95.38	24.09	75.91
Fruit Amendment	FA1	Yes	No	O	P	84.3	8.1	7.7	0.94	99.06	41.68	58.32
	FA2	No	No	O	P	77.4	6.9	15.7	0.77	99.23	43.24	56.76
	FA3	Yes	No	O	P	79.6	3.8	16.6	1.04	98.96	65.17	34.83
	FA4	Yes	No	O,N	P	66.4	14.1	19.4	0.58	99.42	44.42	55.58
Lawn Amendment	LA1	Yes	No	O	P	81.2	8.8	10.0	3.99	96.01	42.70	57.30
	LA2	No	No	NA	NA	NA	NA	NA	NA	NA	NA	NA
	LA3	No	No	O	NA	NA	NA	NA	NA	NA	NA	NA
	LA4	Yes	No	O	P	NA	NA	NA	NA	NA	NA	NA
Manure	M1	No	No	N	S	90.0	1.6	8.3	3.26	96.74	66.39	33.61
	M2	No	No	NA	S	NA	NA	NA	4.15	95.85	40.14	59.86
	M3	No	No	O	S	NA	NA	NA	3.72	96.28	36.62	63.38
	M4	Yes	No	O	P	90.5	3.8	5.7	3.76	96.24	59.70	40.30
	M5	No	No	NA	P	NA	NA	NA	NA	NA	NA	NA
	M6	No	No	O	P	NA	NA	NA	3.00	97.00	42.51	57.49
Compost	C1	No	No	O	NA	NA	NA	NA	4.99	95.01	31.92	68.08
	C2	NA	NA	NA	NA	NA	NA	NA	4.94	95.06	68.43	31.57
	C3	No	Yes	NA	D	96.6	1.6	1.9	2.34	97.66	75.52	24.48
Recently Landscaped Soil	RL1	NA	NA	NA	NA	NA	NA	NA	2.44	97.56	84.58	15.42
	RL2	NA	NA	NA	NA	NA	NA	NA	4.96	95.04	47.09	52.91
	RL3	NA	NA	NA	NA	NA	NA	NA	4.44	95.56	34.29	65.71
Native Soil	NS1	NA	NA	NA	NA	NA	NA	NA	1.38	98.62	88.16	11.84
	NS2	NA	NA	NA	NA	NA	NA	NA	1.46	98.54	94.44	5.56
	NS3	NA	NA	NA	NA	NA	NA	NA	1.99	98.01	91.07	8.93
	NS4	NA	NA	NA	NA	NA	NA	NA	1.49	98.51	96.22	3.78
	NS5	NA	NA	NA	NA	NA	NA	NA	1.55	98.45	95.59	4.41

[a] Not available (NA). [b] Natural (N), organic (O), premium (P), and not available (NA). [c] Dairy cow (D), bat guano (G), poultry (P), steer (S), and not available (NA).

4. Results and Discussion

3.1 Gene Quantities

sul, *tet*, and *erm* confer resistance to sulfonamides, tetracyclines, and macrolides, respectively, three major classes of antibiotics approved for use in livestock (USFDA 2018). *intI*1 is a useful indicator of anthropogenic pollution (Gillings et al. 2015; Gillings 2018) and 16S rRNA is a total bacteria surrogate measure. Quantities of ARGs and *intI*1 for commercially available garden products, recently landscaped soils, and native soils can be found in Fig. 2-3 and Table A2-6.

*sul*1 was detected in 30 out of 34 garden products, 3 out of 3 recently landscaped soils, and 1 out of 5 native soils. Mean absolute and relative gene quantities were roughly three orders of magnitude higher in garden products (10^6 gene copies/gram and 10^{-2} gene copies/16S rRNA gene copies) than in native soils (10^3 gene copies/gram and 10^{-5} gene copies/16S rRNA gene copies). *sul*2 was detected in 33 out of 34 garden products, 3 out of 3 recently landscaped soils, and 1 out of 5 native soils. *sul*2 mean gene abundances showed a four order magnitude difference between garden products (10^6 gene copies/gram and 10^{-2} gene copies/16S rRNA gene copies) and native soils (10^2 gene copies/gram and 10^{-6} gene copies/16S rRNA gene copies).

tet(L) was detected in 34 out of 34 garden products, 3 out of 3 recently landscaped soils, and 4 out of 5 native soils. Mean absolute and relative abundances of the gene were three orders of magnitude higher in garden products (10^6 gene copies/gram and 10^{-2} gene copies/16S rRNA gene copies) in comparison to native soils (10^3 gene copies/gram and 10^{-5} gene copies/16S rRNA gene copies). *tet*(W) was detected in all garden products, 3 out of 3 recently landscaped soils, and 3 out of 5 native soils. *tet*(W) mean gene quantities were high in garden products (10^7 gene

copies/gram and 10^{-1} gene copies/16S rRNA gene copies) and low in native soils (10^{3} gene copies/gram and 10^{-5} gene copies/16S rRNA gene copies).

erm(F) quantities were detected in 26 out of 34 garden products, 3 out of 3 recently landscaped soils, and 1 out of the 5 native soils. While *erm*(F) mean abundances in garden products were 10^{6} gene copies/gram and 10^{-2} gene copies/16S rRNA gene copies, in native soils they were 10^{3} gene copies/gram and 10^{-5} gene copies/16S rRNA gene copies.

*intI*1 was detected in 29 out of 34 garden products and in 3 out of 3 recently landscaped soils. While the mean absolute and relative concentrations in garden products was 10^{6} gene copies/gram and 10^{-3} gene copies/16S rRNA gene copies, respectively, *intI*1 was undetected in native soils.

Relative gene abundances in commercial garden products are comparable to soils amended with manure-based commercial organic fertilizers (COFs) (Zhou et al. 2017). This may be attributed to COFs introducing approximately 60-70% of ARGs to soils amended with COFs (Zhou et al. 2019).

3.2 Inter-gene Observations

In the present study, the absolute quantities of *intI*1 and *sul*1 were found to exhibit a strong positive correlation ($r = 0.9648$, $p < 0.0001$). When analyzing relative abundances, *intI*1 was found to be highly correlated with *sul*2 ($r = 0.8505$, $p < 0.0001$) and slightly correlated with *erm*(F) ($r = 0.52623$, $p < 0.0001$). Additionally, *erm*(F) and *sul*2 were also slightly correlated ($r = 0.5804$, $p < 0.0001$) (Table A2-7). Several environmental studies have found strong associations between *intI*1 and *sul*1 gene quantities (Gillings et al. 2015; Lin et al. 2016; Nardelli et al. 2012; Peng et al. 2017), attributable to *intI*1 and *sul*1 being components of class 1 integrons (Gillings et al. 2008;

Gillings et al. 2015). Correlations of *intI*1 with *sul*2 (Lin et al. 2016; Peng et al. 2017) and *erm*(F) (Peng et al. 2017) have also been reported for fertilized soils.

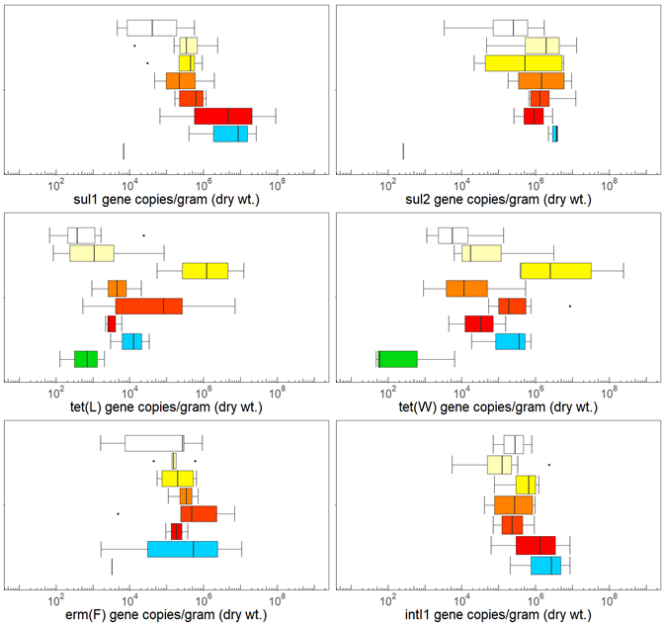

Fig. 2-2 Absolute gene abundances for potting soil (white, n=10), garden soil (light yellow, n=7), fruit amendment (yellow, n=4), lawn amendment (light orange, n=4), manure (orange, n=6), compost (red, n=3), recently landscaped soil (blue, n=3), and native soil (green, n=5).

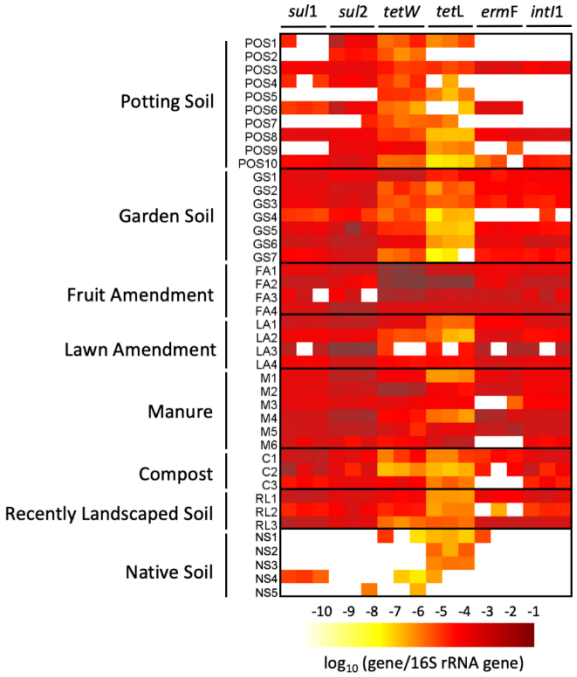

Fig. 2-3 Heatmap of relative gene abundances for 10 potting soils, 7 garden soils, 4 fruit amendments, 4 lawn amendments, 6 manures, 3 composts, 3 recently landscaped soils, and 5 native soils.

3.3 Garden Products Versus Native Soils

A Wilcoxon test for difference between the means of the native soils and garden products were significant ($p < 0.05$) for all absolute and relative gene quantities except *tet*(L). The p-values for absolute gene quantities are 0.003, 0.001, 0.011, 0.078, 0.002, and 0.004 for *sul*1, *sul*2, *erm*(F), *tet*(L), *tet*(W), and *intI*1, respectively. The p-values for relative gene quantities are 0.003, 0.001, 0.013, 0.115, 0.001, and 0.004 for *sul*1, *sul*2, *erm*(F), *tet*(L), *tet*(W), and *intI*1, respectively (Table A2-7). These results indicate the garden products are a source of ARGs when compared to native soils.

3.4 Certifications and Genes

With 33% of garden products listed as OMRI approved, OMRI was the most advertised certification. OMRI-certified and not certified garden products were found to contain gene quantities that were generally comparable ($p > 0.05$) (Table A2-7). Indicating that the OMRI certification cannot serve as an indicator for ARG introduction via garden products.

Demeter certification applies exclusively to biodynamic farms and corresponded to two garden products from just one brand (POS9 and C3). More garden products of this certification are needed to determine if the Demeter certification may serve as an ARG predictor.

3.5 Manure Sourcing and Genes

A Wilcoxon test for difference between the means of manured and non-manured sources proved to be insignificant ($p > 0.05$) except for *tet*(L) and *tet*(W) (Table A2-7). However, manure source information was not consistently available across gardening products. Even when manure source was available, proportions and pretreatments of manure were considered proprietary, largely limiting the ability to screen for pre-treatment effects on final garden product ARG levels. Results in this this study indicate that regulations considering product labelling, pre-treatment, and antibiotic, ARG, and ARB loading are needed.

5. Appendix

5.1 DNA Extraction and qPCR

Every extraction included an additional 2 mL screw cap tube preloaded with 1.00 ± 0.05 g of 0.7 mm diameter garnet beads as an extraction blank to confirm absence of contamination during the extraction process. Eluted DNA was aliquoted and stored at -20 °C awaiting qPCR analysis. Total DNA concentration was measured using UV absorption via a Nanodrop 2000C (Thermo Scientific, Waltham MA), as were 260/280 absorbance ratios.

All assays consisted of 40 cycles and were conducted using PowerUp SYBR Green Master Mix and consisted of: 12.5 µL of PowerUp SYBR Green MasterMix (Life Technologies, Grand Island, NY), 1.25 µL of each primer, 2 µL of template DNA, and 8 µL of molecular grade water. Primers and primer concentrations and reaction specifics as validated previously in the literature can be found in Table A2-1 and Table A2-2 (Ji et al. 2012; Knapp et al. 2010; Luo et al. 2010; Pei et al. 2006; Zhou et al. 2014). Each assay run included a 7-point standard curve positive control, applicable extraction blanks, and a negative control of molecular grade water, with each sample plated in triplicate wells.

Well spike and serial dilution tests were used to determine the appropriate DNA concentration and dilutions were accomplished using molecular grade water. Serial dilution involved picking random samples and serially diluting DNA by a factor of 4 and performing qPCR on all dilutions to determine the ideal dilution factor. All study samples were quantified for DNA concentration and the dilution factor was used in conjunction with the lowest DNA yield to determine an appropriate standardized dilution concentration. A second set of randomly selected samples were then used to verify absence of inhibition through performing well spikes. Unquantifiable samples were run at higher concentrations to verify absence of gene and ensure that over-dilution was not occurring.

Standard curves were designed using sequences obtained through the NCBI database and ordered through IDT Technologies (Echeverria-Palencia et al. 2017). Known concentrations of the designed DNA fragment were run alongside environmental samples, yielding a seven-point standard curve and allowing for quantitation of gene copies. Standard curve efficiencies were at or above 91% across all qPCR assays and all R^2 values were at or above 0.99. Melt curves were used to further verify target gene amplification specificity.

Table A2-1. Forward and reverse primers for qPCR assays.

Target Gene		Concentration (nM)	Sequence (5'-3')	Amplicon Size (bp)
*sul*1[a]	F	200	CGCACCGGAAACATCGCTGCAC	258
	R		TGAAGTTCCGCCGCAAGGCTCG	
*sul*2[b]	F	200	CTCCGATGGAGGCCGGTAT	449
	R		GGGAATGCCATCTGCCTTGA	
tet(L)[c]	F	900	GGTTTTGAACGTCTCATTACCTGAT	250
	R		CCAATGGAAAAGGTTAACATAAAGG	
tet(W)[d]	F	200	GAG AGC CTG CTA TAT GCC AGC	385
	R		GGG CGT ATC CAC AAT GTT AAC	
erm(F)[c]	F	500	TCGTTTTACGGGTCAGCACTT	246
	R		CAACCAAAGCTGTGTCGTTT	
*int*I1[b]	F	200	GGCTTCGTGATGCCTGCTT	424
	R		CATTCCTGGCCGTGGTTCT	
16S rRNA[e]	F	100	CCTACGGGAGGCAGCAG	257
	R		ATTACCGCGGCTGCTGG	

[a]Pei et al. 2006 [b]Luo et al. 2010 [c]Knapp et al. 2010 [d]Zhou et al. 2014 [e]Ji et al. 2012

Table A2-2. qPCR reaction conditions.

Target Gene	Holding		Denaturation		Annealing		Extension		R^2	Amp. Eff.
	Temp. (°C)	Time (min)	Temp. (°C)	Time (s)	Temp. (°C)	Time (s)	Temp. (°C)	Time (s)		
*sul*1[a]	95	10	95	15	65	30	72	30	0.991 ± 0.020	97 ± 5.8
*sul*2[b]	95	15	95	15	58.5	30	72	30	0.992 ± 0.010	91 ± 0.8
tet(L)[c]	95	10	95	15	60	30	-	-	1.000 ± 0.000	97 ± 2.0
tet(W)[d]	95	15	95	15	60	30	72	30	0.995 ± 0.001	98 ± 3.5
erm(F)[c]	95	10	94	20	60	60	-	-	0.999 ± 0.001	97 ± 1.9
*intI*1[b]	95	10	95	15	55	30	72	30	0.999 ± 0.000	98 ± 2.2
16S rRNA[e]	95	15	95	15	60	30	72	30	0.999 ± 0.005	97 ± 2.1

[a]Pei et al. 2006 [b]Luo et al. 2010 [c]Knapp et al. 2010 [d]Zhou et al. 2014 [e]Ji et al. 2012

Table A2-3. Average Log_{10} gene abundances (gene copies/gram (dry wt.)) for product categories.

Category		*sul*1		*sul*2		*tet*(L)		*tet*(W)		*erm*(F)		*intI*1	
	n	Mean	Max	Mean	Max	Mean	Max	Mean	Max	Mean	Max	Mean	Max
Potting Soil	10	5.0	5.7	5.7	6.2	3.4	4.4	4.3	5.1	5.2	6.0	5.1	5.9
Garden Soil	7	5.8	6.4	6.6	7.1	4.1	7.1	5.7	6.5	5.3	5.8	5.6	6.4
Fruit Amend.	4	5.7	6.0	6.4	6.8	6.6	7.1	8.1	8.4	5.5	5.8	5.8	6.1
Lawn Amend.	4	5.8	6.3	6.6	7.0	3.9	4.3	5.2	5.7	5.6	5.9	5.7	6.0
Manure	6	5.8	6.1	6.5	7.1	6.1	6.9	6.2	6.9	6.2	6.8	5.5	6.0
Compost	3	7.5	8.0	6.1	6.5	3.6	3.8	4.8	5.2	5.2	5.6	6.5	6.9
Recently Landscaped Soil	3	7.1	7.4	6.5	6.6	4.2	4.5	5.6	5.9	6.6	7.0	6.6	6.9
Native Soil	5	3.1	3.8	1.7	2.4	2.9	3.3	3.1	3.8	2.8	3.5	ND	ND

Table A2-4. Average Log_{10} gene abundances (gene copies/16S rRNA gene copies) for product categories.

Category		*sul*1		*sul*2		*tet*(L)		*tet*(W)		*erm*(F)		*intI*1	
	n	Mean	Max	Mean	Max	Mean	Max	Mean	Max	Mean	Max	Mean	Max
Potting Soil	10	-3.4	-2.6	-2.6	-1.9	-4.8	-4.1	-3.8	-3.0	-3.2	-2.5	-3.4	-2.5
Garden Soil	7	-2.7	-2.2	-1.8	-1.1	-4.2	-1.1	-2.8	-2.0	-3.3	-2.8	-2.9	-2.2
Fruit Amend.	4	-2.3	-1.9	-1.8	-1.3	-1.0	-0.4	-0.6	-0.2	-2.3	-2.0	-2.1	-1.8
Lawn Amend.	4	-2.2	-1.8	-0.8	-0.2	-3.9	-3.5	-3.1	-2.6	-2.0	-1.5	-2.0	-1.5
Manure	6	-2.4	-2.1	-1.6	-1.1	-2.5	-1.8	-1.7	-0.9	-1.9	-1.4	-2.6	-2.2
Compost	3	-1.7	-1.3	-2.8	-2.7	-4.8	-4.5	-3.4	-3.0	-3.8	-3.6	-2.6	-2.4
Recently Landscaped Soil	3	-2.0	-1.7	-2.6	-2.5	-4.9	-4.6	-3.4	-3.0	-2.5	-2.1	-2.4	-2.2
Native Soil	5	-4.9	-4.2	-6.1	-5.4	-5.2	-4.8	-5.2	-4.5	-5.5	-4.8	ND	ND

Table A2-5. Average Log_{10} gene abundances (gene copies/gram (dry wt.)) for samples.

Category	Sample	*sul*1	*sul*2	*tet*(L)	*tet*(W)	*erm*(F)	*intI*1
Potting Soil	POS1	3.9	6.2	3.2	3.7	ND	ND
	POS2	ND	4.4	ND	3.3	ND	ND
	POS3	5.3	5.7	4.4	4.5	6.0	5.4
	POS4	3.7	4.8	2.2	3.8	ND	ND
	POS5	ND	ND	2.6	3.7	ND	ND
	POS6	4.1	5.8	1.8	3.1	5.5	ND
	POS7	ND	3.5	2.8	3.2	ND	ND
	POS8	5.7	5.4	2.5	4.3	5.4	5.9
	POS9	ND	5.3	3.0	5.1	3.2	ND
	POS10	5.2	6.1	2.3	3.9	3.9	4.8
Garden Soil	GS1	5.9	5.6	4.9	6.5	5.1	5.5
	GS2	5.7	6.3	3.5	4.2	5.3	5.1
	GS3	5.2	5.8	3.6	3.8	4.6	4.5
	GS4	4.1	4.7	2.4	3.8	ND	3.7
	GS5	5.5	7.1	2.4	4.4	5.2	4.9
	GS6	6.4	6.8	3.0	5.7	5.8	6.4
	GS7	5.5	6.5	1.9	4.2	5.1	5.2
Fruit Amendment	FA1	6.0	6.7	6.5	8.4	5.8	6.1
	FA2	5.6	4.7	7.1	7.2	4.9	5.7
	FA3	4.5	4.3	4.7	5.6	4.7	4.9
	FA4	5.7	6.8	5.7	5.6	5.7	6.0
Lawn Amendment	LA1	6.3	6.7	3.8	5.7	5.0	6.0
	LA2	5.1	5.3	3.0	3.8	5.6	4.6
	LA3	5.6	7.0	3.5	3.0	5.9	5.9
	LA4	4.7	5.6	4.3	4.3	5.5	5.0
Manure	M1	5.2	6.4	2.7	4.9	5.4	5.0
	M2	5.2	5.8	4.7	6.9	5.7	4.9
	M3	5.9	6.0	5.5	5.9	3.7	5.4
	M4	6.0	7.1	3.2	4.7	6.8	6.0
	M5	5.7	6.3	5.2	5.3	6.4	5.7
	M6	6.1	5.8	6.9	5.3	ND	5.3
Compost	C1	6.7	6.0	3.8	4.5	5.0	6.1
	C2	8.0	6.5	3.3	3.6	5.6	6.9
	C3	4.8	5.4	3.4	5.2	ND	4.8
Recently Landscaped Soil	RL1	6.9	6.3	3.5	5.9	5.7	6.4
	RL2	5.6	6.6	4.1	5.6	3.2	5.3
	RL3	7.4	6.6	4.5	4.3	7.0	6.9
Native Soil	NS1	ND	ND	2.6	3.8	3.5	ND
	NS2	ND	ND	3.1	ND	ND	ND
	NS3	ND	ND	3.3	ND	ND	ND
	NS4	3.8	ND	2.1	1.8	ND	ND
	NS5	ND	2.4	ND	1.7	ND	ND

Table A2-6. Average Log_{10} gene abundances (gene copies/16S rRNA gene copies) for samples.

Category	Sample	*sul*1	*sul*2	*tet*(L)	*tet*(W)	*erm*(F)	*intI*1
Potting Soil	POS1	-4.3	-1.9	-4.6	-4.1	ND	ND
	POS2	ND	-3.6	ND	-4.7	ND	ND
	POS3	-3.1	-2.8	-4.1	-3.9	-2.5	-3.0
	POS4	-4.1	-3.1	-6.1	-4.1	ND	ND
	POS5	ND	ND	-5.1	-4.0	ND	ND
	POS6	-4.0	-2.2	-6.4	-5.0	-2.6	ND
	POS7	ND	-4.2	-4.9	-4.5	ND	ND
	POS8	-2.6	-3.0	-5.9	-4.1	-3.0	-2.5
	POS9	ND	-2.8	-5.1	-3.0	-5.0	ND
	POS10	-3.4	-2.5	-6.2	-4.7	-4.7	-3.8
Garden Soil	GS1	-2.6	-2.9	-3.4	-2.0	-3.3	-3.1
	GS2	-2.8	-2.3	-4.7	-4.1	-3.3	-3.4
	GS3	-2.9	-2.3	-4.5	-4.3	-3.5	-3.6
	GS4	-4.1	-3.6	-5.9	-4.4	ND	-4.5
	GS5	-2.8	-1.1	-6.0	-4.0	-3.1	-3.5
	GS6	-2.2	-1.8	-5.5	-2.8	-2.8	-2.2
	GS7	-3.2	-2.3	-6.8	-4.5	-3.6	-3.5
Fruit Amendment	FA1	-2.8	-2.0	-2.2	-0.4	-2.9	-2.6
	FA2	-1.9	-2.8	-0.4	-0.2	-2.5	-1.8
	FA3	-2.4	-2.6	-2.0	-1.1	-2.0	-2.0
	FA4	-2.4	-1.3	-2.4	-2.5	-2.4	-2.1
Lawn Amendment	LA1	-2.1	-1.7	-4.6	-2.6	-3.3	-2.4
	LA2	-3.0	-2.9	-5.1	-4.3	-2.5	-3.5
	LA3	-1.8	-0.2	-3.8	-4.6	-1.5	-1.5
	LA4	-3.1	-2.2	-3.5	-3.5	-2.4	-2.8
Manure	M1	-2.8	-1.6	-5.3	-3.1	-2.6	-3.0
	M2	-2.7	-2.1	-3.2	-0.9	-2.2	-3.0
	M3	-2.8	-2.6	-3.2	-2.7	-5.1	-3.3
	M4	-2.2	-1.1	-4.9	-3.5	-1.4	-2.2
	M5	-2.1	-1.6	-2.7	-2.5	-1.6	-2.2
	M6	-2.4	-2.7	-1.8	-3.4	ND	-3.1
Compost	C1	-1.9	-2.7	-4.5	-3.8	-3.6	-2.5
	C2	-1.3	-2.7	-5.8	-5.4	-3.6	-2.4
	C3	-3.4	-2.9	-4.8	-3.0	ND	-3.4
Recently Landscaped Soil	RL1	-1.9	-2.5	-5.4	-3.0	-3.1	-2.3
	RL2	-3.6	-2.7	-5.1	-3.7	-6.1	-3.9
	RL3	-1.7	-2.5	-4.6	-4.9	-2.1	-2.2
Native Soil	NS1	ND	ND	-5.8	-4.5	-4.8	ND
	NS2	ND	ND	-4.8	ND	ND	ND
	NS3	ND	ND	-4.9	ND	ND	ND
	NS4	-4.2	ND	-5.9	-6.3	ND	ND
	NS5	ND	-5.4	ND	-6.1	ND	ND

Table A2-7. P-values from Wilcoxon hypothesis tests.

	OMRI vs Non-OMRI		Garden Products vs Native Soils		Manure Sourcing vs Non-manure Sourcing	
	Absolute	Relative	Absolute	Relative	Absolute	Relative
*sul*1	0.244	0.330	0.003	0.003	0.985	0.660
*sul*2	0.560	0.375	0.001	0.001	0.721	0.612
erm(F)	0.155	0.098	0.011	0.013	0.527	0.150
tet(L)	0.036	0.053	0.078	0.115	0.002	0.002
tet(W)	0.166	0.143	0.002	0.001	0.008	0.008
*int*I1	0.111	0.111	0.004	0.004	0.745	0.292

6. References

Allen, H. K., Donato, J., Wang, H. H., Cloud-Hansen, K. A., Davies, J., & Handelsman, J. Call of the wild: Antibiotic resistance genes in natural environments. *Nature Reviews Microbiology*. **2010**, *8*(4), 251–259. https://doi.org/10.1038/nrmicro2312

Ashworth, J., Keyes, D., Kirk, R., Lessard, R. Standard procedure in the hydrometer method for particle size analysis. *Commun. Soil Sci. Plant Anal*. **2001**, 32, 633–642. https://doi.org/10.1081/CSS-100103897

EPA. *METHOD 1684 Total , Fixed , and Volatile Solids in Water , Solids , and Biosolids Draft January 2001 U . S . Environmental Protection Agency Office of Water Office of Science and Technology Engineering and Analysis Division (4303)*. **2001**, (January), 1–13.

Cheng, W., Chen, H., Su, C., & Yan, S. Abundance and persistence of antibiotic resistance genes in livestock farms: A comprehensive investigation in eastern China. **2013**, *Environment International*, *61*, 1–7. https://doi.org/10.1016/j.envint.2013.08.023

Code of Federal Regulations https://www.ecfr.gov/cgi-bin/text-idx?SID=4835b8a48e2533555547c742ae912ed2&mc=true&node=sp7.3.205.d&rgn=div6#se7.3.205_1300.

Dungan, R. S., Strausbaugh, C., Leytem, A. Survey of Selected Antibiotic Resistance Genes in Agricultural and Non-Agricultural Soils in South-Central Idaho. *FEMS Microbiol. Ecol.* **2019**, *95*.

Echeverria-Palencia, C. M., Thulsiraj, V., Tran, N., Ericksen, C. A., Melendez, I., Sanchez, M. G., Walpert, D., Yuan, T., Ficara, E., Senthilkumar, N., et al. Disparate Antibiotic Resistance Gene Quantities Revealed across 4 Major Cities in California: A Survey in Drinking Water, Air, and Soil at 24 Public Parks. *ACS Omega* **2017**, *2*, 2255–2263. https://doi.org/10.1021/acsomega.7b00118.

Fahrenfeld, N., Knowlton, K., Krometis, L. A., Hession, W. C.; Xia, K., Lipscomb, E., Libuit, K., Green, B. L., Pruden, A. Effect of Manure Application on Abundance of Antibiotic Resistance Genes and Their Attenuation Rates in Soil : Field-Scale Mass Balance Approach. *Environ. Sci. Technol.* **2014**, https://doi.org/10.1021/es404988k.

Gillings, M. R. DNA as a Pollutant: The Clinical Class 1 Integron. *Curr. Pollut. Reports* **2018**, *4* (1), 49–55. https://doi.org/10.1007/s40726-018-0076-x.

Gillings, M., Boucher, Y., Labbate, M., Holmes, A., Krishnan, S., Holley, M., & Stokes, H. W. The evolution of class 1 integrons and the rise of antibiotic resistance. *Journal of Bacteriology*. **2008**, *190*(14), 5095–5100. https://doi.org/10.1128/JB.00152-08

Gillings, M. R., Gaze, W. H., Pruden, A., Smalla, K., Tiedje, J. M., Zhu, Y.-G. Using the Class 1 Integron-Integrase Gene as a Proxy for Anthropogenic Pollution. *ISME J.* **2015**, *9* (10), 1269–1279. https://doi.org/10.1038/ismej.2014.226.

Hall, B. G., & Barlow, M. Evolution of the serine β-lactamases: Past, present and future. *Drug Resistance Updates*. **2004**, *7*(2), 111–123.https://doi.org/10.1016/j.drup.2004.02.003

He, Y., Yuan, Q., Mathieu, J., Stadler, L., Senehi, N., Sun, R., Alvarez, P. J. J. Antibiotic Resistance Genes from Livestock Waste: Occurrence, Dissemination, and Treatment. *npj Clean Water* **2020**, *3* (1), 4. https://doi.org/10.1038/s41545-020-0051-0.

Heuer, H., Schmitt, H., Smalla, K. Antibiotic Resistance Gene Spread Due to Manure Application on Agricultural Fields. **2011**, 236–243. https://doi.org/10.1016/j.mib.2011.04.009.

Heuer, H., Solehati, Q., Zimmerling, U., Kleineidam, K., Schloter, M., Müller, T., Focks, A., Thiele-Bruhn, S., Smalla, K. Accumulation of Sulfonamide Resistance Genes in Arable Soils Due to Repeated Application of Manure Containing Sulfadiazine. *Appl. Environ. Microbiol.* **2011**, *77* (7), 2527–2530. https://doi.org/10.1128/AEM.02577-10.

Jacobs, K., Wind, L., Krometis, L.-A., Hession, W. C., Pruden, A. Fecal Indicator Bacteria and Antibiotic Resistance Genes in Storm Runoff from Dairy Manure and Compost-Amended Vegetable Plots. *J. Environ. Qual.* **2019**, *48* (4), 1038–1046. https://doi.org/10.2134/jeq2018.12.0441.

Jechalke, S., Kopmann, C., Rosendahl, I., Groeneweg, J., Weichelt, V., Krögerrecklenfort, E., Brandes, N., Nordwig, M., Ding, G.-C., Siemens, J., et al. Increased Abundance and Transferability of Resistance Genes after Field Application of Manure from Sulfadiazine-Treated Pigs. *Appl. Environ. Microbiol.* **2013**, *79* (5), 1704–1711. https://doi.org/10.1128/AEM.03172-12.

Ji, X., Shen, Q., Liu, F., Ma, J., Xu, G., Wang, Y., Wu, M. Antibiotic Resistance Gene Abundances Associated with Antibiotics and Heavy Metals in Animal Manures and Agricultural Soils Adjacent to Feedlots in Shanghai; China. *J. Hazard. Mater.* **2012**, *235–236*, 178–185. https://doi.org/10.1016/j.jhazmat.2012.07.040.

Knapp, C. W.; Dolfing, J., Ehlert, P. A. I., Graham, D. W. Evidence of Increasing Antibiotic Resistance Gene Abundances in Archived Soils since 1940. *Environ. Sci. Technol.* **2010**, *44* (2), 580–587. https://doi.org/10.1021/es901221x.

Lin, H., Sun, W., Zhang, Z., Chapman, S. J., Freitag, T. E., Fu, J., … Ma, J. Effects of manure and mineral fertilization strategies on soil antibiotic resistance gene levels and microbial community in a paddy-upland rotation system. **2016**, *Environmental Pollution*, *211*, 332–337. https://doi.org/10.1016/j.envpol.2016.01.007

Liu, J., Zhao, Z., Orfe, L., Subbiah, M., & Call, D. R. Soil-borne reservoirs of antibiotic-resistant bacteria are established following therapeutic treatment of dairy calves. *Environmental Microbiology*. **2016**, *18*(2), 557–564. https://doi.org/10.1111/1462-2920.13097

Looft, T., Johnson, T. A., Allen, H. K.; Bayles, D. O., Alt, D. P., Stedtfeld, R. D., Sul, W. J., Stedtfeld, T. M., Chai, B., Cole, J. R., et al. In-feed antibiotic effects on the swine

intestinal microbiome. *Proc. Natl. Acad. Sci.* **2012**, *109* (5), 1691–1696.

Luo, Y. I., Mao, D., Rysz, M. Trends in Antibiotic Resistance Genes Occurrence in the Haihe River , China. **2010**, *44* (19), 7220–7225.

Marti, R., Scott, A., Tien, Y. C., Murray, R., Sabourin, L., Zhang, Y., & Topp, E. Impact of manure fertilization on the abundance of antibiotic-resistant bacteria and frequency of detection of antibiotic resistance genes in soil and on vegetables at harvest. *Applied and Environmental Microbiology*. **2013**, *79*(18), 5701–5709. https://doi.org/10.1128/AEM.01682-13

McEachran, A. et al. Antibiotics, Bacteria, and Antibiotic Resistance Genes: Aerial Transport from Cattle Feed Yards via Particulate Matter. *Environ. Health Perspect.* **2012**, No. May, 337–343. https://doi.org/10.1289/ehp.0800317.

McKinney, C.; Dungan, R.; Moore, A.; Leytem, A. Occurrence and Abundance of Antibiotic Resistance Genes in Agricultural Soils Receiving Dairy Manure. *FEMS Microbiol. Ecol.* **2018**, *94* (fiy010).

Munir, M., & Xagoraraki, I. Levels of Antibiotic Resistance Genes in Manure, Biosolids, and Fertilized Soil. **2011**, *Journal of Environmental Quality*, *40*(1), 248–255. https://doi.org/10.2134/jeq2010.0209

Nardelli, M.; Scalzo, P. M.; Ramírez, M. S.; Quiroga, M. P.; Cassini, M. H.; Centrón, D. Class 1 Integrons in Environments with Different Degrees of Urbanization. *PLoS One* **2012**, *7* (6). https://doi.org/10.1371/journal.pone.0039223.

National Organic Program Handbook https://www.ams.usda.gov/sites/default/files/media/Program%20Handbk_TOC.pdf

O'Neill, J. *Antimicrobial Resistance: Tackling a crisis for the health and wealth of nations The Review on Antimicrobial Resistance Chaired*. **2014**, (December).

Pei, R., Kim, S.-C., Carlson, K. H., Pruden, A. Effect of River Landscape on the Sediment Concentrations of Antibiotics and Corresponding Antibiotic Resistance Genes (ARG). *Water Res.* **2006**, *40* (12), 2427–2435. https://doi.org/10.1016/j.watres.2006.04.017.

Peng, S., Feng, Y., Wang, Y., Guo, X., Chu, H., & Lin, X. Prevalence of antibiotic resistance genes in soils after continually applied with different manure for 30 years. **2017**, *Journal of Hazardous Materials*, *340*, 16–25. https://doi.org/10.1016/j.jhazmat.2017.06.059

Sancheza, H. M., Echeverria, C., Thulsiraj, V., Zimmer-Faust, A., Flores, A., Laitz, M., Healy, G., Mahendra, S., Paulson, S. E., Zhu, Y., et al. Antibiotic Resistance in Airborne Bacteria Near Conventional and Organic Beef Cattle Farms in California, USA. *Water. Air. Soil Pollut.* **2016**, *227* (8). https://doi.org/10.1007/s11270-016-2979-8.

Sandberg, K. D., LaPara, T. M. The fate of antibiotic resistance genes and class 1 integrons

following the application of swine and dairy manure to soils. *FEMS Microbiol. Ecol.* **2016**, *92* (2), 1–7.

Sarmah, A. K., Meyer, M. T., Boxall, A. B. A. A global perspective on the use, sales, exposure pathways, occurrence, fate and effects of veterinary antibiotics (VAs) in the environment. *Chemosphere*. **2006**, *65* (5), 725–759.

Tien, Y. C., Li, B., Zhang, T., Scott, A., Murray, R., Sabourin, L., Marti, R., Topp, E. Impact of Dairy Manure Pre-Application Treatment on Manure Composition, Soil Dynamics of Antibiotic Resistance Genes, and Abundance of Antibiotic-Resistance Genes on Vegetables at Harvest. *Sci. Total Environ.* **2017**, *581–582*, 32–39. https://doi.org/10.1016/j.scitotenv.2016.12.138.

USFDA. Antimicrobials Sold or Distributed for Use in Food-Producing Animals. **2018**

Wang, L., Gutek, A., Grewal, S., Michel, FC, J., Yu, Z. Changes in Diversity of Cultured Bacteria Resistant to Erythromycin and Tetracycline in Swine Manure during Simulated Composting and Lagoon Storage. *Lett. Appl. Microbiol.* **2015**, *61* (3), 245–251.

Zhou, T., Lu, J., Tong, Y., Li, S., & Wang, X. Distribution of antibiotic resistance genes in Bosten Lake, Xinjiang, China. **2014**, *Water Science and Technology*, *70*(5), 925–931. https://doi.org/10.2166/wst.2014.321

Zhou, X., Qiao, M., Su, J. Q., & Zhu, Y. G. High-throughput characterization of antibiotic resistome in soil amended with commercial organic fertilizers. **2019**, *Journal of Soils and Sediments*, *19*(2), 641–651. https://doi.org/10.1007/s11368-018-2064-6

Zhou, X., Qiao, M., Wang, F. H., & Zhu, Y. G. Use of commercial organic fertilizer increases the abundance of antibiotic resistance genes and antibiotics in soil. **2017**, *Environmental Science and Pollution Research*, *24*(1), 701–710. https://doi.org/10.1007/s11356-016-785

Chapter 3: Antibiotic resistance genes in reclaimed water for irrigation in the Maneadero Valley, Mexico

1. Introduction

Water sustainability, food security, and increasing global antibiotic resistance are issues of paramount importance for humanity, linked in complex ways and cast on a landscape of changing climate and rising population. Over the last century, major advances in water quality, food production, and treatment of diseases with antibiotics have improved the quality of life of the human population immeasurably. Again, in parallel, each now faces issues of sustainability that if left unaddressed, could seriously threaten the gains we have enjoyed (WHO, 2014).

Changes in our approach to how we consume and recycle water offer tremendous synergistic benefits. Far from being waste products, wastewaters are virtually untapped sources of freshwater, nutrients, and even energy. The numerous and far-reaching benefits of reuse include incentivizing higher levels of treatment, reducing water pollution, increasing water supplies, minimizing stress on environmental water flows (thus enhancing ecosystem services), mitigating seawater intrusion, and lowering costs compared to other water supplies that may need to travel long distances. In the face of changing water cycles and increasing populations, significantly increased use of recycled water will be critical to achieving water and food sustainability across the globe.

New knowledge is needed both to inform the safe application of this resource and to address the stigma frequently associated with its use. Issues of particular concern for human health are the persistence of pathogens and antibiotic resistance genes (ARGs) in soil irrigated with treated wastewater and the synergistic effect that chemical contaminants can have on the proliferation of antibiotic resistance. While chemical contaminants themselves are not the main

focus of the study, the speciation and bioavailability of those that have been shown to promote antibiotic resistance will be investigated in detail.

There have been previous studies dealing with the presence of ARG's in water, soils, and other matrices in Mexico and even in the border region between Mexico and the USA. Fuentes et al. (2019) evaluated the concentration of antibiotic residues, to determine the presence of genetic elements conferring antibiotic resistance and to characterize multi-drug resistant bacteria in the waters of the Rio Grande. Antibiotics were found in 92% of both water and sediment samples. Antibiotic concentrations ranged from 0.38 ng/L - 742.73 ng/L and 0.39 ng/l - 66.3 ng/g dry weight in water and sediment samples, respectively. Genetic elements conferring resistance were recovered from all collection sites. Of the isolated bacteria, 91 (64.08%) were resistant to at least two synergistic antibiotic combinations and 11 (14.79%) were found to be resistant to 20 or more individual antibiotics. Fecal contamination was higher during the months of April and July.

The presence of pharmaceuticals in wastewater- irrigated soils has been documented for several sites worldwide. However, it is currently unclear whether and to which degree continuous irrigation with wastewater may lead to a long-term accumulation of these agents in soil (Dalkmann et al., 2012).

The Maneadero Valley in Mexico is a coastal agricultural region, which was historically irrigated by the Maneadero aquifer. The aquifer serves as the main water source to the cities of Ensenada and Maneadero, but has been over-abstracted at a rate of 5.4 million cubic meters per year, causing significant seawater intrusion. This salinity has caused severe deterioration of the groundwater quality for agriculture and domestic water supply (Daesslé et al., 2005). Mendoza-Espinosa and Daesslé-Heuser (2012) proposed using plant effluent as reclaimed water (RW) from the nearby *El Naranjo* for the irrigation of these farms, and beginning in 2014, this RW irrigates

at least 140-150 ha of flowers and crops not for human consumption and when there is excess RW after supply to farms for irrigation, the water is discharged into the nearby Las Animas Creek (Mendoza-Espinosa and Daesslé-Heuser, 2018).

Soils and sediments have been implicated as reservoirs and potential havens for pathogens (Echeverria-Palencia et al., 2017; Jeanneau et al., 2012; Knapp et al., 2011) as these environments can provide protection from both ultraviolet radiation and predation by microorganisms in the overlying water column (Korajkic et al., 2019). However, while viable pathogens and ARGs can persist for extended periods in soils, their fate in these compartments is particularly understudied. Our work aims to fill this knowledge gap by specifically quantifying antibiotic resistance genes (ARGs) in the RW, point of use RW storage tanks, and the agricultural soil irrigated with the RW. In order to more readily assess the public health relevance of ARGs detected, we also use PMA-qPCR (propidium monoazide-qPCR) to quantify genes detected from viable versus non-viable cells.

2. Methods

2.1 Sample Collection and Study Site

Sampling was undertaken in two periods: June 2019 and January 2020. The first period served as method optimization for the research, and the data and methods discussed in this work are all from the second sampling period. After the first sampling period the DNA extraction kit was changed, the filtration process was optimized for power and efficiency, and five soil samples per farm (rather than three) were taken.

Sampling sites are shown in Figure 3-1, with the corresponding GPS coordinates shown in Table 3-1. Water samples collected were the El Naranjo WWTP effluent, Maneadero WWTP UV effluent, Las Animas Creek water, RW at the point of use of 3 different farms, and groundwater (GW) from a fourth farm to serve as a RW control. At the 3 farms irrigating with RW, two samples

were taken – from running influent into the farm's storage tank, and from the opposite side of the tank). The latter serves as a representation of the water used for irrigation, but it should be noted that the grab sample is from the surface of the open-air tank and is not a sample of the effluent from the holding tank.

El Naranjo WWTP is an activated sludge system operated as an oxidation ditch, providing nitrification/denitrification in addition to the oxidation of organic matter; the effluent is chlorinated before discharge.

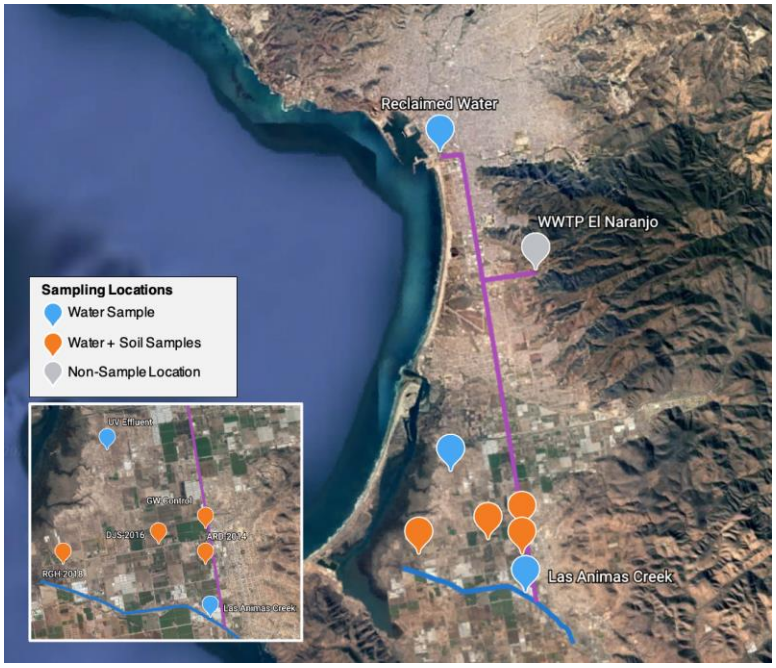

Figure 3-1. Sampling locations in Ensenada and Maneadero Valley.

2.2 Water Collection and Processing

At each site, sample water was collected in autoclaved polypropylene plastic bottles prewashed with sample. Samples were transported on ice to the field laboratory location and were processed immediately upon arrival.

For the measurement of gene copies per mL, sample water was vacuum-filtered through 37-mm, 0.45 um pore-size, mixed cellulose ester (MCE filters) (Millipore Sigma, Darmstadt, Germany) using a gast vacuum pressure pump in the field. For quantification by qPCR, water was

filtered in at least triplicate of turbidity-dependent maximum volumes. Filters were washed with phosphate buffered saline (PBS) before removal, unless the sample was very turbid, in which case volume-filtered was prioritized over the final wash. Each filter was folded and placed in an individual 2 mL polypropylene screw-cab and stored at -20°C until extraction, with the exception of car transport from Rosarito, Mexico to the laboratory at UCLA. From Rosarito to the Mexico-US border, samples were stored on ice alone because of the unavailability of dry ice in the region. Immediately upon crossing the border, samples were stored for transport with dry ice for the remainder of transport to the laboratory that evening. Filter blanks, consisting of 100 mL volume of PBS passed through the MCE filter, were also generated with the processed samples.

For PMA-qPCR experiments, an additional equivalent volume was filtered and washed similarly for each sample, followed by further processing as explained below.

For all water samples, at the time of collection, conductivity, temperature, and dissolved oxygen (DO) was measured using a Hydrolab Quanta Multiparameter Sonde (Hach Hydromet, Loveland, CO), and pH was estimated using test strips. DO measurements from the Hydrolab could not be measured due to a manufacturer defect that affected the probe during sampling. Turbidity of water samples was measured when the samples were brought back to the field lab location using a LaMotte Turbidimeter 2020.

2.3 Soil Collection and Processing

Soil samples were collected in acid-washed 60-mL glass screw-top jars. Five samples were taken for each farm – ARD, DJS, RGH, and GW. Sample locations for each farm were decided by a random matrix, and were at least ten meters apart. For each farm, all samples were taken in the field plot that had most recently been harvested in order to avoid damaging crops.

For qPCR, Soil samples were sieved (2 mm) and weighed to approximately 0.25 g (wet weight) and stored in individual 2 mL polypropylene screw-cab and stored at -20°C until extraction

(with the same extenuating transport circumstance as explained for water filter transportation). For PMA-qPCR, a homogenous soil sample was created from the quintuplicate soil field samples, and this sample was weighed to approximately 1.25 g (wet weight). Gravimetric soil moisture was determined in quintuplicate by sequential loss on ignition (LOI) at 105 °C for 24 hours.

2.4 DNA Extraction and qPCR

DNA from samples was extracted by either using the ZymoBIOMICS DNA Miniprep Kit (Zymo Research, Irvine, CA) or the FastDNA Spink Kit for Soil (MP Biomedicals, Irvine, CA). Because of the COVID-19 pandemic, a different DNA extraction kit during the study had to be used due to supply chain issues. DNA was extracted according to the manufacturer's protocol, with the addition of a pre-extraction protocol modified from Li et al. (2018) in order to maximize DNA recovered from the water filters. Nucleic acid concentration was determined using UV absorption with a Nanodrop 2000C (Thermo Scientific, Waltham, MA). A preloaded tube used to assess any possible contamination during the extraction process (extraction blank) was extracted in parallel.

Briefly, for all assays other than the 16S rRNA gene (with 16S volumes following in parentheses), the qPCR mixture consisted of 3 μL (2 μL) of appropriately diluted DNA template added to 10 μL (12.5 μL) of SYBR PowerUp^{TM} Master Mix (Thermo Fisher Scientific, Waltham, MA), 1 μL (1.25 μL) each of both forward and reverse primer working concentrations, and 5 μL (3 μL) of molecular grade RNAse-free molecular biological grade water (Fisher Scientific, Pittsburgh, PA), for a final reaction volume of 20 μL (25 μL). DNA template was diluted prior to qPCR to offset inhibition effects, which were determined by the dilution protocol defined by Cao et al. (2012). All assays were performed in 96-well reaction plates using a StepOne Plus Real-Time PCR System (Applied Biosystems, Foster City, CA). Cycling conditions, primer sequences,

and concentrations have been previously validated and are detailed in Tables A3-1 and A3-2 in Appendix B. All qPCR samples were run in triplicate. Standard curves covering over 7 orders of magnitude were constructed with 10-fold serial dilutions of known amounts of dsDNA from Integrated DNA Technologies, Inc. (Coralville, IA). All applicable negative controls were run for each assay, and a no template control was run in each plate. Quantification thresholds were converted into units of gene copies for each plate using a standard curve. Threshold and baseline values were determined automatically for each plate by the machine's associated software. Following qPCR, melting curves were generated and analyzed to verify that nonspecific amplification did not occur. R^2 values were more than 0.99 for all standard curves, and efficiencies ranged from 90% to 110%.

2.5 PMA-qPCR

PMA was applied to samples in order to understand whether ARGs were from viable cells. PMA was applied to both water and soil samples. Although we found that the PMA application to soil would have to be further optimized, we include the procedure used.

Prior to the field work, the PMA method was optimized in the laboratory at UCLA for highest yield of bacterial elution from soil, proper sedimentation velocities for soil and bacterial cells, PMA concentration applied, and storage method of the solution after application.

The main problem with using the PMA-qPCR method for the measurement of low environmental concentration genes such as ARGs in soil is that the light activation of the PMA cannot occur in a turbid sample, but high amounts of soil are needed for gene quantities above the lower limit of detection. Because of this, bacterial soil extractions were used to maximize the cells retrieved from the soil before beginning the PMA application.

Approximately 1.25 g of soil were added to 10 mL of PBS in a 50 mL falcon tube and was hand shaken for 2 minutes. The sample was then aliquoted into 10-1.7 mL microcentrifuge tubes, at approximately 1.1 mL each. (In the field, due to the unavailability of a centrifuge with a rotor that could hold 50 mL Falcon tubes, soil suspension were aliquoted into 1.7 mL tubes). These tubes were centrifuged at 500 xg for 2 minutes in order to remove soil particulates, and the suspension was transferred to new 1.7 mL tubes and centrifuged at 10,000 xg for 3 minutes (Robe et al., 2003; Fægri et al., 1977; Thulsiraj et al., 2017)**.** The liquid was removed, being conservative to not disturb the cell pellet, and the pellet was resuspended to 50 µL. These 50 µL suspensions were then all combined and suspended to exactly 1 mL in PBS.

To prepare water filters for application of PMA, each filter was placed in 5 mL of PBS and hand-shaken for two minutes. One mL of resuspension was used for analysis of PMA treatment.

Following respective water filter and soil sample preparations, the application of PMA was identical and was generally according to the manufacturer's (Biotium, Fremont, CA) protocol with some slight modifications based upon the literature. Each 1-mL resuspension was aliquoted into 2-500 µL volumes, for which one had PMA added and one did not. The one that did not still underwent all further steps. PMAxx Dye (Biotium, Fremont, CA) was added to a final concentration of 50 uM to half of the subsamples (Nocker and Camper, 2009), and was vortexed gently (Vortex level 2 on Fisher Vortex Genie 2) in the dark for 2 minutes at room temperature (Carini et al., 2016; Nocker and Camper, 2009). The PMA was activated by exposure to a 10,000 lux, flat, Verilux LED light from 20 cm distance for a total of two minutes. After 1 minute, the sample was manually rotated for even activation. The samples were then centrifuged at 10,000 xg for 5 minutes at room temperature and resuspended in 500 µL of PBS and stored at -20 C° until

extraction. Dead cell controls were performed according to the manufacturer's protocol, with modifications made to adjust for our optimized PMA application procedure.

3. Results

3.1 Field sampling measurements

Sample names used from here forward are given in Table 3-1, along with water quality parameters measured, soil moisture content, and site location.

3.2 qPCR Results of Water Samples

The ARGs, *int*I1, and 16S rRNA genes per volume of water filtered were all quantified using qPCR. From Figure 3-2, it can be seen that the RW is consistently similar to the water on farms that use RW, and that water on farms using RW is consistently higher than that of the GW (or control) site. Additionally, for all genes, the creek water is similar in gene abundance to that of the RW and the water used on farms irrigating with RW.

On average on farms using RW, *sul*1 and *sul*2 genes are approximately 1.0E5 – 1.0E6 genes per mL. *tet*W and *erm*F genes are approximately between 1.0E4 – 1.0E5 genes per mL, and *int*I1 genes are between 1.0E4 and 1.0E6 genes per mL.

The abundance of the ARGs, *int*I1, and the 16S rRNA gene is less in the GW and the UV effluent than in all other samples. The abundance of all ARGs and *int*I1 in the GW is notable either non-detected or at least five orders of magnitude less than the abundance of the RW. Even for the 16S rRNA gene, which is an approximation of the total number of cells present, the gene abundance is approximately four orders of magnitude less than in the RW. In the UV effluent, gene abundances are generally greater than in the GW but still significantly less than in the other samples.

All genes were normalized to the 16S rRNA gene in order to obtain normalized values of the gene per approximate total bacterial cells. These results are shown in Figure 3-3. The relative

abundance of *int*I1 in the RW is greater than that in the ARGs, where the relative abundance of *intI*1 is 11.8% +/- 5.6% and those of the ARGs range from 0.32% +/- 0.05% (*tet*W) to 3.95% ± 1.95% (*sul*1).

Most notable from these results is that normalized genes in the GW sample are zero for all genes, compared to those from the farms using RW. A general trend from Figure 3-3 is that the relative abundance of most genes is less in the irrigation water than it is in the on-site RW storage. *intI*1 is unique in that it is significantly higher in the RW than in the farm's water, with the exception of the 2018 – Present On-site RW Storage sample. While the absolute abundance of ARGs in the creek water was comparable to the gene abundances of the RW farms, the result is less comparable when using relative abundance. For *sul*1 and *erm*F, it is still comparable to on-site RW Storage waters, while for *sul*2 it is less than the farms' storage, on average. For *tet*W and *intI*1, the creek has in general less genes per 16S rRNA gene than the RW storage on the farms.

Another observation is that the irrigation water from the farm that began irrigating with RW in 2018 is less than that of either one or both of the farms that began irrigating with RW in 2014 or 2016.

Table 3-1. Field measurements summary table.

Site	Sample	Reclaimed Water Use Start	Location (decimal degrees)	Soil Moisture Content	Water SpCond (mS/cm)	Water Temp (C)	Water pH	Water Turbidity
RW	RW	-	31.846520, -116.611520	-	4.838	19.85	6.5	8.4
UV Eff	UV Eff	-	31.7463972, -116.6075833	-	4.517	20.82	7.1	1.6
Control	Control	Never	31.7285222, -116.581275	-	8.468	22.22	6.8	2.9
	Soil-A			18.68%	-	-	-	-
	Soil-B			24.72%	-	-	-	-
	Soil-C			16.97%	-	-	-	-
	Soil-D			26.52%	-	-	-	-
	Soil-E			24.05%	-	-	-	-
ARD	Tank	2014	31.7204139, -116.6193556	-	4.171	20.13	6.5	4.2
	Irrigation			-	4.162	15.95	6.5	144.4
	Soil-A			20.12%	-	-	-	-
	Soil-B			23.21%	-	-	-	-
	Soil-C			26.08%	-	-	-	-
	Soil-D			19.26%	-	-	-	-
	Soil-E			22.03%	-	-	-	-
DJS	Tank	2016	31.7250033, -116.593825	-	4.199	19.52	6.5	18.2
	Irrigation			-	4.596	15.83	6.5	15.8
	Soil-A			22.35%	-	-	-	-
	Soil-B			21.24%	-	-	-	-
	Soil-C			20.26%	-	-	-	-
	Soil-D			23.24%	-	-	-	-
	Soil-E			23.20%	-	-	-	-
RGH	Tank	2018	31.7204139, -116.6193556	-	4.777	19.33	6.0	6.1
	Irrigation			-	4.346	16.98	6.0	12.7
	Soil-A			8.52%	-	-	-	-
	Soil-B			13.91%	-	-	-	-
	Soil-C			9.23%	-	-	-	-
	Soil-D			14.35%	-	-	-	-
	Soil-E			19.24%	-	-	-	-
Creek	Creek	-	31.7084139, -116.5799722	-	4.12	21.03	6.8	11.2

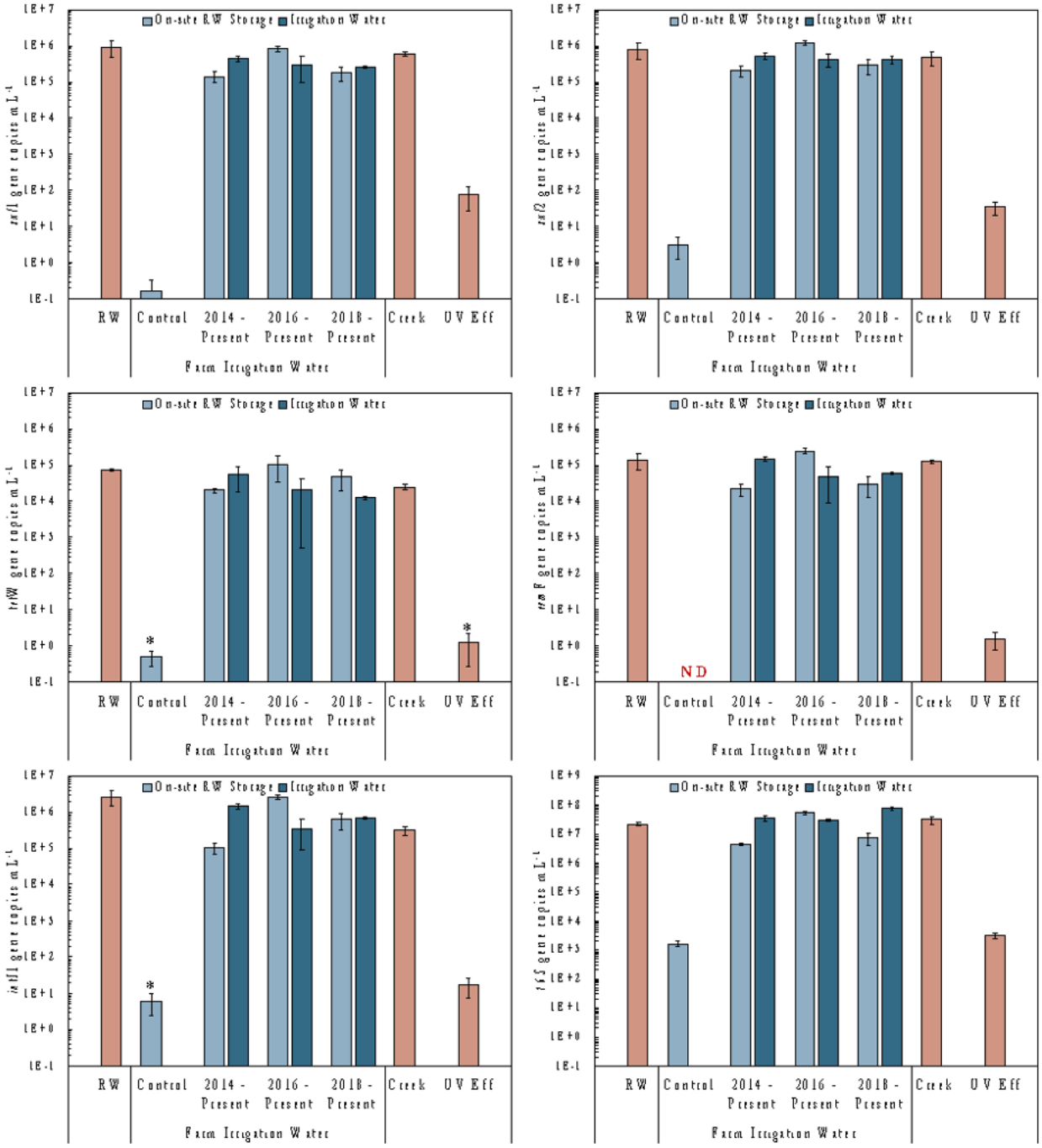

Figure 3-2. Absolute gene abundances in all water samples. *Samples for which at least one replicate were less than the LLOD.

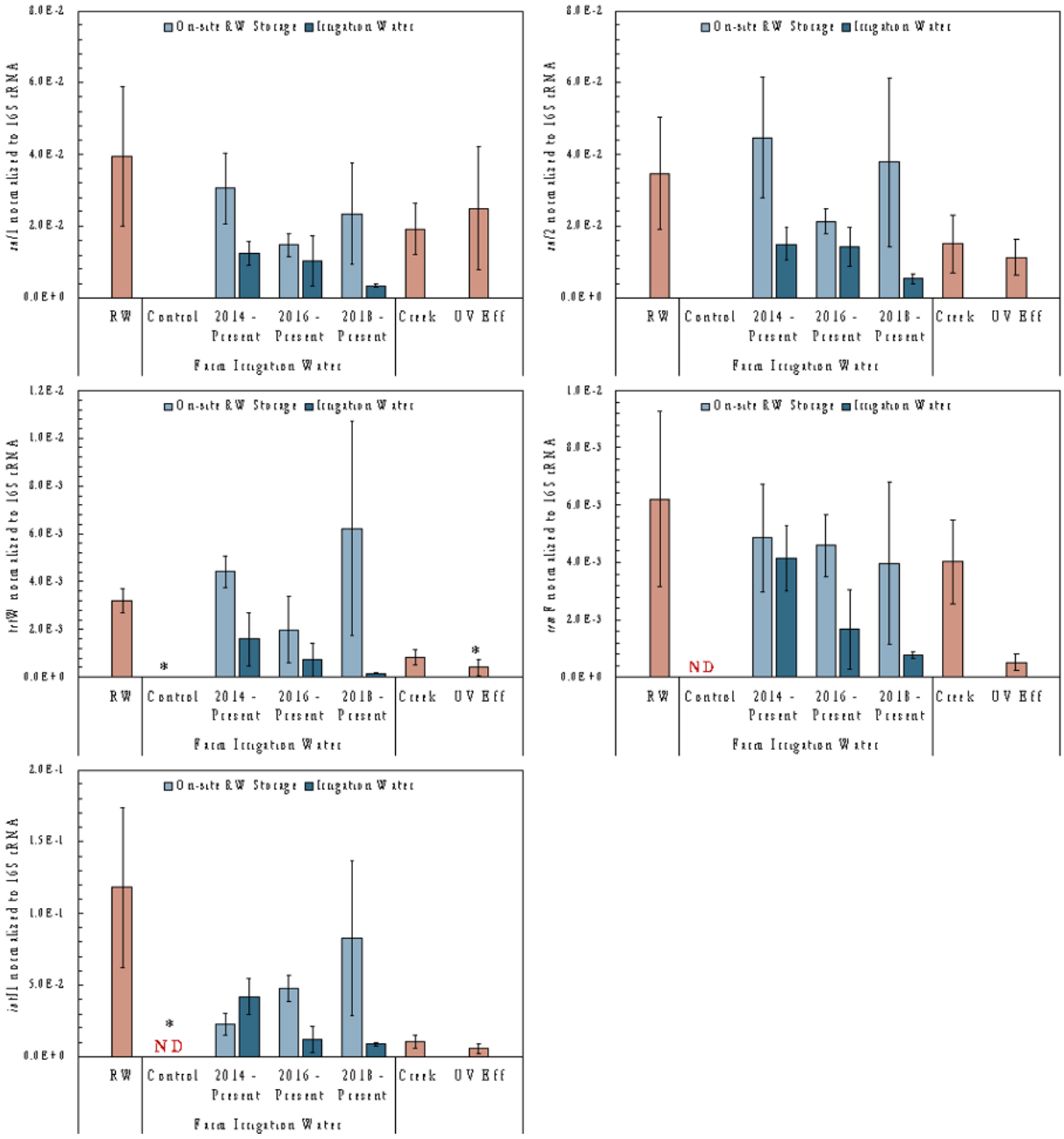

Figure 3-3. Relative gene abundances in all water samples. ND indicates that all well replicates were less than the LLOD. *Samples for which at least one replicate were less than the LLOD.

3.3 qPCR Results of Soil Samples

For all genes, it is notable that the soil irrigated with GW has significantly less genes per gram of soil than at least two of the farms irrigated with RW.

*tet*W and *erm*F gene abundances in soil are less than *sul*1 and *sul*2 abundances. There is a noticeably higher abundance in *sul*2 at the site that began using RW in 2016 than in the GW and

2014 site. The 16S abundance is consistent for the GW, 2014 and 2016 site, but is less in the 2018 site.

While the *intI*1 relative abundance was higher than other genes in the water, this is not true in the soil. In soil, although the *intI*1relative abundance is in general an order of magnitude greater than the *tet*W and *intI*1 relative abundances, it is an order of magnitude less than *sul*1 and *sul*2 abundances. Also different from the water results, there is not a downward trend in relative gene abundances with time, but instead the opposite occurs where the 2018 site has a greater relative abundance than other sites, with the exclusion of the *erm*F gene.

3.4 PMA-qPCR Results

PMA-qPCR results are shown in Figures 3-6 and 3-7 for select water samples. The RW samples show a fairly even divide between genes that come from viable and non-viable cells, with the exception of *sul*2 genes, which are almost all (94.1%) from live cells. This is strikingly different than the viability of cells that have been through the distribution system and are from water flowing into the on-site holding tanks (On-Site Storage on the graphs). In these samples, almost all (over 90%) of the genes measured were from non-viable cells, for all genes and for both the 2014 and the 2016 sites. The 2018 site is not included in this analysis because of sample damage.

After the water has been in the storage tank and is used for irrigation, there are more ARGs from viable cells than when the water entered the tank. Not surprisingly, there are almost no ARGs or *intI*1 genes from viable or non-viable cells in the UV effluent from the Maneadero WWTP. In the creek, there are high abundances of genes, but these are almost all from non-viable cells.

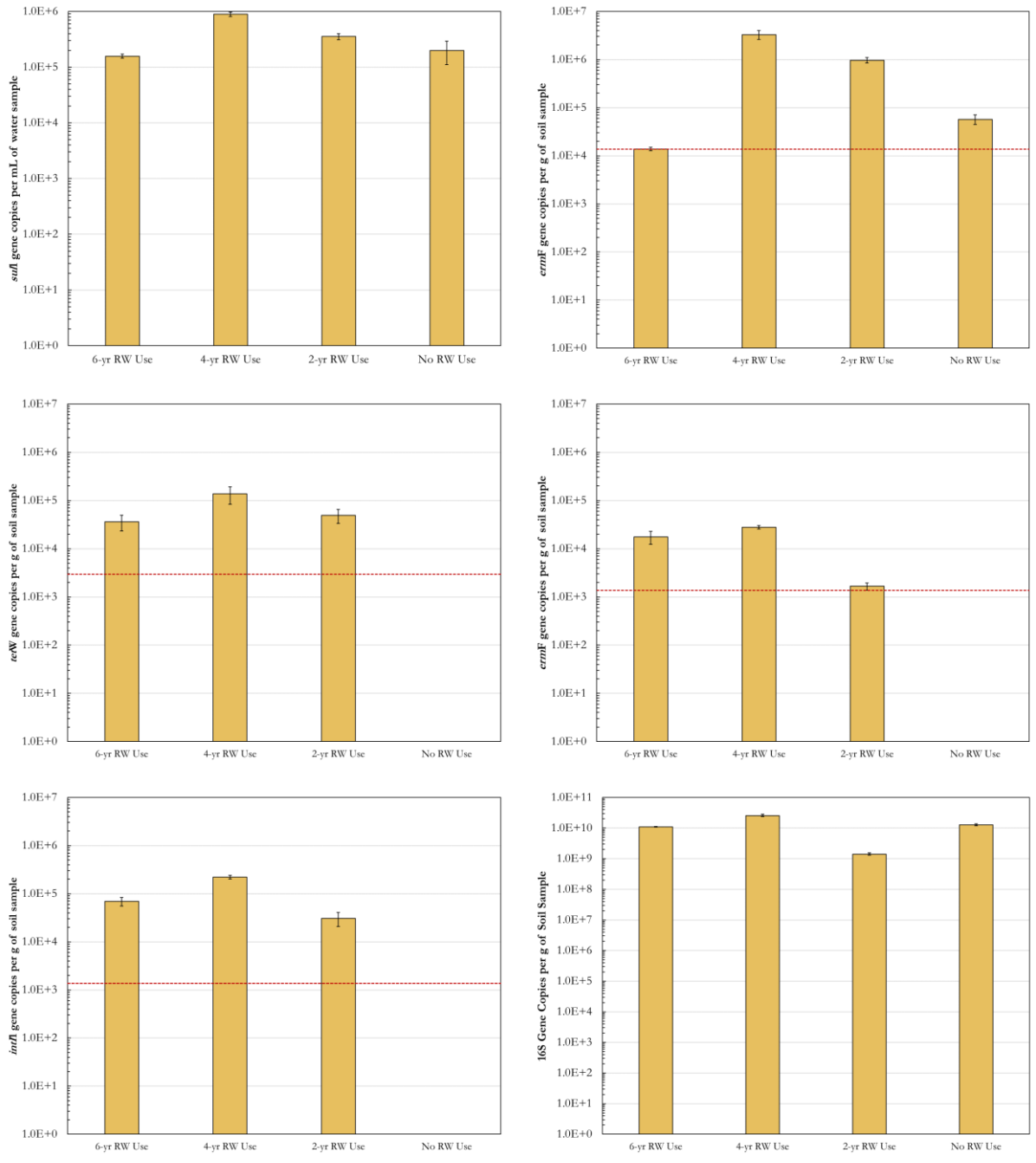

Figure 3-4. Absolute gene abundances in all soil samples.

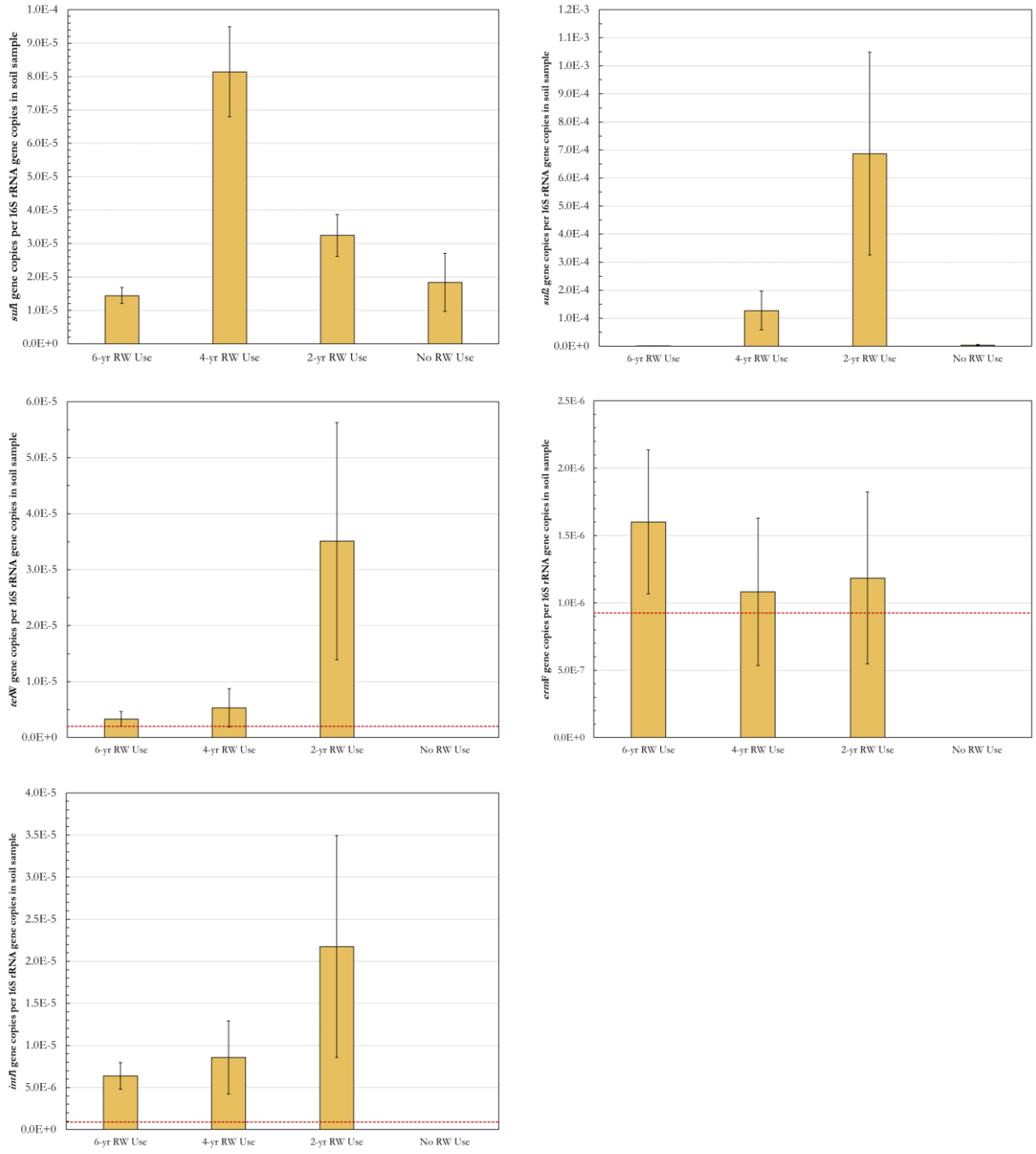

Figure 3-5. Relative gene abundances in all soil samples.

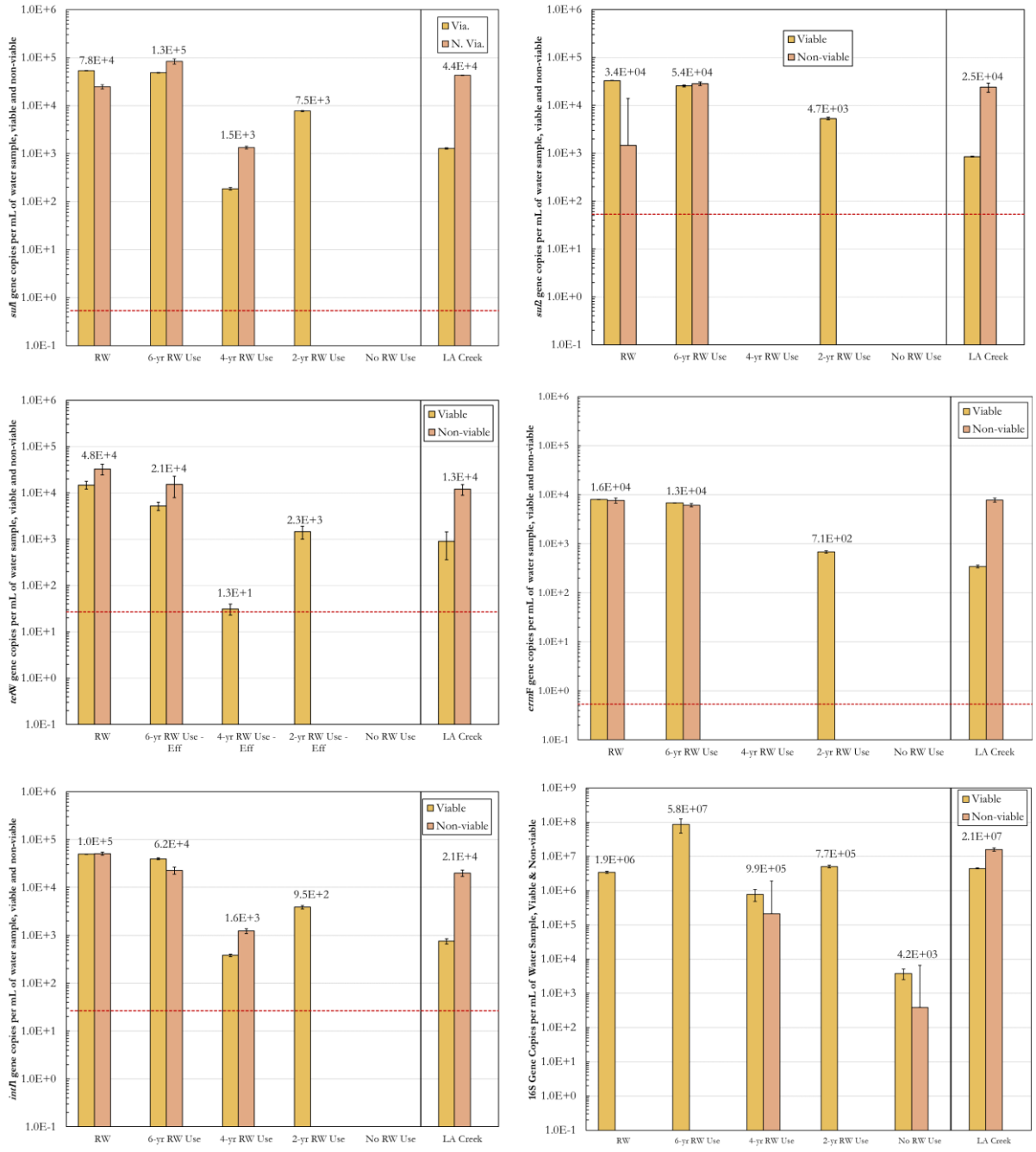

Figure 3-6. PMA-qPCR results, genes from viable and non-viable cells for RW and On-Site Storage Effluent of the RW and the Las Animas Creek.

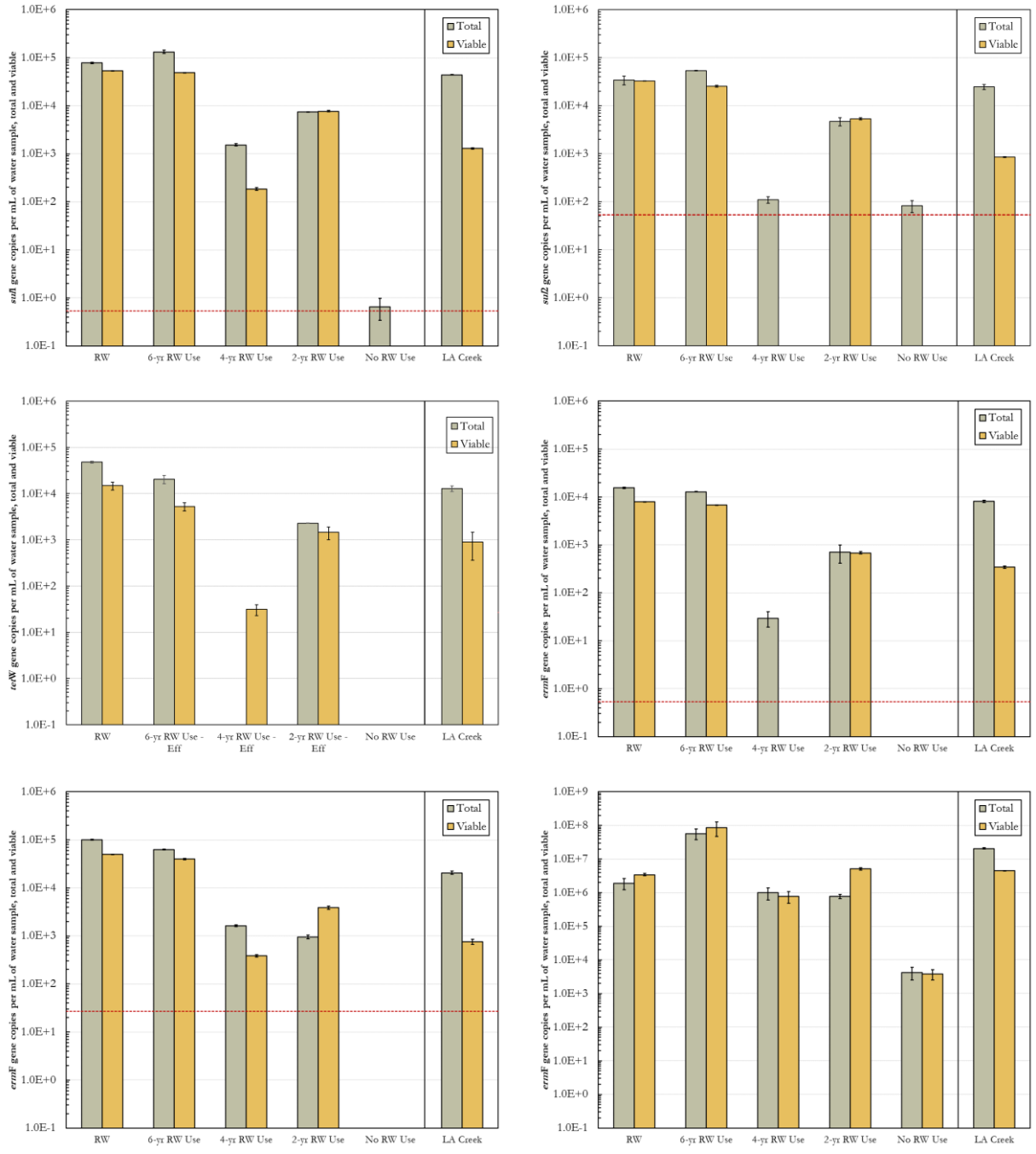

Figure 3-7. PMA-qPCR results, genes from total and viable cells for RW and On-Site Storage Effluent of the RW and the Las Animas Creek.

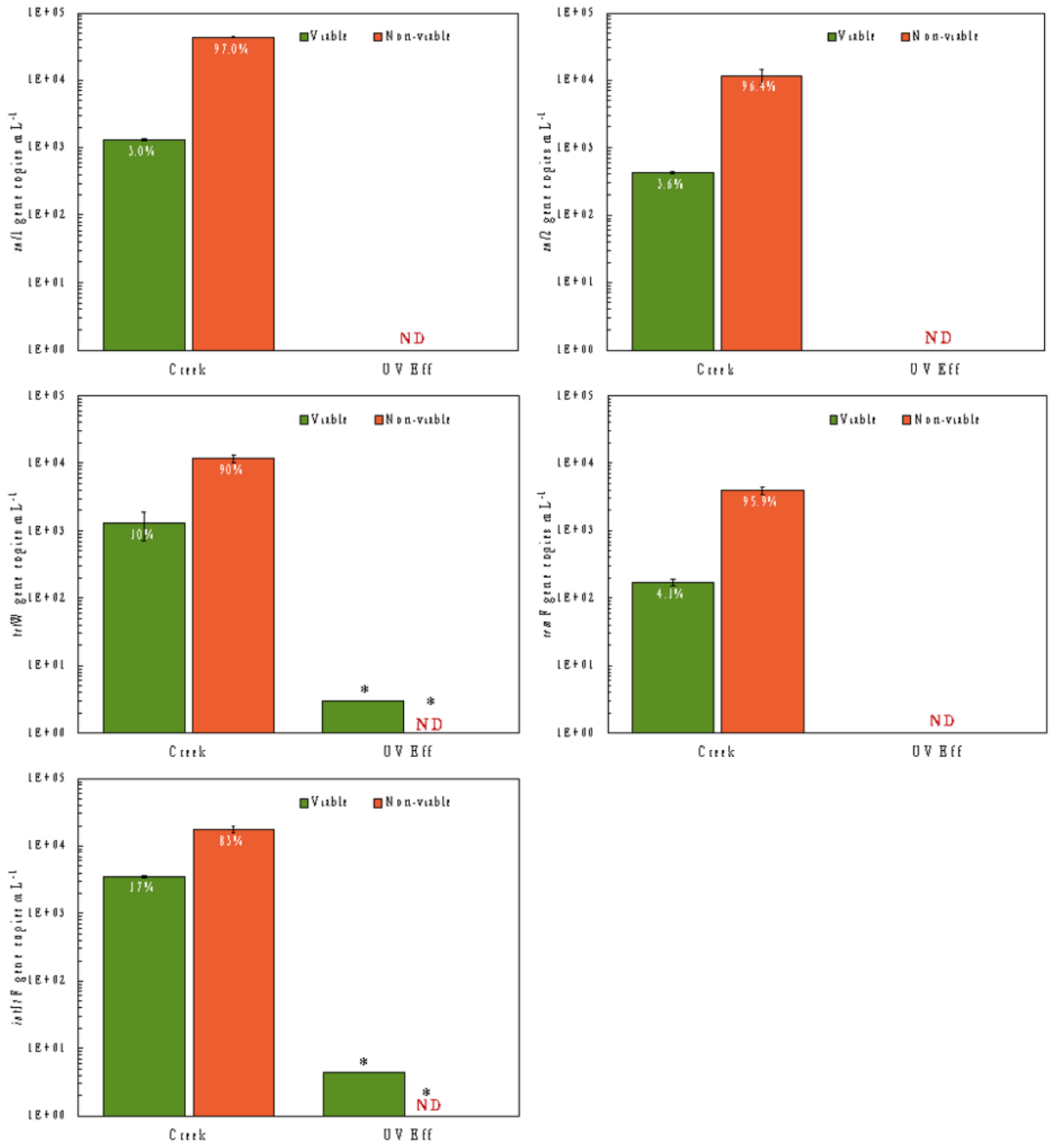

Figure 3-8. PMA-qPCR results for Las Animas Creek and the Maneadero Treatment Plant UV Effluent for *sul*1, *sul*2, *tet*W, *erm*F, and *int*I1. ND indicates that all well replicates were non-detected. *Samples for which at least one well replicate were less than the LLOD. **Non-viable result that is the difference between total cell and viable cell samples, for which at least one well replicate from each were less than the LLOD.

4. Discussion

GW (control) has very low gene abundances of all ARGs and *intI*1 when compared to the RW, water in the holding tanks, and water used for irrigation. This is in line with what is expected of GW. The 16S rRNA gene abundance is additionally lower in the GW than the RW samples. It is known that there are low levels of bacterial cells in GW. Similarly, it has been previously found that UV is effective at denaturing ARGs, which aligns with what is seen in our work.

In Mexico, studies about ARG's are uncommon. Most studies have focused on the Mezquital Valley, located in central Mexico, where wastewater has been used for the irrigation of crops for more than 100 years. Dalkmann et al. (2012) found that there was a significant correlation between the absolute concentration of *sul*1 genes and irrigation time. However, relative concentrations of *sul* genes were not correlated with the duration of irrigation. Soils irrigated with wastewater for 100 years did not contain more *sul* resistance genes in relation to their content of 16S rRNA than did a soil irrigated with wastewater for 1.5 years. Broszat et al. (2014) investigated the effects of wastewater irrigation for different periods on the occurrence of pathogenic bacteria and antibiotic resistance determinants in the affected Mezquital Valley soils and compared wastewater-irrigated soils with rain-fed agriculture in the same area, incorporating possible seasonal effects by sampling the same soils in the rainy and dry seasons. They found up to six types of antibiotic resistance in isolates from wastewater-irrigated soils; sulfamethoxazole resistance was the most abundant (33.3% of the isolates), followed by oxacillin resistance (21.9% of the isolates). An increase of potentially harmful bacteria and a larger incidence of resistance determinants in wastewater-irrigated soils was detected, which might result in health risks for farm workers and consumers of wastewater-irrigated crops. Jechalke et al. (2015) confirmed the results by Dalkmann et al. (2012), the absolute abundance of 16S rRNA genes in the samples increased significantly over time (linear regression model, $p < 0.05$) suggesting an increase in bacterial

biomass due to repeated irrigation with wastewater. Correspondingly, all tested ARGs as well as *int*I1 and korB significantly increased in abundance over the period of 100 years of irrigation. However, no significant positive correlations were observed between the relative abundance of selected genes and years of irrigation.

More recently, Tapia-Arreola et al. (2022) studied the frequency of Gram-negative bacteria resistant to antimicrobials along the Lerma River, a basin in central Mexico basin, that sustains the activity of 750,000 ha of irrigation, livestock, more than 1500 industries, and important urban centers, using phenotypic and molecular methods. They found that, throughout the entire the Lerma River, Gram-negative bacteria resistant to ß-lactams, aminoglycosides, and quinolones were detected, as a results of contamination by residual antimicrobials that are released through different sources, such as agricultural runoff, wastewater discharges, and leaching from nearby farms throughout the basin.

There is a general trend in irrigation water where the RGH-2018 sample has less ARGs and *int*I1 per 16S rRNA than one or both of the ARD-2014 and DJS-2016 sample. One hypothesis to explain this would be that over time, the bacterial community in the holding tanks changes and becomes either a more hospitable environment to ARGs or is conducive to horizontal gene transfer. Relative gene abundances are generally lower in the water used for irrigation than the RW entering the tanks. The RW entering the tanks has just been chlorinated at *El Naranjo* WWTP and likely has a low count of live cells, but the proportion of the cells (viable or non-viable) that host the ARGs measured decreases with time in the tank. It is also true that the irrigation samples were grab samples from the surface of the open-air tanks, and these samples were exposed to the sun and could have been affected by UV radiation.

Relative abundances of soil samples are variable. In several cases, the farm that most recently began using RW (RGH-2018) has the highest relative abundance of ARGs, which could be because the 16S rRNA gene abundance of this sample was lower than those of the others. In all cases, the soil irrigated with GW has very low relative abundances, which is to be expected. It does not appear that the relative abundances of ARGs increase with the time that the soil has been irrigated with RW. Regardless of the relative abundances of the genes, the high levels of ARGs in the soils can be a concern to farmworkers handling the soil. It is especially important for people working in direct contact with soils containing ARGs, especially if these genes are from a live cell, that their skin is protected from exposure when there is an open wound. A major source of ARGs to soils is manure fertilization, which was not explicitly investigated in this work.

The context of this study is that RW is used for irrigation in an agricultural region where the GW has historically been used for irrigation, but that GW now has intolerable levels of salinity because of seawater intrusion. It is important to understand that qPCR detects *all* target genes in a sample, indiscriminate of whether the gene is hosted by a viable or non-viable cell. Because of the importance of prioritizing the use of RW for irrigation in this region, we also used PMA-qPCR to evaluate the fraction of genes from water samples that were from viable and non-viable cells.

From this method, we are able to see that although there are significant levels of ARGs in the irrigation water from live cells, there were minimal levels of ARGS in the RW entering the tanks after traveling through the distribution system. This result is promising because it means that any antibiotic resistance present in the tanks could potentially be treated at the tanks with an engineering solution.

5. Conclusions

This work evaluates the effect on antibiotic resistance of the use of RW for agriculture. Genes were quantified by qPCR as well as PMA-qPCR to determine the viability of host cells. The groundwater was found to have very low levels of ARGs and *int*I1, and the soil irrigated with the GW also had low absolute and relative abundances of these genes. There is some evidence that time spent in the RW holding tanks allows for proliferation of antibiotic resistance, but despite this, there are not increased relative levels of ARGs in soils that have been irrigated with RW for longer periods of time. While there were live cells hosting ARGs and *int*I1 in the effluent from the *El Naranjo* WWTP, by the time it traveled through the distribution system, the levels of absolute ARGs were comparable but most of these genes were hosted by non-viable cells. Future work is needed to better understand the complex effects that RW has on antibiotic resistance in agricultural soil in order to both ensure public safety while also understanding the magnitude of the benefit that the use of RW has for the region.

6. Appendix

Table A3-1. Primer Sequences and Concentrations

Target Gene		Concentration (nM)	Sequence (5'-3')	Amplicon size (bp)	Reference
16S rRNA	F	600	ATGGCTGTCGTCAGCT	351	Pan and Chu, 2018
	R		ACGGGCGGTGTGTAC		
*erm*F	F	500	TCGTTTTACGGGTCAGCACTT	246	Knapp et al., 2009
	R		CAACCAAAGCTGTGTCGTTT		
*int*I1	F	200	GGCTTCGTGATGCCTGCTT	424	Lou et al., 2010
	R		CATTCCTGGCCGTGGTTCT		
*sul*1	F	200	CGCACCGGAAACATCGCTGCAC	258	Pei et al., 2006
	R		TGAAGTTCCGCCGCAAGGCTCG		
*sul*2	F	200	CTCCGATGGAGGCCGGTAT	449	Lou et al., 2010
	R		GGGAATGCCATCTGCCTTGA		
*tet*W	F	700	GAGAGCCTGCTATATGCCAGC	700	Aminov et al., 2001
	R		GGGCGTATCCACAATGTTAAC		

Table A3-2. qPCR Thermocycling Conditions

Target Gene	Holding		Denaturation		Annealing		Extension		R^2	Eff.
	Temp. (°C)	Time (min)	Temp. (°C)	Time (s)	Temp. (°C)	Time (s)	Temp. (°C)	Time (s)		
16S rRNA	94	4	94	40	60	45	72	60	1	0.93
*erm*F	95	10	94	20	60	60	-	-	1	0.93
*int*I1	95	10	95	15	55	30	72	30	1	0.97
*sul*1	95	10	95	15	65	30	72	30	1	0.97
*sul*2	95	15	95	15	58.5	30	72	30	1	0.90
*tet*W	95	30	95	30	60	30	72	30		

7. References

Broszat, M., Nacke, H., Blasi, R., Siebe, C., Huebner, J., Daniel, R., et al. (2014). Wastewater irrigation increases abundance of potentially harmful Gammaproteobacteria in soils from Mezquital Valley, Mexico. Appl. Environ. Microbiol. 80, 5282–5291. doi: 10.1128/AEM.01295-14

Cao, Y., Griffith, J.F., Dorevitch, S., Weisberg, S.B., 2012. Effectiveness of qPCR permutations, internal controls and dilution as means for minimizing the impact of inhibition while measuring Enterococcus in environmental waters. J. Appl. Microbiol. 113, 66–75. https://doi.org/10.1111/j.1365-2672.2012.05305.x

Carini, P., Marsden, P.J., Leff, J.W., Morgan, E.E., Strickland, M.S., Fierer, N., 2016. Relic DNA is abundant in soil and obscures estimates of soil microbial diversity. Nat. Microbiol. 2. https://doi.org/10.1038/nmicrobiol.2016.242

Daesslé, L.W., Sánchez, E.C., Camacho-Ibar, V.F., Mendoza-Espinosa, L.G., Carriquiry, J.D., Macias, V.A., Castro, P.G., 2005. Geochemical evolution of groundwater in the Maneadero coastal aquifer during a dry year in Baja California, Mexico. Hydrogeol. J. 13, 584–595. https://doi.org/10.1007/s10040-004-0353-1

Dalkmann P, Broszat M, Siebe C, Willaschek E, Sakinc T, et al. (2012) Accumulation of Pharmaceuticals, Enterococcus, and Resistance Genes in Soils Irrigated with Wastewater for Zero to 100 Years in Central Mexico. PLoS ONE 7(9): e45397. doi:10.1371/journal.pone.0045397

Echeverria-Palencia, C.M., Thulsiraj, V., Tran, N., Ericksen, C.A., Melendez, I., Sanchez, M.G., Walpert, D., Yuan, T., Ficara, E., Senthilkumar, N., Sun, F., Li, R., Hernandez-Cira, M., Gamboa, D., Haro, H., Paulson, S.E., Zhu, Y., Jay, J.A., 2017. Disparate Antibiotic Resistance Gene Quantities Revealed across 4 Major Cities in California: A Survey in

Drinking Water, Air, and Soil at 24 Public Parks. ACS Omega 2, 2255–2263. https://doi.org/10.1021/acsomega.7b00118

Fægri, A., Torsvik, V.L., GoksÖyr, J., 1977. Bacterial and fungal activities in soil: Separation of bacteria and fungi by a rapid fractionated centrifugation technique. Soil Biol. Biochem. 9, 105–112. https://doi.org/10.1016/0038-0717(77)90045-1

Fuentes MD, Gutierrez S, Sahagun D, Gomez J, Mendoza J, Ellis CC, Bauer S, Blattner J, Lee WY, Alvarez M, Domínguez DC. Assessment of Antibiotic Levels, Multi-Drug Resistant Bacteria and Genetic Biomarkers in the Waters of the Rio Grande River Between the United States-Mexico Border. J Health Pollut. 2019 Aug 22;9(23):190912. doi: 10.5696/2156-9614-9.23.190912. PMID: 31497375; PMCID: PMC6711330.

Jeanneau, L., Solecki, O., Wéry, N., Jardé, E., Gourmelon, M., Communal, P.Y., Jadas-Hécart, A., Caprais, M.P., Gruau, G., Pourcher, A.M., 2012. Relative decay of fecal indicator bacteria and human-associated markers: A microcosm study simulating wastewater input into seawater and freshwater. Environ. Sci. Technol. 46, 2375–2382. https://doi.org/10.1021/es203019y

Jechalke S, Broszat M, Lang F, Siebe C, Smalla K and Grohmann E (2015) Effects of 100 years wastewater irrigation on resistance genes, class 1 integrons and IncP-1 plasmids in Mexican soil. Front. Microbiol. 6:163. doi: 10.3389/fmicb. 2015.00163

Kibret, M., Abera, B., 2011. Antimicrobial susceptibility patterns of E. coli from clinical sources in northeast Ethiopia. Afr. Health Sci. 11, S40. https://doi.org/10.4314/ahs.v11i3.70069

Knapp, C.W., McCluskey, S.M., Singh, B.K., Campbell, C.D., Hudson, G., Graham, D.W., 2011. Antibiotic Resistance Gene Abundances Correlate with Metal and Geochemical Conditions in Archived Scottish Soils. PLoS One 6, e27300.

https://doi.org/10.1371/journal.pone.0027300

Korajkic, A., Wanjugi, P., Brooks, L., Cao, Y., Harwood, V.J., 2019. Persistence and Decay of Fecal Microbiota in Aquatic Habitats. Microbiol. Mol. Biol. Rev. 83. https://doi.org/10.1128/mmbr.00005-19

Li, A.D., Metch, J.W., Wang, Y., Garner, E., Zhang, A.N., Riquelme, M. V., Vikesland, P.J., Pruden, A., Zhang, T., 2018. Effects of sample preservation and DNA extraction on enumeration of antibiotic resistance genes in wastewater. FEMS Microbiol. Ecol. 94, 1–11. https://doi.org/10.1093/femsec/fix189

Mendoza-Espinosa, L., Daesslé-Heuser, W., 2012. 2012 Guidelines for Water Reuse, Maneadero Aquifer, Ensenada, Baja California, Mexico 2011–2013.

Mendoza-Espinosa L. G. & Daesslé L. W. (2018). Consolidating the use of reclaimed water for irrigation and infiltration in a semi-arid agricultural valley in Mexico: water management experiences and results. Journal of Water, Sanitation and Hygiene for Development, vol. 8, no 4, 679-687. DOI: 10.2166/washdev.2018.021

Nocker, A., Camper, A.K., 2009. Novel approaches toward preferential detection of viable cells using nucleic acid amplification techniques. FEMS Microbiol. Lett. https://doi.org/10.1111/j.1574-6968.2008.01429.x

Robe, P., Nalin, R., Capellano, C., Vogel, T.M., Simonet, P., 2003. Extraction of DNA from soil. Eur. J. Soil Biol. 39, 183–190. https://doi.org/10.1016/S1164-5563(03)00033-5

Tapia-Arreola, A.K.; Ruiz-Garcia, D.A.; Rodulfo, H.; Sharma, A.; De Donato, M. High Frequency of Antibiotic Resistance Genes (ARGs) in the Lerma River Basin, Mexico. Int. J. Environ. Res. Public Health 2022, 19, 13988. https://doi.org/10.3390/ ijerph192113988

Thulsiraj, Vanessa, Zimmer-Faust, Amity G, Jay, Jennifer A, Thulsiraj, V, Zimmer-Faust, A G,

Jay, J A, 2017. Use of Viability-Based Methods for Improved Detection of Recent Fecal Contamination in a Microbial Source Tracking Study Near Tijuana, Mexico. Water Air Soil Pollut. 228. https://doi.org/10.1007/s11270-016-3204-5

WHO, 2014. Antimicrobial Resistance Global Report on Surveillance. Geneva, Switzerland

Chapter 4: Investigating Hospital Sewage as a Source of Antibiotic Resistant Bacteria and Antibiotic Resistance Genes

1. Introduction

Antibiotic resistance is a global public health threat (WHO, 2019). Antibiotic resistance currently results in more than 700,000 deaths each year and is expected to result in more than 10 million deaths each year by 2050 (O'Neill, 2014). While antibiotics are important for the treatment of infections, the overuse and misuse of antibiotics are major drivers of antibiotic resistance.

Antibiotic residues, antibiotic resistant bacteria (ARB), and antibiotic resistance genes (ARGs) are excreted and released into wastewater systems (Kummerer et al., 2003). Although wastewater treatment plants (WWTPs) are highly efficient at removing these constituents, WWTPs still discharge antibiotics, ARB, and ARGs at concentrations that impact downstream environments (Lorenzo et al., 2018; Rodriguez-Mozaz et al., 2015).

Wastewater treatment plants collect municipal, industrial, agricultural, and hospital waste streams. With 50% of hospital patients receiving antibiotics during their stay (Magill et al., 2014), hospitals are hotspots for antibiotic resistance (Berendonk et al, 2015). Although high concentrations of antibiotics, ARB, and ARGs in hospital wastewater have been reported, there are fewer studies on hospital wastewater in comparison to other environments (Korzeniewska et al., 2012; Lamba et al., 2017; Wang et al., 2018).

Studies on hospital wastewater use one of many proposed approaches to study antibiotic resistance. Moreover, due to a lack of standardization of methods, comparison between studies is difficult (Hocquet et al., 2016). Therefore, an integrated approach using various methods would allow for cross validation of methods and a more comprehensive analysis of antibiotic resistance in hospital wastewater (Blake et al., 2021; Lorenzo et al., 2018).

This study uses culture- and molecular-based methodologies to study the ARB and ARG burden hospital wastewater discharges to the sewershed. Samples above, within, and below a hospital and at the receiving WWTP are analyzed. The analysis 1) assesses abundance, diversity, and mobility of ARGs, 2) cross-validates culture and molecular methods, and 3) tests a low-tech and low-cost culture method for identifying hotspots of antibiotic resistance.

2. Methods

2.1 Sample Collection

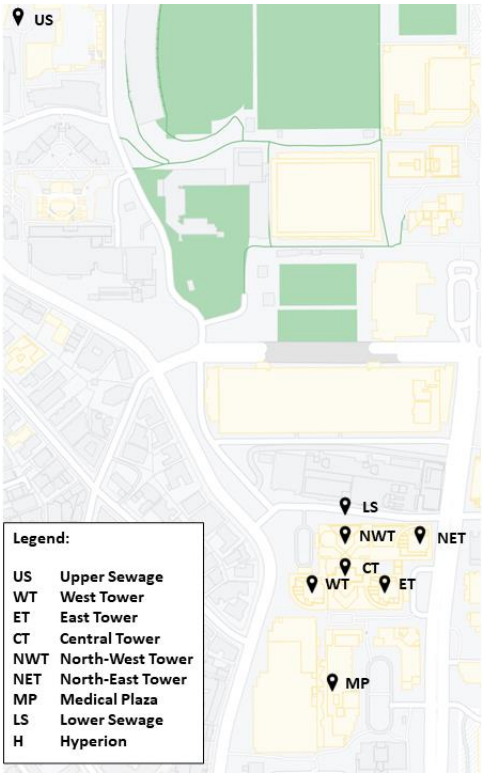

Figure 4-1. The map shows the location of the sampling sites above, below, and within the UCLA Ronald Reagan Medical Center and at the UCLA Medical Plaza.

Sewage samples were collected above, below, and within the UCLA Ronald Reagan Medical Center (Figure 4-1). Comparison samples were also taken at the UCLA Medical Plaza (Figure 4-1) and at the Hyperion Water Reclamation Plant. Sewage samples were collected in January 2020, February 2020, January 2022, and January 2023. Sewage samples were collected in

autoclaved polypropylene bottles pre-washed thrice with sample. Samples were transported to the laboratory on ice for immediate processing.

2.2 FIB Enumeration

Samples were diluted 100 to 100,000-fold in sterile Milli-Q water. Samples were enumerated for total coliform (TC) and *Escherichia coli* (EC) using Colilert-18 (IDEXX Laboratories, Westbrook, Maine) and enterococci using Enterolert (ENT; IDEXX Laboratories, Westbrook, Maine) according to the manufacturer's instructions. The most probable number (MPN)/100 mL and confidence interval will be calculated.

2.3 Heterotrophic Plate Counts

Samples were diluted 10 to 10,000-fold in phosphate buffered saline (PBS). We appled 50 uL of undilute or dilute sample to solid 25% Luria−Bertani (LB) growth medium amended with no antibiotic, 20 mg/L of tetracycline, 4 mg/L of ciprofloxacin, or 10 mg/L of erythromycin in triplicate. Plates will be incubated at 30°C for 24 hours. Antibiotic resistance levels will be calculated as the ratio of colony forming units (CFUs) growing on plates amended with antibiotic to the CFUs growing on plates amended with no antibiotic. The mean and standard deviation of antibiotic resistance levels will be calculated (Negreanu et al., 2012).

2.4 Sample Filtration

Homogenized samples were vacuum filtered in 47 mm diameter, 0.22 um pore size, polycarbonate filters (MilliporeSigma, Burlington, Massachusetts) in quintuplet until clogging, volumes were be recorded. A “filter blank” of 100 mL of autoclaved PBS was also filtered. Four of the five filters were folded and placed in 2 mL microcentrifuge tubes with 1.5 mL of 50% ethanol. Filters were stored in -20°C until extraction.

2.5 Propidium Monoazide (PMA)

One of the five filters was folded and placed in a 25 mL falcon tube with 5 mL of PBS and hand-shaken for two minutes. Two 500 uL aliquots of suspension was placed in a light transparent 2 mL microcentrifuge tube. One of the aliquots was treated with 100 uM of PMAxx Dye (Biotium, Fremont, California). Both aliquots were gently vortexed (at level 2, Vortex Genie 2, FisherScientific, Hampton, New Hampshire) in the dark for 5 mins. Aliquots were then laid horizontally, and light exposed for 2 mins using a flat 10,000 luxe intensity LED light (Verilux, Santa Ana, California) from 20 cm distance. After 1 minute, the aliquots were manually rotated for even exposure. Aliquots were then centrifuged at 10,000 x g for 5 mins (Nocker et al., 2007). The supernatant was removed and discarded. The pellet was resuspended in 500 μL of PBS and 500 uL of 50% ethanol. Aliquots were stored in -20℃ until extraction.

2.6 DNA Extraction

Filters were fragmented with flame sterilized tweezers and scissors and transferred to 2 mL lysing matrix e tubes (MP Biomedicals, Irvine, California). The remaining solution from the 2 mL microcentrifuge tubes were centrifuged at 5,000 x g for 10 mins. The supernatant was removed and discarded. The remaining pellet was resuspended with 978 uL of sodium phosphate buffer (MP Biomedicals, Irvine, California) and transferred to the 2 mL lysing matrix e tubes (Li et al., 2018).

Aliquots were centrifuged at 15,000 x g for 5 mins. The top 500 uL of supernatant was removed and discarded. The remaining pellet and PBS were resuspended with 978 uL of sodium phosphate buffer (MP Biomedicals, Irvine, California) and transferred to the 2 mL lysing matrix e tubes.

DNA from the filters and aliquots was extracted using the FastDNA Spin Kit for Soil (MP Biomedicals, Irvine, California) following the manufacturer's protocol, except for where samples

are homogenized a Mini-Beadbeater-16 (BioSpec Products, Bartlesville, Oklahoma) was used twice for 1.5 mins with a 5 min rest in between. An "extraction blank" was extracted in parallel in all extractions. The eluted DNA was aliquoted. Nucleic acid concentration and 260/280 absorbance ratios were measured via UV absorption using a Nanodrop 2000C (Thermo Scientific, Waltham, Massachusetts). Aliquots of eluted DNA will be stored in -80℃ until use.

2.7 qPCR

*sul*1 (Pei et al., 2006), *erm*F (Knapp et al., 2010), *tet*A (Ng et al., 2001), $bla_{\text{CTX-M}}$ (Kim et al., 2005), *van*A (Volkmann et al., 2004), *int*I1 (Stokes et al., 2006), and 16S rRNA (Galley et al., 2021; Suzuki et al., 2000) primers, primer concentrations, and thermocycling conditions previously validated in the literature were used (Table A4-1 and A4-2). To determine the appropriate DNA concentration, serial dilution and well spike tests were performed for all samples. All assays were performed in 96-well reaction plates that contain triplicate: diluted DNA, filter blanks, extraction blanks, a RNase-free molecular biology grade water negative control, and a standard curve positive control. A standard curve, covering 7 orders of magnitude, were constructed with 10-fold serial dilutions of known amounts of dsDNA (Integrated DNA Technologies, Coralville, Iowa). All assays were run in a StepOne Plus Real-Time PCR System (Applied Biosystems, Foster City, California), which generated quantification thresholds and melt curves for each assay. Quantification thresholds were converted into gene copies using the standard curve. Melt curves were used to further verify target gene amplification specificity. The limit of detection was set as the lowest standard that amplified at least in duplicate. Standard curve efficiencies were at or above 90% and R^2 values were at or above 0.99 across all qPCR assays (Table A4-2).

2.8 Metagenomic Sequencing and Bioinformatic Analysis

We sent DNA from each sample to MR DNA Molecular Research Lab (Shallowater, Texas) for library preparation using a NexteraXT DNA Library Prep Kit and for 2 x 150 bp paired-end shotgun metagenomic sequencing using an Illumina NovaSeq 6000. Quality trimming, annotation, and assembly of metagenomes were perfomed via Galaxy. Metagenomes were analyzed against the Comprehensive Antibiotic Resistance Database (CARD), Structured ARG (SARG), A CLAssification of Mobile Genetic Elements (ACLAME), Pathosystems Resource Integration Center (PATRIC) databases via ARGs-OAP and MetaCompare (Yang et al., 2016; Oh et al., 2018).

2.9 Systematic Literature Review

We conducted a systematic literature review using Web of Science to identify clinically relevant antibiotic resistance genes and pathogens in Los Angeles. We will use the following keywords: “antibiotic OR antimicrobial”, “resist*”, “clinic”, and “Los Angeles” (Davis et al., 2020; Fresia et al., 2019).

3. Results and Discussion

3.1 ARB in Hospital and Non-Hospital Sewage

The resistance ratios in hospital and non-hospital sewage were comparable. The mean erythromycin resistance ratio in hospital sewage was 0.533 and in non-hospital sewage it was 0.409. The mean tetracycline resistance ratio in hospital sewage was 0.013 and in non-hospital sewage it was 0.013. The mean ciprofloxacin resistance ratio in hospital sewage was 0.009 and in non-hospital sewage it was 0.017 (Figure 4-2). Wilcoxon Rank-Sum tests showed no statistically significant ($p > 0.05$) differences for all resistance ratios between hospital and non-hospital sewage (Table A4-3). The higher resistance ratios observed for erythromycin in comparison to tetracycline

and ciprofloxacin has been previously observed in agricultural soils irrigated with treated wastewater and biosolids (Hung et al., 2022; Negreanu et al., 2012).

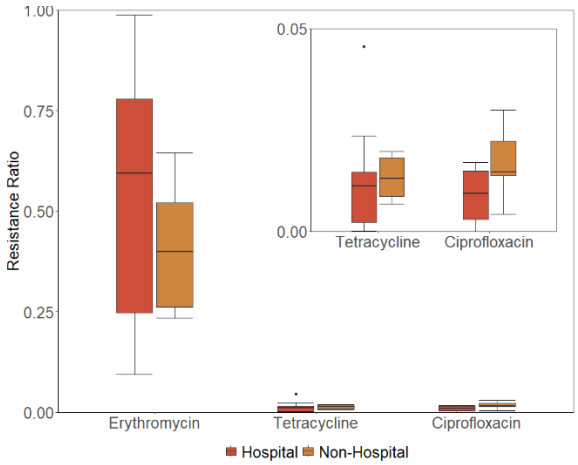

Figure 4-2. Erythromycin, tetracycline, and ciprofloxacin resistance ratios for hospital and non-hospital sewage.

3.2 ARGs in Hospital and Non-Hospital Sewage

Relative gene abundances in hospital sewage were up to 2 orders of magnitude greater than in non-hospital sewage. Mean *intI*1 relative abundances were 10^{-1} gene copies/16S rRNA gene copies in hospital sewage and non-hospital sewage. *sul*1 relative abundances were 10^{-1} gene copies/16S rRNA gene copies in hospital sewage and 10^{-2} gene copies/16S rRNA gene copies non-hospital sewage. *erm*F relative abundances were 10^{-2} gene copies/16S rRNA gene copies in hospital sewage and non-hospital sewage. *tet*A relative abundances were 10^{-3} gene copies/16S rRNA gene copies in hospital sewage and non-hospital sewage. $bla_{CTX\text{-}M}$ relative abundances were 10^{-3} gene copies/16S rRNA gene copies in hospital sewage and 10^{-5} gene copies/16S rRNA gene copies non-hospital sewage. *van*A relative abundances were 10^{-3} gene copies/16S rRNA gene copies in hospital sewage and 10^{-6} gene copies/16S rRNA gene copies non-hospital sewage (Figure 4-3). Wilcoxon Rank-Sum tests confirmed that differences in all relative gene abundances between hospital and non-hospital sewage were insignificant ($p > 0.05$) (Table A4-4). It is important to

note, that differences in *bla*$_{CTX\text{-}M}$ and *van*A relative abundances can be of concern since they are clinically relevant ARGs that encode resistance to last-resort antibiotics (Keenum et al., 2022).

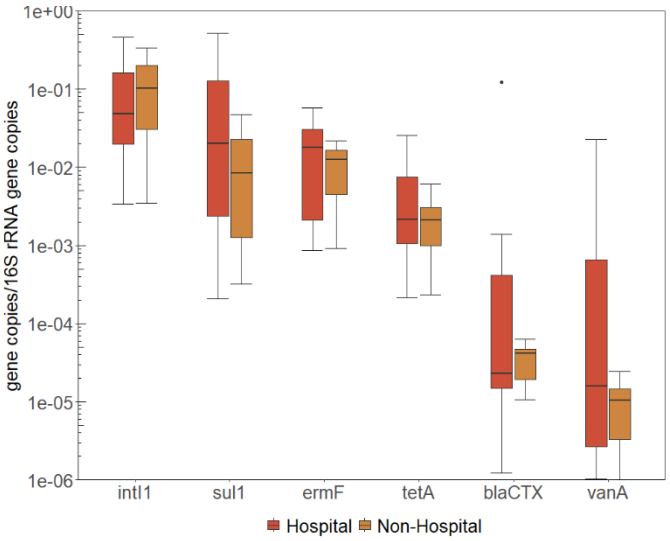

Figure 4-3. Relative gene abundances for hospital and non-hospital sewage.

3.3 Risk Scores in Hospital and Non-Hospital Sewage

Risk scores in hospital and non-hospital sewage were also comparable. The mean risk score in hospital sewage was 32.38 and in non-hospital sewage it was 29.14 (Figure 4-4). The risk scores observed in this study do match those observed in other studies for hospital sewage (Oh et al., 2018) and wastewater influent (Majeed et al., 2021).

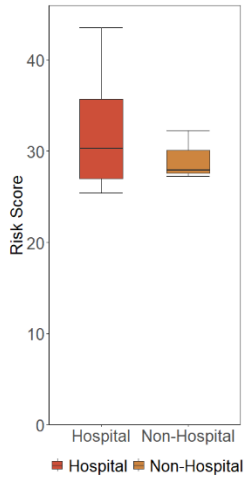

Figure 4-4. Risk scores for hospital and non-hospital sewage.

3.4 Cross-validation of Culture and Molecular Methods

Culture and molecular-based methods correlated with one another. Erythromycin resistance ratios from the culture method correlated significantly ($p < 0.05$) with macrolide, *sul*1, *tet*A, $bla_{CTX\text{-}M}$, *and vanA* relative abundances from the metagenomic sequencing method. When comparing qPCR and metagenomic sequencing, relative abundances of *sul*1 and $bla_{CTX\text{-}M}$ had high statistically significant correlations ($p < 0.001$) and relative abundances of *erm*F and *tet*A had moderate statistically significant correlations ($p < 0.01$) (Figure 4-5).

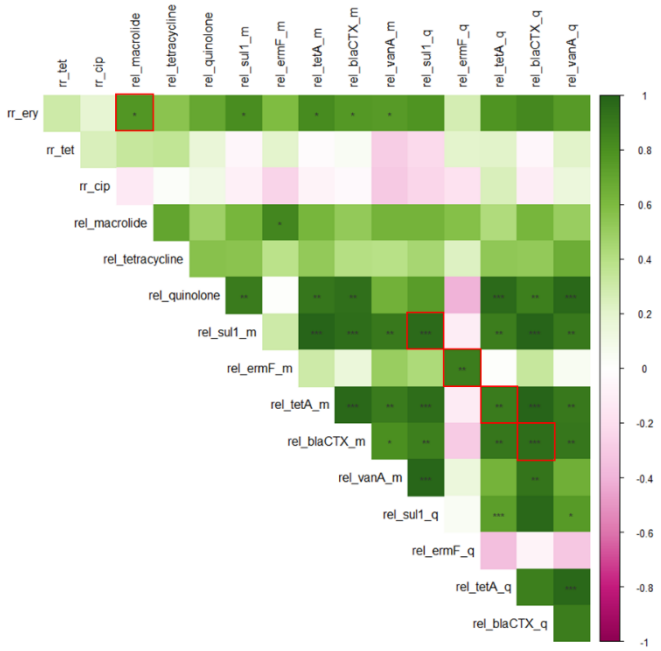

Figure 4-5. Pearson correlations for culture and molecular methods.

Relative gene abundances from the qPCR and metagenomics method were not exact. A scatter plot of qPCR versus metagenomics relative gene abundances against a 1:1 line showed little agreement. Boxplots showed that relative abundances from the qPCR method were 1 order of magnitude greater than from the metagenomics method. Mean *sul*1 relative abundances were 10^{-1} gene copies/16S rRNA gene copies by qPCR and 10^{-2} gene copies/16S rRNA gene copies by metagenomics. *erm*F relative abundances were 10^{-2}gene copies/16S rRNA gene copies by qPCR

and 10^{-3} gene copies/16S rRNA gene copies by metagenomics. *tet*A relative abundances were 10^{-3} gene copies/16S rRNA gene copies by qPCR and metagenomics. $bla_{CTX\text{-}M}$ relative abundances were 10^{-4} gene copies/16S rRNA gene copies by qPCR and 10^{-5} gene copies/16S rRNA gene copies by metagenomics. *van*A relative abundances were 10^{-3} gene copies/16S rRNA gene copies by qPCR and 10^{-4} gene copies/16S rRNA gene copies by metagenomics (Figure 4-6). Welch's t-tests confirmed that differences in *sul*1, *tet*A, $bla_{CTX\text{-}M}$, and *van*A relative gene abundances between qPCR and metagenomics were insignificant ($p > 0.05$). However, differences in *erm*F relative gene abundances between qPCR and metagenomics were moderately significant ($p < 0.01$) (Table A4-4). Differences in the relative gene abundances between qPCR and metagenomics methods may be due to the detection limitations of the metagenomic approach (Crossette et al., 2021).

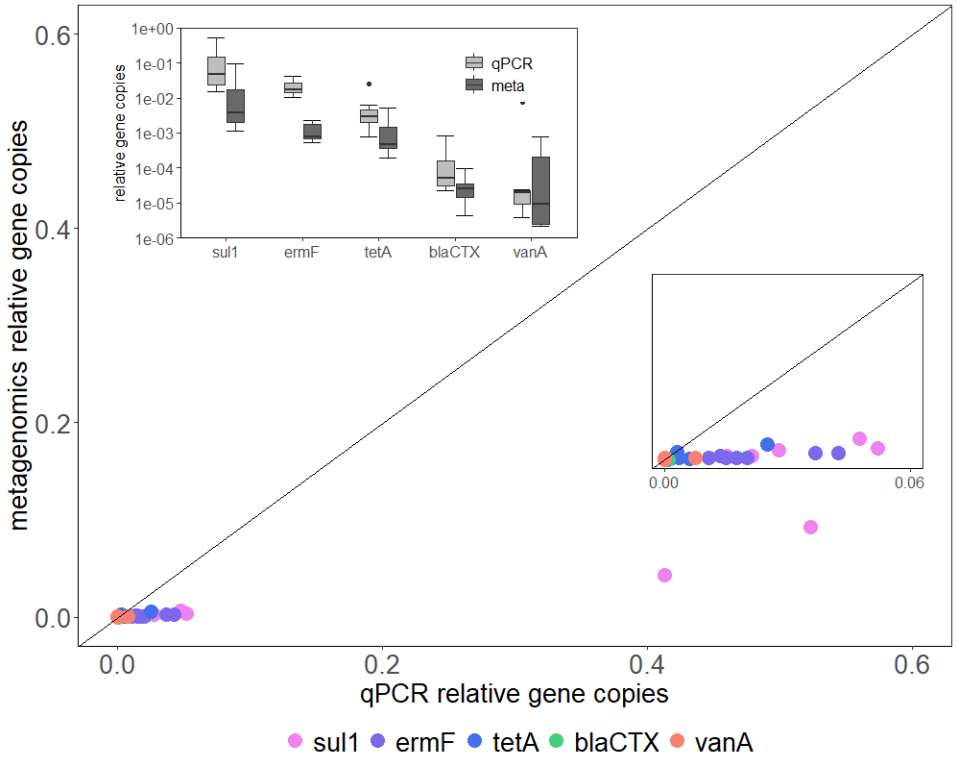

Figure 4-6. Boxplot and scatter plot of qPCR versus metagenomic relative gene abundances.

4. Appendix

Table A4-1. Primer Sequences and Concentrations.

Target Gene		Concentration (nM)	Sequence (5'-3')	Amplicon size (bp)	Reference
*sul*1	F	200	CGCACCGGAAACATCGCTGCAC	258	Pei et al., 2006
	R		TGAAGTTCCGCCGCAAGGCTCG		
*erm*F	F	500	TCGTTTTACGGGTCAGCACTT	246	Knapp et al., 2009
	R		CAACCAAAGCTGTGTCGTTT		
*tet*A	F	200	GCTACATCCTGCTTGCCTTC	210	Ng et al., 2010
	R		CATAGATCGCCGTGAAGAGG		
bla_{CTX-M}	F	900	CGTCACGCTGTTGTTAGGAA	791	Kim et al., 2005
	R		ACGGCTTTCTGCCTTAGGTT		
*van*A	F	200	CTGTGAGGTCGGTTGTGCG	185	Volkmann., 2004
	R		TTTGGTCCACCTCGCCA		
*int*I1	F	650	CTGGATTTCGATCACGGCACG	483	Stokes et al., 2006
	R		ACATGCGTGTAAATCATCGTCG		
16S rRNA	F	1000	CGGTGAATACGTTCYCGG	152	Suzuki et al., 2000
	R		GGWTACCTTGTTACGACTT		

Table A4-2. qPCR Thermocycling Conditions. *Assay has an initial denaturation step at 50°C for 2 minutes.

Target Gene	Holding		Denaturation		Annealing		Extension		R^2	Eff.
	Temp. (°C)	Time (min)	Temp. (°C)	Time (s)	Temp. (°C)	Time (s)	Temp. (°C)	Time (s)		
*sul*1	95	10	95	15	65	30	72	30	0.999	91
*erm*F	95	10	94	20	60	60	-	-	0.999	93
*tet*A	95	4	95	5	55	30	72	30	0.999	91
bla_{CTX-M}	95	10	95	8	60	60	-	-	0.996	97
*van*A	95	5	95	15	60	60	-	-	0.998	96
*int*I1*	95	2	95	15	58	15	72	60	0.998	93
16S rRNA*	95	10	95	15	56	75	-	-	1.000	90

Table A4-3. Wilcoxon Rank-Sum tests comparing hospital and non-hospital resistance ratios.

Resistance Ratio	p-value
Erythromycin	0.409
Tetracycline	0.480
Ciprofloxacin	0.195

Table A4-4. Wilcoxon Rank-Sum tests comparing hospital and non-hospital relative gene abundances.

Gene	p-value
rel *intI*1	0.505
rel *sul*1	0.267
rel *erm*F	0.374
rel *tet*A	0.617
rel $bla_{\text{CTX-M}}$	0.956
rel *van*A	0.165

Table A4-5. Welch's t-tests comparing qPCR and metagenomics relative gene abundances.

Gene	p-value
rel *sul*1	0.149
rel *erm*F	0.004
rel *tet*A	0.200
rel $bla_{\text{CTX-M}}$	0.178
rel *van*A	0.458

5. References

Berendonk, T. U. *et al.* Tackling antibiotic resistance: The environmental framework. *Nat. Rev. Microbiol.* **13**, 310–317 (2015).

Blake, K. S., Choi, J. & Dantas, G. Approaches for characterizing and tracking hospital-associated multidrug-resistant bacteria. *Cell. Mol. Life Sci.* (2021) doi:10.1007/s00018-020-03717-2.

Cao, Y., Griffith, J. F. & Weisberg, S. B. The next-generation PCR-based quantification method for ambient waters: Digital PCR. *Methods Mol. Biol.* **1452**, 113–130 (2016).

Cira, M. *et al.* Commercially available garden products as important sources of antibiotic resistance genes—a survey. *Environ. Sci. Pollut. Res.* **28**, 43507–43514 (2021).

Crossette, Emily, et al. Metagenomic quantification of genes with internal standards. MBio 12.1 (2021): e03173-20.

Davis, B. C. *et al*. Demonstrating an Integrated Antibiotic Resistance Gene Surveillance Approach in Puerto Rican Watersheds Post-Hurricane Maria. *Environmental Science & Technology*, ***54*** (23), 15108-15119 (2020).

Dutka-Malen, S., Evers, S. & Courvalin, P. Detection of glycopeptide resistance genotypes and identification to the species level of clinically relevant enterococci by PCR. *J. Clin. Microbiol.* **33**, 24–27 (1995).

Fresia, P. *et al.* Urban metagenomics uncover antibiotic resistance reservoirs in coastal beach and sewage waters. *Microbiome* **7**, 1–9 (2019).

Galley, Jeffrey D., et al. Prenatal stress-induced disruptions in microbial and host tryptophan metabolism and transport. *Behavioural brain research* 414 (2021): 113471.

Goldstein, C. *et al*. Incidence of Class 1 and 2 Integrases in Clinical and Commensal Bacteria from Livestock, Companion Animals, and Exotics. *American Society for Microbiology*. **45**, 723–726 (2001).

González-Escalona, N. *et al.* Detection of live Salmonella sp. cells in produce by a taqman-based quantitative reverse transcriptase real-time PCR Targeting invA mRNA. *Appl. Environ. Microbiol.* **75**, 3714–3720 (2009).

Haugland, R. A. *et al.* Evaluation of genetic markers from the 16S rRNA gene V2 region for use in quantitative detection of selected Bacteroidales species and human fecal waste by qPCR. *Syst. Appl. Microbiol.* **33**, 348–357 (2010).

Hocquet, D., Muller, A. & Bertrand, X. What happens in hospitals does not stay in hospitals: antibiotic-resistant bacteria in hospital wastewater systems. *J. Hosp. Infect.* **93**, 395–402 (2016).

Hung, Wei-Cheng, et al. Tracking antibiotic resistance through the environment near a biosolid spreading ground: Resistome changes, distribution, and metal (loid) co-selection. Science of The Total Environment 823 (2022): 153570.

Keenum, Ishi, et al. A framework for standardized qPCR-targets and protocols for quantifying antibiotic resistance in surface water, recycled water and wastewater. *Critical Reviews in Environmental Science and Technology* 52.24 (2022): 4395-4419.

Kim, J., Lim, Y., Jeong, Y., Scol, S. Occurrence of CTX-M-3, CTX-M-15, CTX-M-14, and CTX-M-9 extended-spectrum B-Lactameses in Enterobacteriaceae clinical isolates in Korea. *American Society for Microbiology*. **49**, 1572–1575 (2005).

Knapp, C. W.; Dolfing, J., Ehlert, P. A. I., Graham, D. W. Evidence of Increasing Antibiotic Resistance Gene Abundances in Archived Soils since 1940. *Environ. Sci. Technol. 44* (2), 580–587 (2010).

Korzeniewska, E., Korzeniewska, A. & Harnisz, M. Antibiotic resistant Escherichia coli in hospital and municipal sewage and their emission to the environment. *Ecotoxicol. Environ. Saf.* **91**, 96–102 (2013).

Kümmerer, K. Promoting resistance by the emission of antibiotics from hospitals and households into effluent. *Clin. Microbiol. Infect.* **9**, 1203–1214 (2003).

Lamba, M., Graham, D. W. & Ahammad, S. Z. Hospital Wastewater Releases of Carbapenem-Resistance Pathogens and Genes in Urban India. *Environ. Sci. Technol.* **51**, 13906–13912 (2017).

Li, A. D. *et al.* Effects of sample preservation and DNA extraction on enumeration of antibiotic resistance genes in wastewater. *FEMS Microbiol. Ecol.* **94**, 1–11 (2018).

Lorenzo, P. *et al.* Antibiotic resistance in urban and hospital wastewaters and their impact on a receiving freshwater ecosystem. *Chemosphere* **206**, 70–82 (2018).

Majeed, Haniyyah J., et al. Evaluation of metagenomic-enabled antibiotic resistance surveillance at a conventional wastewater treatment plant. *Frontiers in microbiology* 12 (2021): 657954.

Magill, S. S. *et al.* Multistate Point-Prevalence Survey of Health Care–Associated Infections. *N. Engl. J. Med.* **370**, 1198–1208 (2014).

Negreanu, Y., Pasternak, Z., Jurkevitch, E. & Cytryn, E. Impact of treated wastewater irrigation on antibiotic resistance in agricultural soils. *Environ. Sci. Technol.* **46**, 4800–4808 (2012).

Ng, L. K., Martin, I., Alfa, M. & Mulvey, M. Multiplex PCR for the detection of tetracycline resistant genes. *Mol. Cell. Probes* **15**, 209–215 (2001).

Nocker, A., Sossa-Fernandez, P., Burr, M. D. & Camper, A. K. Use of propidium monoazide for live/dead distinction in microbial ecology. *Appl. Environ. Microbiol.* **73**, 5111–5117 (2007).

Pei, R., Kim, S. C., Carlson, K. H. & Pruden, A. Effect of River Landscape on the sediment concentrations of antibiotics and corresponding antibiotic resistance genes (ARG). *Water Res.* **40**, 2427–2435 (2006).

Oh, Min, et al. MetaCompare: a computational pipeline for prioritizing environmental resistome risk. FEMS microbiology ecology 94.7 (2018): fiy079.

O'Neill, J. Antimicrobial Resistance: Tackling a crisis for the health and wealth of nations The Review on Antimicrobial Resistance Chaired. (2014).

Rodriguez-Mozaz, S. *et al.* Occurrence of antibiotics and antibiotic resistance genes in hospital and urban wastewaters and their impact on the receiving river. *Water Res.* **69**, 234–242 (2015).

Stachler, E. *et al.* Quantitative CrAssphage PCR Assays for Human Fecal Pollution Measurement. *Environ. Sci. Technol.* **51**, 9146–9154 (2017).

Stokes, H. W., et al. Class 1 integrons potentially predating the association with Tn 402-like transposition genes are present in a sediment microbial community. Journal of bacteriology 188.16 (2006): 5722-5730.

Suzuki, M. T., Taylor, L. T. & DeLong, E. F. Quantitative analysis of small-subunit rRNA genes in mixed microbial populations via 5'-nuclease assays. *Appl. Environ. Microbiol.* **66**, 4605–4614 (2000).

Volkmann, H.; Schwartz, T.; Bischoff, P.; Kirchen, S.; Obst, U. Detection of Clinically Relevant Antibiotic-Resistance Genes in Municipal Wastewater Using Real-Time PCR (TaqMan). *J. Microbiol. Methods* **2004**, *56* (2), 277–286. https://doi.org/10.1016/J.MIMET.2003.10.014.

Wang, Q., Wang, P. & Yang, Q. Occurrence and diversity of antibiotic resistance in untreated hospital wastewater. *Sci. Total Environ.* **621**, 990–999 (2018).

WHO. Ten threats to global health in 2019 Air pollution and climate change. *Ten Threat. To Glob. Heal. 2019* 1–18 (2019).

Yang, Ying, et al. ARGs-OAP: online analysis pipeline for antibiotic resistance genes detection from metagenomic data using an integrated structured ARG-database. *Bioinformatics* 32.15 (2016): 2346-2351.

Chapter 5: Fate and Transport of Antibiotic Resistant Bacteria and Antibiotic Resistance Genes in Natural and Urbanized Coastal Watersheds in Los Angeles

1. Introduction

Antibiotic resistance is a global public health threat (WHO, 2019) resulting in more than 700,000 deaths each year (O'Neill, 2014). A sustained rise in antibiotic resistance may result in more than 10 million deaths each year by 2050 (O'Neill, 2014). Therefore, to combat antibiotic resistance a globally coordinated effort across multiple sectors, including the environment, is crucial (WHO, 2015).

The environment plays an important role in the persistence, selection, and spread of antibiotic resistance (CDC, 2019; JPIAMR, 2019; WHO et al., 2019). Runoff and wastewater which may contain antimicrobial residues, antibiotic resistant bacteria (ARB), and antibiotic resistance genes (ARGs) are discharged into surface waters and coastal waters (JPIAMR, 2019). Antibiotic resistance in recreational waters may pose a public health risk (Nappier, 2020). Thus, agencies are interested in extending surveillance systems to include water environments (FDA et al, 2020; JPIAMR, 2019; O'Neill, 2016).

However, standardized methods for surveillance of antibiotic resistance in the environment are still needed. Various methods have been proposed, including culture, quantitative polymerase chain reaction (qPCR), and next generation sequencing (NGS) methods (Berendonk et al., 2015). However, since studies typically use one of these methods, cross validation of methods is urgently needed. Additionally, the methods proposed are technologically intensive and costly, making them inaccessible to low- and middle-income countries.

Nonetheless, recent methodological advances have helped answer questions on the emergence and dissemination of antibiotic resistance in the environment. For example, a recent

study used qPCR and NGS to assess sources, clinical relevance, and mobility of ARGs in watersheds (Davis et al., 2020).

The purpose of this study is to examine the impacts of urbanization on antibiotic resistance by comparing ARGs and ARB in an urban watershed and an adjacent natural watershed in Los Angeles. The urban Ballona Creek Watershed (BCW) is 91% developed and the adjacent natural Topanga Creek Watershed (TCW) is 15% developed (Manago and Hoague, 2017). While previous studies have detected ARGs and ARB in the surface waters of these watersheds (Noble et al., 2006; Kawecki et al., 2017), the coastal waters have been largely overlooked. However, the Ballona Creek Watershed and the Topanga Creek Watershed are the first and third largest inputs to the Santa Monica Bay, respectively (LACDPWa, LACDPWb). Therefore, the coastal waters may represent an important point of environmental exposure to antibiotic resistance for the 50 million people that recreate in these beaches every year (Los Angeles County, 2021; USGS, 2003). The analysis1) assesses abundance, diversity, and mobility of ARGs, 3) cross-validated culture, qPCR, and NGS methods, and 4) determines if a low-tech and low-cost culture method can be utilized to identify hotspots.

2. Methods

2.1 Sample Collection

Sampling locations are shown in Figure 5-1. Sampling occured during one dry and one wet weather event. We measured temperature, pH, turbidity, specific conductivity, and dissolved oxygen using a Hydrolab HL4 Multiparameter Sonde (Hydrolab, Loveland, Colorado). Surface water samples were collected in autoclaved polypropylene bottles pre-washed thrice with sample. Samples were transported to the laboratory on ice for immediate processing.

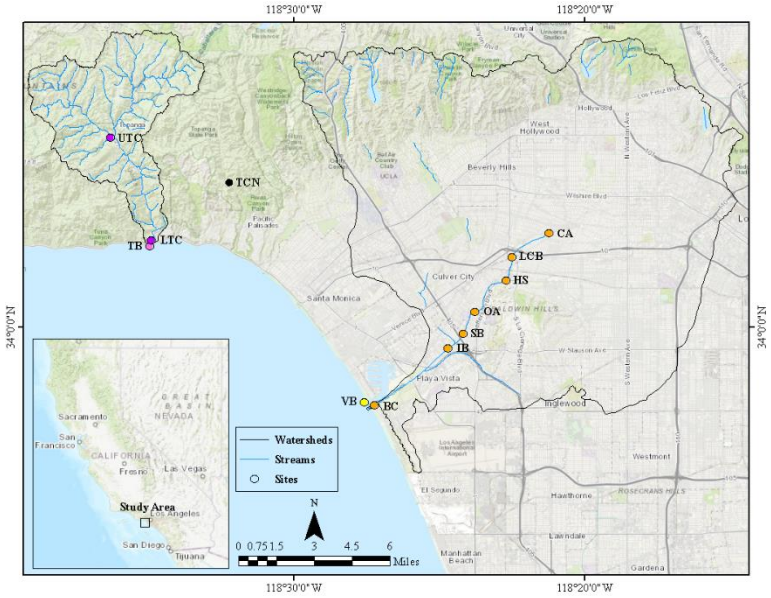

Figure 5-1. The study area map shows the Ballona Creek watershed (to the right in black lines) and the Topanga Creek Watershed (to the left in black lines), and their corresponding streams (blue lines). The map also shows the location of the 7 sites in Ballona Creek (orange circles), 1 site in Venice Beach (yellow circle), 2 sites in Topanga Creek (purple circles), 1 site in Topanga Beach (pink circle), and 1 control site in Temescal Canyon (black circle).

2.2 FIB Enumeration

Samples will be diluted 10 to 10,000-fold in sterile Milli-Q water. Samples were enumerated for total coliform (TC) and *Escherichia coli* (EC) using Colilert-18 (IDEXX Laboratories, Westbrook, Maine) and enterococci using Enterolert (ENT; IDEXX Laboratories, Westbrook, Maine) according to the manufacturer's instructions. The most probable number (MPN)/100 mL and confidence interval will be calculated.

Samples were analyzed using the standards set by the State Water Resources Control Board (SWRCB) for recreational marine waters at 10,000 colony-forming units (CFU)/100 mL for TC and 104 CFU/100 mL for ENT, and for freshwater at 235 CFU/100 mL for EC (EPA, 2012; SWRCB, 2019).

2.3 Heterotrophic Plate Counts

Samples were diluted 10 to 10,000-fold in phosphate buffered saline (PBS). We appled 50 uL of undilute or dilute sample to solid 25% Luria−Bertani (LB) growth medium amended with

no antibiotic, 20 mg/L of tetracycline, 4 mg/L of ciprofloxacin, or 10 mg/L of erythromycin in triplicate. Plates will be incubated at 30°C for 24 hours. Antibiotic resistance levels will be calculated as the ratio of colony forming units (CFUs) growing on plates amended with antibiotic to the CFUs growing on plates amended with no antibiotic. The mean and standard deviation of antibiotic resistance levels will be calculated (Negreanu et al., 2012).

2.4 Sample Filtration

Homogenized samples were vacuum filtered in 47 mm diameter, 0.22 um pore size, polycarbonate filters (MilliporeSigma, Burlington, Massachusetts) in quintuplet until clogging, volumes were be recorded. A "filter blank" of 100 mL of autoclaved PBS was also filtered. Four of the five filters were folded and placed in 2 mL microcentrifuge tubes with 1.5 mL of 50% ethanol. Filters were stored in -20°C until extraction.

2.5 Propidium Monoazide (PMA)

One of the five filters was folded and placed in a 25 mL falcon tube with 5 mL of PBS and hand-shaken for two minutes. Two 500 uL aliquots of suspension was placed in a light transparent 2 mL microcentrifuge tube. One of the aliquots was treated with 100 uM of PMAxx Dye (Biotium, Fremont, California). Both aliquots were gently vortexed (at level 2, Vortex Genie 2, FisherScientific, Hampton, New Hampshire) in the dark for 5 mins. Aliquots were then laid horizontally, and light exposed for 2 mins using a flat 10,000 luxe intensity LED light (Verilux, Santa Ana, California) from 20 cm distance. After 1 minute, the aliquots were manually rotated for even exposure. Aliquots were then centrifuged at 10,000 x g for 5 mins (Nocker et al., 2007). The supernatant was removed and discarded. The pellet was resuspended in 500 μL of PBS and 500 uL of 50% ethanol. Aliquots were stored in -20°C until extraction.

2.6 DNA Extraction

Filters were fragmented with flame sterilized tweezers and scissors and transferred to 2 mL lysing matrix e tubes (MP Biomedicals, Irvine, California). The remaining solution from the 2 mL microcentrifuge tubes will be were entrifuge at 5,000 x g for 10 mins. The supernatant was removed and discarded. The remaining pellet was resuspended with 978 uL of sodium phosphate buffer (MP Biomedicals, Irvine, California) and transferred to the 2 mL lysing matrix e tubes (Li et al., 2018).

Aliquots were centrifuged at 15,000 x g for 5 mins. The top 500 uL of supernatant was removed and discarded. The remaining pellet and PBS were resuspended with 978 uL of sodium phosphate buffer (MP Biomedicals, Irvine, California) and transferred to the 2 mL lysing matrix e tubes.

DNA from the filters and aliquots was extracted using the FastDNA Spin Kit for Soil (MP Biomedicals, Irvine, California) following the manufacturer's protocol, except for where samples are homogenized a Mini-Beadbeater-16 (BioSpec Products, Bartlesville, Oklahoma) was used twice for 1.5 mins with a 5 min rest in between. An "extraction blank" was extracted in parallel in all extractions. The eluted DNA was aliquoted. Nucleic acid concentration and 260/280 absorbance ratios were measured via UV absorption using a Nanodrop 2000C (Thermo Scientific, Waltham, Massachusetts). Aliquots of eluted DNA will be stored in -80℃ until use.

2.7 qPCR

*sul*1 (Pei et al., 2006), *erm*F (Knapp et al., 2010), *tet*A (Ng et al., 2001), $bla_{\text{CTX-M}}$ (Kim et al., 2005), *van*A (Volkmann et al., 2004), *int*I1 (Stokes et al., 2006), and 16S rRNA (Galley et al., 2021; Suzuki et al., 2000) primers, primer concentrations, and thermocycling conditions previously validated in the literature were used (Table A5-1 and A5-2). To determine the appropriate DNA concentration, serial dilution and well spike tests were performed for all samples.

All assays were performed in 96-well reaction plates that contain triplicate: diluted DNA, filter blanks, extraction blanks, a RNase-free molecular biology grade water negative control, and a standard curve positive control. A standard curve, covering 7 orders of magnitude, were constructed with 10-fold serial dilutions of known amounts of dsDNA (Integrated DNA Technologies, Coralville, Iowa). All assays were run in a StepOne Plus Real-Time PCR System (Applied Biosystems, Foster City, California), which generated quantification thresholds and melt curves for each assay. Quantification thresholds were converted into gene copies using the standard curve. Melt curves were used to further verify target gene amplification specificity. The limit of detection was set as the lowest standard that amplified at least in duplicate. Standard curve efficiencies were at or above 90% and R^2 values were at or above 0.99 across all qPCR assays (Table A5-2).

2.8 Metagenomic Sequencing and Bioinformatic Analysis

We sent DNA from each sample to MR DNA Molecular Research Lab (Shallowater, Texas) for library preparation using a NexteraXT DNA Library Prep Kit and for 2 x 150 bp paired-end shotgun metagenomic sequencing using an Illumina NovaSeq 6000. Quality trimming, annotation, and assembly of metagenomes were perfomed via Galaxy. Metagenomes were analyzed against the Comprehensive Antibiotic Resistance Database (CARD), Structured ARG (SARG), A CLAssification of Mobile Genetic Elements (ACLAME), Pathosystems Resource Integration Center (PATRIC) databases via ARGs-OAP and MetaCompare (Yang et al., 2016; Oh et al., 2018).

2.9 Systematic Literature Review

We conducted a systematic literature review using Web of Science to identify clinically relevant antibiotic resistance genes and pathogens in Los Angeles. We will use the following

keywords: “antibiotic OR antimicrobial”, “resist*”, “clinic”, and “Los Angeles” (Davis et al., 2020; Fresia et al., 2019).

3. Results and Discussion

3.1 ARB in the Ballona and Topanga Creek Watersheds

The resistance ratios in the BCW were up to an order of magnitude greater that those in the TCW. The mean erythromycin resistance ratio in BCW was 0.109 and in TCW it was 0.068. The mean tetracycline resistance ratio in BCW was 0.005 and in TCW it was 0.0002. The mean ciprofloxacin resistance ratio in BCW was 0.006 and in TCW it was 0.0007 (Figure 5-2). Wilcoxon Rank-Sum tests for resistance ratios between BCW and TCW showed no statistically significant ($p > 0.05$) differences for the erythromycin and ciprofloxacin resistance rations, but did show statistically significant ($p < 0.05$) differences for the tetracycline resistance ratios (Table A5-3). The higher resistance ratios observed for erythromycin in comparison to tetracycline and ciprofloxacin has been previously observed in agricultural soils irrigated with treated wastewater and biosolids (Hung et al., 2022; Negreanu et al., 2012).

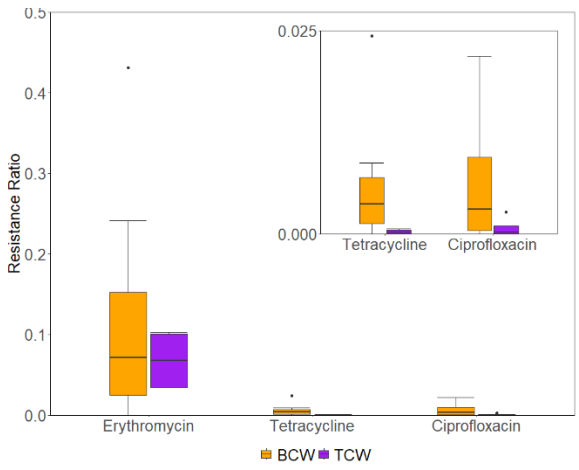

Figure 5-2. Erythromycin, tetracycline, and ciprofloxacin resistance ratios for the BCW and TCW.

3.2 ARGs in the Ballona and Topanga Creek Watersheds

Relative gene abundances in the BCW were up to 1 order of magnitude greater than in the TCW. Mean *intI*1 and *sul*1 relative abundances were 10^{-2} gene copies/16S rRNA gene copies in

BCW and 10^{-3} gene copies/16S rRNA gene copies in TCW. *erm*F relative abundances were 10^{-3} gene copies/16S rRNA gene copies in BCW and 10^{-5} gene copies/16S rRNA gene copies in TCW. *tet*A relative abundances were 10^{-4} gene copies/16S rRNA gene copies in BCW and 10^{-5} gene copies/16S rRNA gene copies in TCW. $bla_{CTX\text{-}M}$ and *van*A relative abundances were 10^{-5} gene copies/16S rRNA gene copies in hospital sewage and 10^{-5} gene copies/16S rRNA gene copies non-hospital sewage (Figure 5-3). Wilcoxon Rank-Sum tests confirmed that differences in relative gene abundances between BCW and TCW were statistically significant ($p < 0.05$) for all genes except $bla_{CTX\text{-}M}$ and *van*A (Table A5-4). While $bla_{CTX\text{-}M}$ and *van*A relative abundances were not high, detection of these genes in the environment is of importance since they are clinically relevant ARGs that encode resistance to last-resort antibiotics (Keenum et al., 2022).

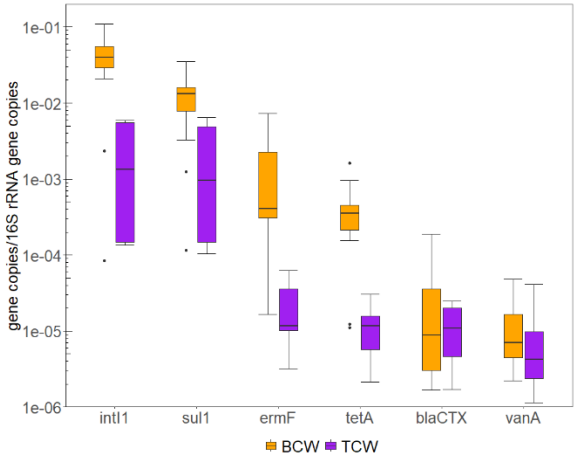

Figure 5-3. Relative gene abundances for the BCW and TCW.

3.3 Risk Scores in the Ballona and Topanga Creek Watersheds

Risk scores in the BCW and TCW were comparable. The mean risk score in the BCW was 22.99 and in the TCW it was 23.85 (Figure 5-4). A Wilcoxon Rank-Sum test showed that these differences were not statistically significant ($p > 0.05$).

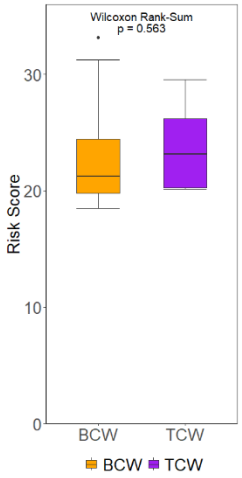

Figure 5-4. Risk scores for the BCW and TCW.

3.4 Cross-validation of Culture and Molecular Methods

Culture and molecular-based methods had few correlations with one another. Erythromycin resistance ratios from the culture method correlated significantly ($p < 0.05$) with quinolone and *sul*1 relative abundances from the metagenomic sequencing method and $bla_{CTX\text{-}M}$ relative abundances from the qPCR method. The tetracycline resistance ratios from the culture method also correlated significantly ($p < 0.05$) with *sul*1 relative abundances from the metagenomic sequencing method. Similarly, ciprofloxacin resistance ratios from the culture method also correlated significantly ($p < 0.05$) with quinolone and *sul*1 relative abundances from the metagenomic sequencing method. When comparing qPCR and metagenomic sequencing, only the relative abundances of $bla_{CTX\text{-}M}$ had statistically significant correlations ($p < 0.05$) (Figure 5-5).

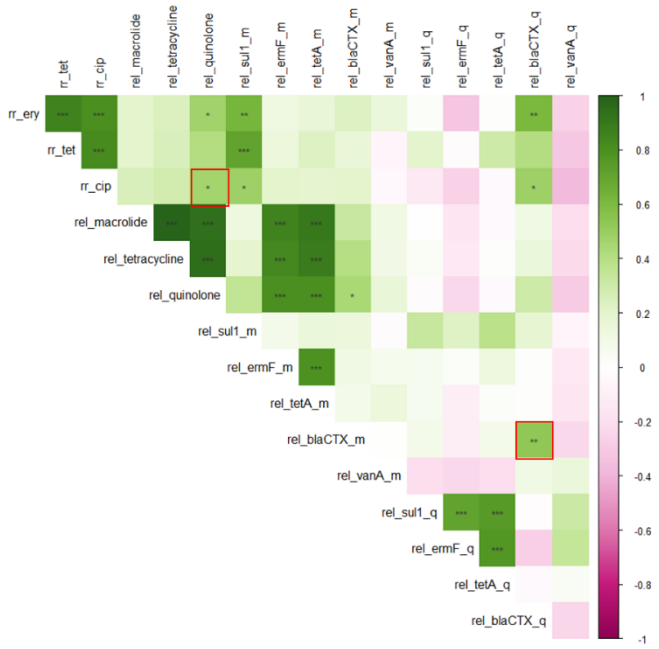

Figure 5-5. Pearson correlations for culture and molecular methods.

Relative gene abundances from the qPCR and metagenomics method were not exact. A scatter plot of qPCR versus metagenomics relative gene abundances against a 1:1 line showed little agreement. Boxplots showed that relative abundances from the qPCR method were up to 2 orders of magnitude greater than from the metagenomics method. Mean *sul*1 relative abundances were 10^{-2} gene copies/16S rRNA gene copies by qPCR and 10^{-4} gene copies/16S rRNA gene copies by metagenomics. *erm*F relative abundances were 10^{-3} gene copies/16S rRNA gene copies by qPCR and 10^{-5} gene copies/16S rRNA gene copies by metagenomics. *tet*A relative abundances were 10^{-4} gene copies/16S rRNA gene copies by qPCR and metagenomics. $bla_{CTX\text{-}M}$ relative abundances were 10^{-5} gene copies/16S rRNA gene copies by qPCR and 10^{-6} gene copies/16S rRNA gene copies by metagenomics. *van*A relative abundances were 10^{-5} gene copies/16S rRNA gene copies by qPCR and metagenomics (Figure 5-6). Welch's t-tests confirmed that differences in *sul*1, *tet*A, $bla_{CTX\text{-}M}$, and *van*A relative gene abundances between qPCR and metagenomics were insignificant

(p > 0.05). However, differences in *sul*1, *erm*F, and *bla*$_{CTX\text{-}M}$ relative gene abundances between qPCR and metagenomics were significant (p < 0.05), while differences in *tet*A and *van*A relative gene abundances between qPCR and metagenomics were not significant (p > 0.05) (Table A5-5). Differences in the relative gene abundances between qPCR and metagenomics methods may be due to the detection limitations of the metagenomic approach (Crossette et al., 2021).

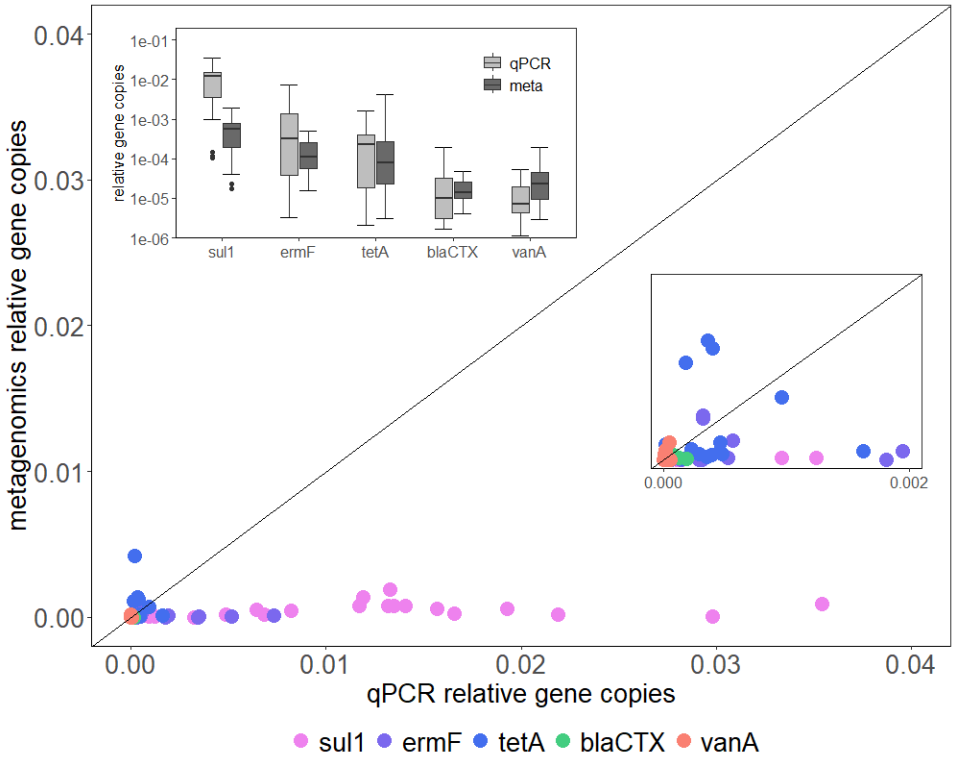

Figure 5-6. Boxplot and scatter plot of qPCR versus metagenomic relative gene abundances.

4. Appendix

Table A5-1. Primer Sequences and Concentrations.

Target Gene		Concentration (nM)	Sequence (5'-3')	Amplicon size (bp)	Reference
*sul*1	F	200	CGCACCGGAAACATCGCTGCAC	258	Pei et al., 2006
	R		TGAAGTTCCGCCGCAAGGCTCG		
*erm*F	F	500	TCGTTTTACGGGTCAGCACTT	246	Knapp et al., 2009
	R		CAACCAAAGCTGTGTCGTTT		
*tet*A	F	200	GCTACATCCTGCTTGCCTTC	210	Ng et al., 2010
	R		CATAGATCGCCGTGAAGAGG		
bla_{CTX-M}	F	900	CGTCACGCTGTTGTTAGGAA	791	Kim et al., 2005
	R		ACGGCTTTCTGCCTTAGGTT		
*van*A	F	200	CTGTGAGGTCGGTTGTGCG	185	Volkmann., 2004
	R		TTTGGTCCACCTCGCCA		
*int*I1	F	650	CTGGATTTCGATCACGGCACG	483	Stokes et al., 2006
	R		ACATGCGTGTAAATCATCGTCG		
16S rRNA	F	1000	CGGTGAATACGTTCYCGG	152	Suzuki et al., 2000
	R		GGWTACCTTGTTACGACTT		

Table A5-2. qPCR Thermocycling Conditions. *Assay has an initial denaturation step at 50°C for 2 minutes.

Target Gene	Holding		Denaturation		Annealing		Extension		R^2	Eff.
	Temp. (°C)	Time (min)	Temp. (°C)	Time (s)	Temp. (°C)	Time (s)	Temp. (°C)	Time (s)		
*sul*1	95	10	95	15	65	30	72	30	0.999	91
*erm*F	95	10	94	20	60	60	-	-	0.999	92
*tet*A	95	4	95	5	55	30	72	30	0.999	92
bla_{CTX-M}	95	10	95	8	60	60	-	-	0.996	90
*van*A	95	5	95	15	60	60	-	-	0.999	94
*int*I1*	95	2	95	15	58	15	72	60	0.999	90
16S rRNA*	95	10	95	15	56	75	-	-	1.000	92

Table A5-3. Wilcoxon Rank-Sum tests comparing BCW and TCW resistance ratios.

Resistance Ratio	p-value
Erythromycin	0.850
Tetracycline	0.014
Ciprofloxacin	0.106

Table A5-4. Wilcoxon Rank-Sum tests comparing BCW and TCW relative gene abundances.

Gene	p-value
rel *intI*1	0.006
rel *sul*1	0.008
rel *erm*F	0.003
rel *tet*A	0.004
rel $bla_{\text{CTX-M}}$	0.248
rel *van*A	0.364

Table A5-5. Welch's t-tests comparing qPCR and metagenomics relative gene abundances.

Gene	p-value
rel *sul*1	0.000
rel *erm*F	0.014
rel *tet*A	0.542
rel $bla_{\text{CTX-M}}$	0.022
rel *van*A	0.417

5. References

Berendonk, T. U. *et al.* Tackling antibiotic resistance: The environmental framework. *Nat. Rev. Microbiol.* **13**, 310–317 (2015).

Cao, Y., Griffith, J. F. & Weisberg, S. B. The next-generation PCR-based quantification method for ambient waters: Digital PCR. *Methods Mol. Biol.* **1452**, 113–130 (2016).

CDC. Antibiotic resistance threats in the United States. *Centers Dis. Control Prev.* 1–113 (2019).

Cira, M. *et al.* Commercially available garden products as important sources of antibiotic resistance genes—a survey. *Environ. Sci. Pollut. Res.* **28**, 43507–43514 (2021).

Crossette, Emily, et al. Metagenomic quantification of genes with internal standards. MBio 12.1 (2021): e03173-20.

Davis, B. C. *et al*. Demonstrating an Integrated Antibiotic Resistance Gene Surveillance Approach in Puerto Rican Watersheds Post-Hurricane Maria. *Environmental Science & Technology*, ***54*** (23), 15108-15119 (2020).

Dutka-Malen, S., Evers, S. & Courvalin, P. Detection of glycopeptide resistance genotypes and identification to the species level of clinically relevant enterococci by PCR. *J. Clin. Microbiol.* **33**, 24–27 (1995).

EPA. Recreational Water Quality Criteria. *U. S. Environ. Prot. Agency* 1–69 (2012).

FDA, CDC, USDA. The National Antimicrobial Resistance Monitoring System: Strategic Plan 2021-2025. 1-12 (2020).

Fresia, P. *et al.* Urban metagenomics uncover antibiotic resistance reservoirs in coastal beach and sewage waters. *Microbiome* **7**, 1–9 (2019).

Galley, Jeffrey D., et al. Prenatal stress-induced disruptions in microbial and host tryptophan metabolism and transport. *Behavioural brain research* 414 (2021): 113471.

Goldstein, C. *et al*. Incidence of Class 1 and 2 Integrases in Clinical and Commensal Bacteria from Livestock, Companion Animals, and Exotics. *American Society for Microbiology*. **45**, 723–726 (2001).

González-Escalona, N. *et al.* Detection of live Salmonella sp. cells in produce by a taqman-based quantitative reverse transcriptase real-time PCR Targeting invA mRNA. *Appl. Environ. Microbiol.* **75**, 3714–3720 (2009).

Haugland, R. A. *et al.* Evaluation of genetic markers from the 16S rRNA gene V2 region for use in quantitative detection of selected Bacteroidales species and human fecal waste by qPCR. *Syst. Appl. Microbiol.* **33**, 348–357 (2010).

Hung, Wei-Cheng, et al. Tracking antibiotic resistance through the environment near a biosolid spreading ground: Resistome changes, distribution, and metal (loid) co-selection. Science of The Total Environment 823 (2022): 153570.

JPIAMR. Strategic Research and Innovation Agenda on Antimicrobial Resistance. *Strateg. Res. Innov. Agenda Antimicrob. Resist.* 1–54 (2019).

Karkman, A., Pärnänen, K. & Larsson, D. G. J. gene abundances in anthropogenically impacted. *Nat. Commun.* 1–8 doi:10.1038/s41467-018-07992-3.

Kawecki, S., Kuleck, G., Dorsey, J. H., Leary, C. & Lum, M. The prevalence of antibiotic-resistant bacteria (ARB) in waters of the Lower Ballona Creek Watershed, Los Angeles County, California. *Environ. Monit. Assess.* **189**, (2017).

Keenum, Ishi, et al. A framework for standardized qPCR-targets and protocols for quantifying antibiotic resistance in surface water, recycled water and wastewater. *Critical Reviews in Environmental Science and Technology* 52.24 (2022): 4395-4419.

Kim, J., Lim, Y., Jeong, Y., Scol, S. Occurrence of CTX-M-3, CTX-M-15, CTX-M-14, and CTX-M-9 extended-spectrum B-Lactameses in Enterobacteriaceae clinical isolates in Korea. *American Society for Microbiology*. **49**, 1572–1575 (2005).

Knapp, C. W.; Dolfing, J., Ehlert, P. A. I., Graham, D. W. Evidence of Increasing Antibiotic Resistance Gene Abundances in Archived Soils since 1940. *Environ. Sci. Technol. 44* (2), 580–587 (2010).

LACDPW. Ballona Creek Watershed. https://www.ladpw.org/wmd/watershed/bc/

LACDPW. Topanga Creek Watershed. https://dpw.lacounty.gov/wmd/watershed/topanga/index.cfm

Li, A. D. *et al.* Effects of sample preservation and DNA extraction on enumeration of antibiotic resistance genes in wastewater. *FEMS Microbiol. Ecol.* **94**, 1–11 (2018).

Los Angeles County. Department of Beaches and Harbors History. https://beaches.lacounty.gov/history/

Manago, K. F. & Hogue, T. S. Urban Streamflow Response to Imported Water and Water Conservation Policies in Los Angeles, California. *J. Am. Water Resour. Assoc.* **53**, 626–640 (2017).

O'Neill, J. Antimicrobial Resistance: Tackling a crisis for the health and wealth of nations. *The Review on Antimicrobial Resistance Chaired*. (2014).

O'Neill, J. Tackling drug-resistant infections globally: final report and Recommendations. *The Review on Antimicrobial Resistance Chaired*. (2016).

Nappier, S. P., Liguori, K., Ichida, A. M., Stewart, J. R. & Jones, K. R. Antibiotic resistance in recreational waters: State of the science. *Int. J. Environ. Res. Public Health* **17**, 1–28 (2020).

Negreanu, Y., Pasternak, Z., Jurkevitch, E. & Cytryn, E. Impact of treated wastewater irrigation on antibiotic resistance in agricultural soils. *Environ. Sci. Technol.* **46**, 4800–4808 (2012).

Ng, L. K., Martin, I., Alfa, M. & Mulvey, M. Multiplex PCR for the detection of tetracycline resistant genes. *Mol. Cell. Probes* **15**, 209–215 (2001).

Noble, R. T. *et al.* Multitiered approach using quantitative PCR to track sources of fecal pollution affecting Santa Monica Bay, California. *Appl. Environ. Microbiol.* **72**, 1604–1612 (2006).

Nocker, A., Sossa-Fernandez, P., Burr, M. D. & Camper, A. K. Use of propidium monoazide for live/dead distinction in microbial ecology. *Appl. Environ. Microbiol.* **73**, 5111–5117 (2007).

Oh, Min, et al. MetaCompare: a computational pipeline for prioritizing environmental resistome risk. FEMS microbiology ecology 94.7 (2018): fiy079.

Pei, R., Kim, S. C., Carlson, K. H. & Pruden, A. Effect of River Landscape on the sediment concentrations of antibiotics and corresponding antibiotic resistance genes (ARG). *Water Res.* **40**, 2427–2435 (2006).

Stachler, E. *et al.* Quantitative CrAssphage PCR Assays for Human Fecal Pollution Measurement. *Environ. Sci. Technol.* **51**, 9146–9154 (2017).

Stokes, H. W., et al. Class 1 integrons potentially predating the association with Tn 402-like transposition genes are present in a sediment microbial community. Journal of bacteriology 188.16 (2006): 5722-5730.

Suzuki, M. T., Taylor, L. T. & DeLong, E. F. Quantitative analysis of small-subunit rRNA genes in mixed microbial populations via 5'-nuclease assays. *Appl. Environ. Microbiol.* **66**, 4605–4614 (2000).

SWRCB. Water Quality Control Plan Ocean Waters of California State Water Resources Control Board California Environmental Protection Agency. (2019).

USGS. Tracking Contaminants in Santa Monica Bay , Offshore of Greater Los Angeles Shaded Relief Map of Santa Monica Bay. (2003).

Volkmann, H.; Schwartz, T.; Bischoff, P.; Kirchen, S.; Obst, U. Detection of Clinically Relevant Antibiotic-Resistance Genes in Municipal Wastewater Using Real-Time PCR (TaqMan). *J. Microbiol. Methods* **2004**, *56* (2), 277–286.

https://doi.org/10.1016/J.MIMET.2003.10.014.

WHO. Global Action Plan on Antimicrobial Resistance. *Microbe Mag.* **10**, 354–355 (2015).

WHO. Ten threats to global health in 2019 Air pollution and climate change. *Ten Threat. to Glob. Heal. 2019* 1–18 (2019).

WHO, FAO, OIE. *Monitoring and evaluation of the global action plan on antimicrobial resistance*. (2019).

Yang, Ying, et al. ARGs-OAP: online analysis pipeline for antibiotic resistance genes detection from metagenomic data using an integrated structured ARG-database. *Bioinformatics* 32.15 (2016): 2346-2351.

Chapter 6: Confidence and Interest in Research Among Graduate Students Participating in a Course-Based Research Experience (CRE) in Water Quality

1. Introduction

A course-based research experience (CRE) provides students with the opportunity to conduct research during the course. The benefits of CREs are well documented among undergraduate students in STEM laboratory courses. Among this group, CREs have been shown to improve student learning outcomes, academic achievement, retention, and matriculation into graduate and professional programs (NASEM, 2015).

Instructors can implement their own CRE. However, there exists network CREs, which were introduced by an individual instructor and implemented by several other instructors. Examples of such CREs include Science Education Alliance-Phage Hunters Advancing Genomics and Evolutionary Science (SEA-PHAGES), Genomics Education Partnership (GEP), and prevalence of antibiotic resistance in the environment (PARE) among others (Fuhrmeister et al., 2020; Gene-Bacon and Bascom-Slack, 2018; NASEM, 2015; Shaffer et al., 2010). Gene-Bacon and Bascom-Slack (2018) designed PARE, a short CRE in which undergraduate students surveil antibiotic resistant bacteria in environmental soil samples. By engaging students in a project of scientific merit, student skills improved, and students expressed interest in a career in research. Due to the success of this CRE, the CRE has been improved and expanded to other countries, including France, India, and Botswana (Fuhrmeister et al., 2020).

This study investigates how a CRE in a graduate civil engineering course impacts student confidence and interest in research. Students learned how to collect and process environmental water samples and how to analyze and interpret water quality data. Students applied these skills to conduct a research project. Students collected and processed river and beach water samples from the Topanga and Ballona Creek watersheds during dry and wet weather conditions to evaluate

whether stormwater runoff is a source of antibiotic resistance bacteria to beaches in the Santa Monica Bay.

2. Methods

2.1 Course Description

The intervention was implemented at UCLA in the Civil and Environmental and Engineering 254A Environmental Aquatics Inorganic Chemistry course. Generally, students who enroll in the course are completing the first quarter of the Civil and Environmental Engineering graduate program.

2.2 Intervention

The intervention consisted of a course-based research experience that comprised of class, field, and laboratory instruction. In the first three weeks, students learned how to collect environmental water samples in the field and learned how to process environmental water samples in class. In weeks three to six, students conducted three sampling campaigns during dry and wet weather conditions. Students signed up for different laboratory or field timeslots to prepare for a sampling campaign and to collect and process environmental water samples. In weeks six to seven, students completed a reading guide using Liguori et al. (2022) for homework to learn how to read scientific articles and to allow students to contextualize their research. In weeks eight to nine, students learned how to analyze and interpret water quality data in class. In week ten, students were divided into groups to analyze and interpret different parts of the water quality data they have collected in class and for homework (Figure 6-1, Table A6-1).

2.3 Safety

Students went to the field with one or two other students to collect environmental water samples. All students were provided with necessary personal protective equipment at all times.

While students quantified bacteria from enclosed trays and plates, students performing bacterial counts completed laboratory safety trainings.

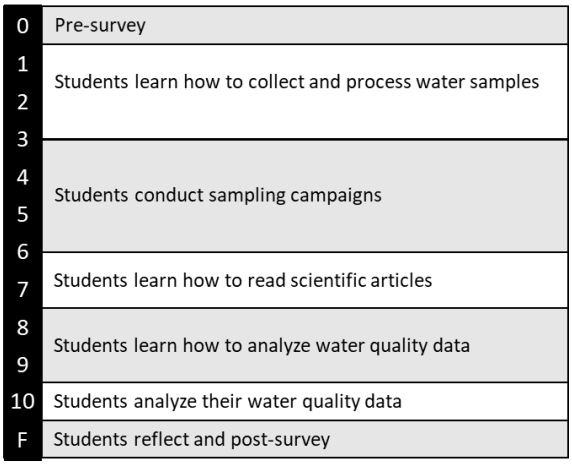

Figure 6-1. Intervention timeline.

2.4 Assessment

We assessed whether students achieved the learning outcomes through completion of sampling campaigns, the reading guide, and the summative final group presentation assignments. The assignments were not optional.

We also assessed the effectiveness of the CRE. We requested IRB approval to assess the intervention through a pre-post survey. Participation in the pre-post survey was anonymous and optional. The three to five minute pre-post survey was administered through Google Forms and contained matching, demographic, attitudinal, and test questions. The attitudinal questions consisted of Likert scale questions that assessed confidence and interest in research and the test questions consisted of multiple-choice questions that assessed mastery of water quality analyses. The pre-post survey questions can be found in the Appendix.

2.5 Analysis

Pre-post survey responses were matched in Excel using the Fuzzy Lookup function. R Studio was used to create bar and Likert scale plots. R Studio was also used to determine the

normality of the matched survey responses. Since the data was found to be normal, paired t-test were performed to determine statistically significant differences between the pre-survey and post-survey responses for all groups.

3. Results

Of the 28 students who enrolled in the course, 19 students completed the pre-post survey. According to the pre-post survey, 42% (n = 8) were women and 58% (n = 11) were men. There were 16% (n = 3) underrepresented minority (URM) students, 21% (n = 4) first generation college students (FGCS), and 37% (n = 7) first generation graduate students (FGCS) (Table A6-2).

Overall, pre-post survey responses showed an increase in student confidence and interest in research. For all students, all means of Likert scale questions assessing student confidence in research, understanding of course topics, sense of community, and interest in research increased. However, when only looking at the "Agree" and "Strongly Agree" responses, LQ05, 12, and 14 showed no increase and LQ04 showed a decrease (Figure 6-2). The paired t-tests showed statistically significant increases for LQ02 and 07-09 (Table A6-3). Further, the test questions showed an increase in mastery of water quality analyses. The number of students that answered TQ1 correctly shifted from 21% in the pre-survey to 58% in the post-survey, and the number of students that answered TQ2 correctly shifted from 16% in the pre-survey to 37% in the post-survey (Figure A6-3).

Pre-post survey responses for women and FGGS also showed an increase in student confidence and interest in research. For women, most means of Likert scale questions increased; LQ04 and LQ06 decreased. However, when only looking at the "Agree" and "Strongly Agree" responses, LQ13 and 14 showed no increase (Figure 6-4). The paired t-tests showed statistically significant increases for LQ03, 09, and 10 (Table A6-3). For FGGS, all means of Likert scale

questions increased. However, when only looking at the "Agree" and "Strongly Agree" responses, LQ05 and 15 showed no increase (Figure 6-5). The paired t-tests showed statistically significant increases for LQ03, 09, and 10 (Table A6-3). Pre-post survey responses for other groups were not analyzed due to their small sample size.

4. Discussion

Results from this study indicate that there were improvements in student confidence in research, understanding of course topics, sense of community, and interest in research. However, for all students, there were only statistically significant improvements to student confidence in wet laboratory skills and understanding of course topics. For women and FGGS, there were only statistically significant improvements to student confidence in ability to collect and process environmental samples, understanding of environmental antibiotic resistance, and class engagement.

Therefore, the results from this study were able to show that this CRE can be used to engage and educate students on antibiotic resistance. Most importantly, the CRE can be used to teach students how to surveil antibiotic resistance in water environments. Gene-Bacon and Bascom-Slack (2018) and Fuhrmeister et al. (2020) also found that PARE, a CRE surveilling antibiotic resistance in soil environments, engaged students in antibiotic stewardship. Since educating the public is critical in combating the antibiotic resistance public health crisis (WHO, 2015), CREs can be used as a tool disseminate this information.

The results of this study also showed that CREs can be used to foster inclusion and diversity in graduate programs. While it was not possible to analyze the impacts of this CRE on URM and FGCS, the CRE did improve FGGS outcomes. Additionally, since CREs occur during classroom time, CREs do remove barriers to academic research (Bangera and Brownell, 2014).

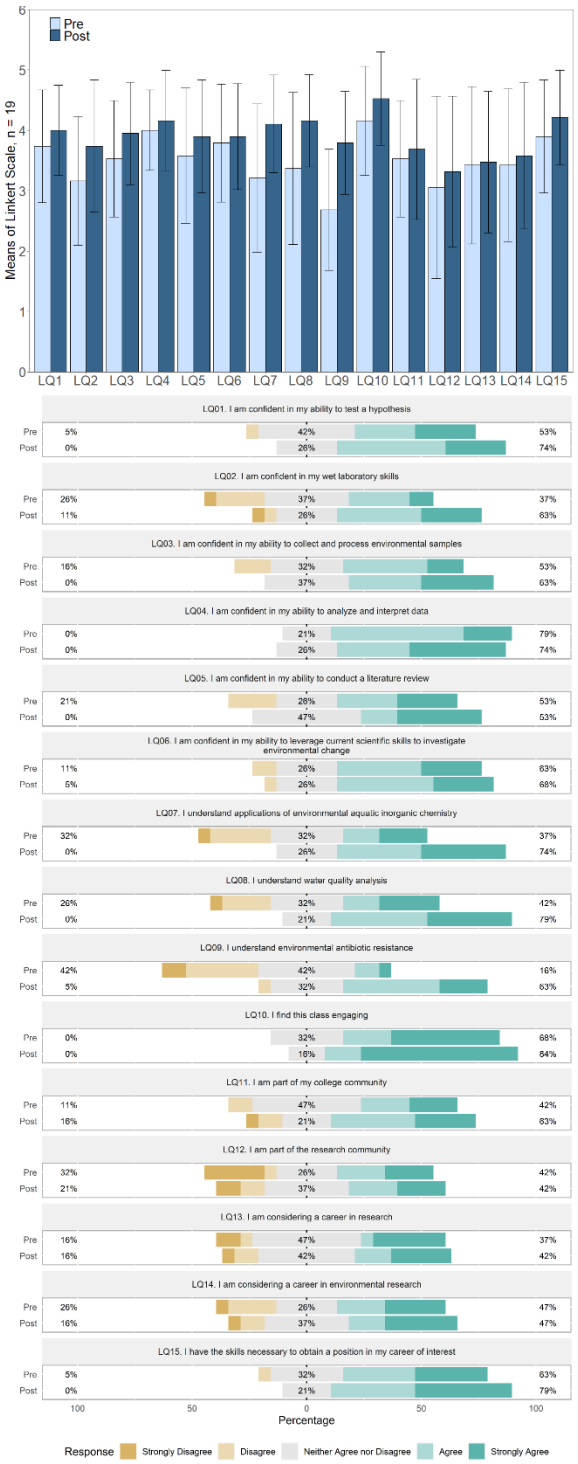

Figure 6-2. Pre-post survey attitudinal responses for all students.

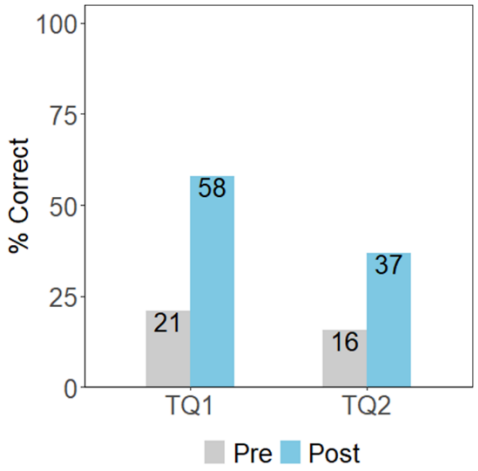

Figure 6-3. Pre-post survey test responses for all students.

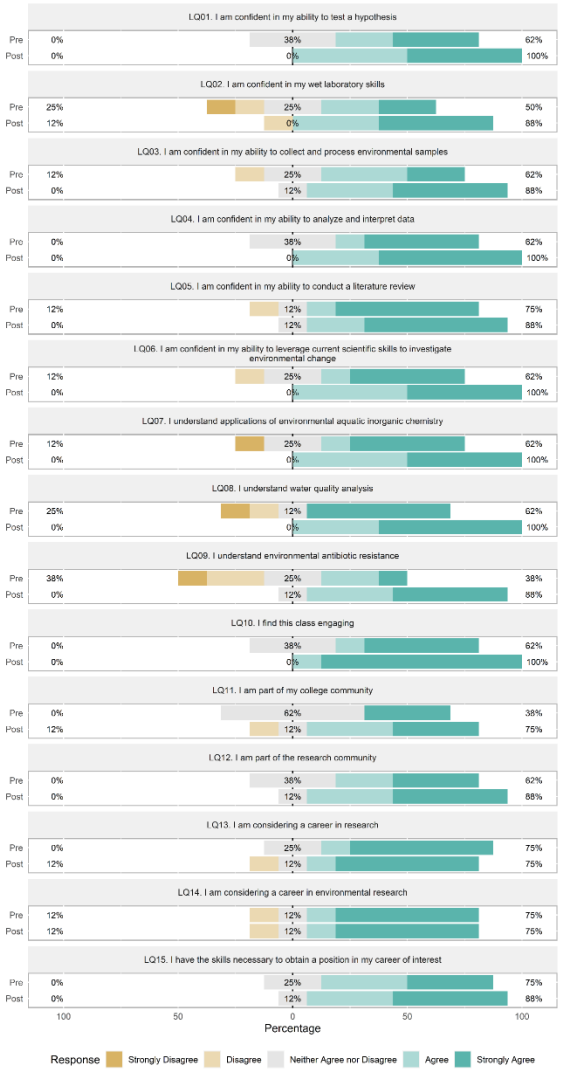

Figure 6-4. Pre-post survey attitudinal responses for women.

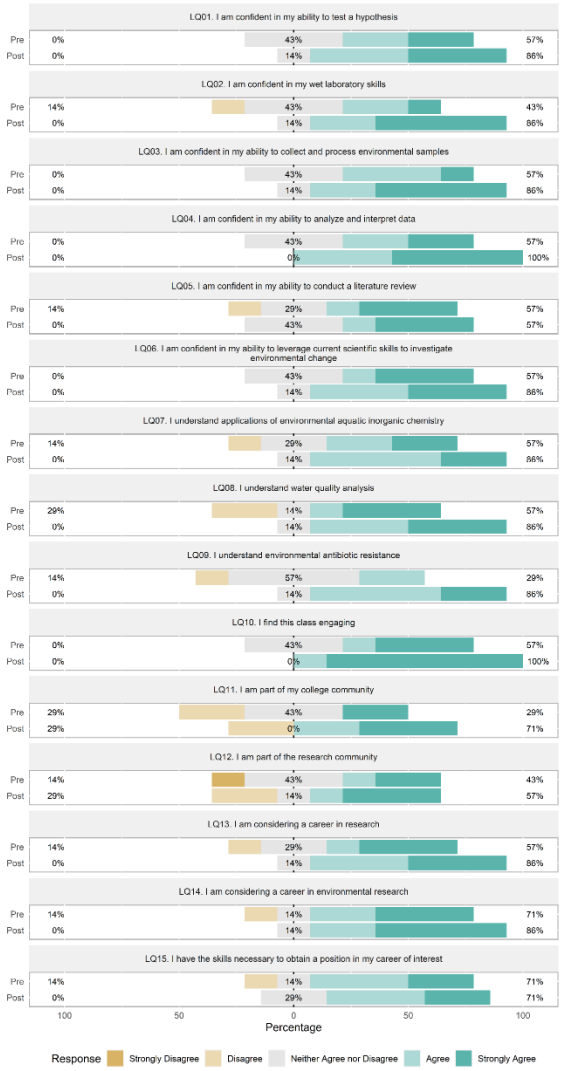

Figure 6-5. Pre-post survey attitudinal responses for FGGS.

Results and feedback from students indicate that the CRE can be further improved. The CRE can be improved by spending more time relating the research to the course material and learning data analysis skills, but by also having students participate in each research activity instead of having them sign up for time slots. The assessment of the CRE can also be improved by increasing the sample size so that overall impacts and impacts to URM and FGCS groups can be better analyzed. Additionally, adding a control group could help assess the impacts of the CRE.

5. Appendix

Table 6-1. Alignment table.

Learning Outcome	Assessment	Learning Activities
Develop and improve their research skills	• Pre-post survey	• In the field, the Professor demonstrated how to collect environmental samples and students practiced • In class, the Professor demonstrated how to perform water quality tests and students practiced • For homework, the students were guided on how to read a research article • In class, the students were guided on how to analyze water quality data
Apply their research skills by conducting a course-based research project	• Pre-post survey • Reflection • Final group presentation	• Students conducted a research project • Students analyzed and interpreted different parts of the data in groups • Students presented their results in class

Table A6-2. Student demographics.

Category		Frequency	Percent
Gender	Woman	8	42
	Man	11	58
Underrepresented Minority (URM)	URM	3	16
	Non-URM	15	79
First Generation College Student (FGCS)	Yes	4	21
	No	15	79
First Generation Graduate Student (FGGS)	Yes	7	37
	No	12	63

Table A6-3.

	LQ1	LQ2	LQ3	LQ4	LQ5	LQ6	LQ7	LQ8	LQ9	LQ10	LQ11	LQ12	LQ13	LQ14	LQ15
All	0.287	0.045	0.088	0.506	0.163	0.650	0.006	0.009	0.000	0.247	0.625	0.399	0.848	0.482	0.209
Woman	0.171	0.087	0.049	0.171	0.563	0.171	0.250	0.197	0.028	0.048	0.517	0.080	0.598	1.000	0.351
Man	0.796	0.307	0.465	0.779	0.167	0.553	0.010	0.020	0.005	0.852	0.858	0.733	0.691	0.465	0.371
FGGS	0.289	0.086	0.047	0.140	0.736	0.356	0.356	0.280	0.038	0.045	0.356	0.356	0.289	0.289	0.736
Non-FGGS	0.615	0.305	0.463	0.504	0.137	1.000	0.009	0.020	0.006	0.851	0.830	0.600	0.658	1.000	0.210

Pre-Post Survey

Matching Questions

1. What was the name of your first pet, or your childhood best friend if you've never had a pet?
2. In what month was your mother born?
3. In what city were you born?

Demographic Questions

1. What is your gender identity?
   a. Woman
   b. Man
   c. Transgender Woman
   d. Transgender Man
   e. Non-Binary
   f. Other
   g. Prefer Not to Answer
2. What is your race? (Select All That Apply)
   a. American Indian or Alaskan Native
   b. Asian
   c. Black or African American
   d. Native Hawaiian or Other Pacific Islander
   e. White
   f. Other
   g. Prefer Not to Answer
3. What is your ethnicity?
   a. Hispanic or Latino or Spanish Origin
   b. Not Hispanic or Latino or Spanish Origin
   c. Prefer Not to Answer
4. What is your major?
5. What program are you completing?
   a. BS
   b. MS
   c. PhD
   d. Other

6. What year are you in your program?
    a. Year 1
    b. Year 2
    c. Year 3
    d. Year 4
    e. Year 5+
7. Are you a first-generation college student (a student whose parent/guardian has not received a four-year bachelor's degree)?
    a. Yes
    b. No
8. Are you a first-generation graduate student (a student whose parent/guardian has not received a four-year bachelor's degree and is now earning a graduate degree)?
    a. Yes
    b. No

Background Questions

1. How much research experience do you have?
    a. No experience
    b. Some experience, but less than one year of experience
    c. One year or more of experience, but less than two years of experience
    d. More than two years of experience
2. How much environmental research experience do you have?
    a. No experience
    b. Some experience, but less than one year of experience
    c. One year or more of experience, but less than two years of experience
    d. More than two years of experience
3. How much wet laboratory (a type of laboratory where experiments involve handling liquids, chemicals, biological matter, and other "wet" hazards) experience do you have?
    a. No experience
    b. Some experience, but less than one year of experience
    c. One year or more of experience, but less than two years of experience
    d. More than two years of experience
4. If you do not have any wet laboratory experience, what factors contributed to this (e.g., no interest, work, limited opportunities, COVID-19, etc.)?

Likert Questions

1. I am confident in my ability to test a hypothesis.
2. I am confident in my wet laboratory skills.
3. I am confident in my ability to collect and process environmental samples.
4. I am confident in my ability to analyze and interpret data.
5. I am confident in my ability to conduct a literature review.
6. I am confident in my ability to leverage current scientific skills to investigate environmental change.

7. I understand applications of environmental aquatic inorganic chemistry.
8. I understand water quality analysis.
9. I understand environmental antibiotic resistance.
10. I find this class engaging.
11. I am part of my college community.
12. I am part of the research community.
13. I am considering a career in research.
14. I am considering a career in environmental research.
15. I have the skills necessary to obtain a position in my career of interest.

Test Questions

1. In Los Angeles County, a single sample of marine water may not exceed an Enterococcus value of?
    a. There is currently no standard.
    b. 104 enterococcus bacteria per 100 mililiters.
    c. 400 enterococcus bacteria per 100 mililiters.
    d. 10,000 enterococcus bacteria per 100 mililiters.
2. I add 50 uL of water sample onto a plate containing 25% Luria-Bertani (LB) agar and 10 mg/L of erythromycin. After incubating at 30°C for 24 hours, I count 100 colonies on the plate. What is the number of colony forming units (CFUs) per 100 mL of water sample?
    a. 50,000 CFU/100 mL
    b. 100,000 CFU/100 mL
    c. 150,000 CFU/100 mL
    d. 200,000 CFU/100 mL

6. References

Alaimo, P. J., Langenhan, J. M., & Suydam, I. T. (2014). Aligning the undergraduate organic laboratory experience with professional work: the centrality of reliable and meaningful data. Journal of Chemical Education, 91(12), 2093-2098.

Bangera, G., & Brownell, S. E. (2014). Course-Based Undergraduate Research Experiences Can Make Scientific Research More Inclusive. *CBE Life Sciences Education*, *13*(4), 602–606. http://doi.org/10.1187/cbe.14-06-0099

Fuhrmeister ER, Larson JR, Kleinschmit AJ, Kirby JE, Pickering AJ and Bascom-Slack CA (2021) Combating Antimicrobial Resistance Through Student-Driven Research and Environmental Surveillance. Front. Microbiol. 12:577821. doi: 10.3389/fmicb.2021.577821.

Genné-Bacon, E. A., & Bascom-Slack, C. A. (2018). The PARE project: a short course-based research project for national surveillance of antibiotic-resistant microbes in environmental samples. Journal of Microbiology & Biology Education, 19(3), 19-3.

Jacobsen M, McDermott M, Brown B, Eaton SE, and Simmons M (2018) Graduate students' research-based learning experiences in an online Master of Education program. Journal of University Teaching & Learning Practice, 15(4), 2018. https://ro.uow.edu.au/jutlp/vol15/iss4/4.

Liguori, K., Keenum, I., Davis, B. C., Calarco, J., Milligan, E., Harwood, V. J., & Pruden, A. (2022). Antimicrobial resistance monitoring of water environments: a framework for standardized methods and quality control. Environmental science & technology, 56(13), 9149-9160.

National Academies of Sciences, Engineering, and Medicine. (2015). Integrating discovery-based research into the undergraduate curriculum: Report of a convocation. National Academies Press.

Shaffer, C. D., Alvarez, C., Bailey, C., Barnard, D., Bhalla, S., Chandrasekaran, C., ... & Elgin, S. C. (2010). The genomics education partnership: successful integration of research into laboratory classes at a diverse group of undergraduate institutions. CBE—Life Sciences Education, 9(1), 55-69.

WHO. (2015). Global Action Plan on Antimicrobial Resistance. *Microbe Mag.* **10**, 354–355.